STIC-ILL

Mic
BS201.B4 J6

From: Schnizer, Richard
Sent: Wednesday, March 26, 2003 3:18 PM
To: STIC-ILL
Subject: 09/627,787

Please send me a copy of:

Sugiyama, Kazuo, J. Macromol. Sci. Chem. (1986), A23(10): 1155-64
102 for broad claims

Lu et al, Bioconjugate Chem. (2000) 11(1): 3-7
Poss interveneing reference

Liso et al J. Controlled Release (1995) 33(3): 429-436)
102 for broad claims?

Rihoiva et al, J. Controlled Release (1985) 2:289-310

Not sure what this is

Omelyanko et al Controlled Release (1998) 53(1-3): 25-37)
Could have fluorescine attached to HPMA

Richard Schnizer, Ph.D.
Patent Examiner
Art Unit 1635
CM1 12E17
703-306-5441
Mail Box CM1 11E12

ELSEVIER

Journal of Controlled Release 33 (1995) 429–436

journal of controlled release

Antinociceptive and antipyretic properties of a new conjugated ibuprofen-methacrylic polymeric controlled delivery system

P.A. Liso [a], M. Rebuelta [a], J. San Román [b,*], A. Gallardo [b], A.M. Villar [a]

[a] *Pharmacology Department, Facultad de Farmacia, Universidad Complutense, pza. Ramón y Cajal, 28040 Madrid, Spain*

[b] *Macromolecular Chemistry Department, Instituto de Ciencia y Tecnología de Polímeros, CSIC, c/ Juan de la Cierva, 3, 28006 Madrid, Spain*

Received 27 July 1994; accepted 16 November 1994

Abstract

Antinociceptive and antipyretic properties of a biocompatible polymer, poly(*N*-(4-(2-(4-isobutylphenyl) propionyloxy) phenyl) methacrylamide (PolyMIA) (Fig. 1) as a carrier drug has been investigated. This new polyacrylic compound and its monomeric form (MIA) were prepared by coupling methacrylic acid, *p*-aminophenol and 2-(4-isobutyl phenyl)propionic acid (Ibuprofen, IB) by means of well-known esterification and amidation reactions and finally by free radical polymerization of the monomeric acrylic derivative in solution, using a conventional free-radical initiator. Plasma levels were determined by gas-liquid chromatography (GLC) after the administration of IB, MIA and PolyMIA in mice. The results obtained indicate that PolyMIA acts as a controlled IB delivery system. Practically constant plasma levels of IB, about 20 μg/ml, were obtained at least for 6 h after the intraperitoneal administration of PolyMIA. Antinociceptive in vivo tests confirm the existence of a prolonged release of IB from the macromolecular systems. PolyMIA shows a time-extended activity and equal or even higher intensity of antinociceptive effects than that of free IB. In antipyretic test, PolyMIA was the only compound which increased its activity beyond the sixth hour of treatment (84.8%, $p < 0.01$ vs. control and vs. IB), doubling the traditional IB activity. The appearance of pharmacological activity of PolyMIA in a very short time after administration, seems to indicate that the system could be active in its polymeric form, since the hydrolytic behaviour followed in vitro in alkaline medium, showed a rate of cleavage of the side IB residue much lower than that indicated by the effects observed in vivo.

Keywords: Ibuprofen; Polymer drug; NSAID-like; Controlled drug delivery

1. Introduction

Ibuprofen (IB) is a quiral drug which shows antinociceptive and antipyretic properties related to its anti-inflammatory effects [1]. It inhibits the synthesis of prostaglandins and has no effect on the adenopituitary axis [2]. Dosage requirements are higher for acute processes and lower but repeated in chronic patients; both dosages lead to adverse reacti ns and side effects. New polymeric drugs have to avoid these drawbacks, since with only one dose (equivalent to an oral single dose of 400 mg) it would be possible to reach a similar antinociceptive and antipyretic potency to that of IB. In addition, these new compounds should provide a larger time-extended activity than that achieved with IB [3].

The aim of this research is to investigate in vivo the pharmacological possibilities of PolyMIA and MIA compounds as IB carrier systems. The synthesis, char-

* C rresponding author.

SSDI 0168-3659(94)00122-7

acterization and preliminary in vitro IB release characteristics have been previously studied [4,5]. Pharmacological trials were oriented to determine antinociceptive and anti-pyretic effects: in this way IB was used as a reference control in all trials to clarify the differences between traditional and polymeric forms of IB. The pharmacokinetic behaviour and pharmacodynamic characteristics were also analysed extensively.

2. Materials and methods

2.1. Animals

Swiss mice were purchased from the Charles River Breeding Laboratories, Barcelona, Spain. Unless otherwise stated, compounds were administered (0.5 ml/mouse) intraperitoneally in 10% Tween-80 in distilled water and the animals were distributed over four groups; (1) positive control (vehicle), (2) reference (traditional Ibuprofen at 5.72 mg/kg) [6], (3) MIA (monomeric form at 17.39 mg/kg) and (4) PolyMIA (polymeric form at 17.39 mg/kg). PolyMIA and MIA doses were molecularly equivalent to IB dose.

2.2. Materials

MIA and PolyMIA forms were prepared as reported elsewhere [4]. Ibuprofen was supplied by Boots Pharmaceuticals. Tween-80, λ-carrageen and carboxymethylcellulose were obtained from Sigma, acetic acid and *n*-hexane from PANREAC and Brewers' yeast from CENTAGE CROWN. All the chemicals were analytical grade, except *n*-hexane (HPLC grade).

2.3. In vitro release studies

The hydrolytic cleavage of IB from polyMIA was studied by measuring the IB concentration by UV spectroscopy (221 nm), in a buffered solution at pH 10 and 37°C. Hydrogel films of 200–300 μm thick, prepared from copolymers f 2-hydroxyethylacrylate (HEMA) and MIA, were used in order to have a heterogeneous system not soluble in the hydrolytical medium. More experimental details are given elsewhere. [5]

2.4. In vivo release studies

Determination of plasma IB

The analysis of the concentration of IB in plasma was carried out by GLC [7] using a capillary column SPB-1 (Sulfur 15 m * 0.32 mm). The column was conditioned before the experiments at 180°C with a carrier gas (nitrogen) at a flow rate of 1.2 ml/min, split 1:10. During analysis, the column, injection port and detector block were maintained isothermally at 180, 300 and 350°C, respectively. Aliquots of plasma (0.2 ml of blood/mouse, 9 mice per group) were prepared and purified for the HPLC assay [8] and compounds were extracted with *n*-hexane. Plasma samples were collected every 30 min after administration over a period of 6 h. Finally, 0.1 μl of final *n*-hexane solution were injected into the chromatograph.

2.5. Acetic acid test

Mice (10 per group) were grouped 2 per cage, and allowed to acclimatise for 30 min before the test. Acetic acid (0.5 ml/mouse of 1% aqueous solution) was injected intraperitoneally into mice weighing 25 ± 1 g. [9]. Animals were pretreated with the compounds under study 10, 40, 70, 100 and 130 min prior to acetic acid. Time for the first abdominal constriction was registered and the number of these during the next 30 min was measured. Results were expressed in time (min) and number of abdominal constrictions.

2.6. Carrageen induced hyperalgesia in mice

Nociception was provoked by compression of inflamed mice paws [10]. Animals (15 per group) were treated with λ-carrageen, 0.02 ml/paw of 3% saline solution, into the plantar region of the right hind paw [11]. Groups were administered with the compounds under study 5 h later. After 10 min, nociception threshold was measured using a modified Randall and Sellito analgesic meter LI-7300. The endpoint was determined as vocalization or paw withdrawal. Left hind paws were considered as individual controls. Results were expressed as the difference between the resistance times (in seconds) for the two hind paws.

2.7. Yeast-induced hyperthermia

To acclimatisee the animals (10 per group) to the experimental conditions, mice were taken out of the cage 5 h before testing. A probe was inserted 1 cm into the rectum. Rectal temperatures were recorded on an electronic thermometer (model Panlab-0331). Brewers' yeast suspension, 6.5 g/kg, was administered subcutaneously 16 h before the experiment (Brewers' yeast vehicle was prepared with carboxymethylcellulose at 1% and Tween-80 at 0.1% 1:1 v/v) [12]. An extra, fifth negative control group, treated only with vehicle, was necessary to determine real fever in positive controls. Ten minutes before starting, compounds were administered. Thereafter, rectal temperatures were taken every 30 min for 6 h.

2.8. Statistical analysis

In order to determine the differences between controls and the various treated groups, the Student t-test was applied. Quantal data differences were determined by the Newman-Keuls t-test. In anti-hyperthermic studies, Dunnet's t-test was used to determine if there was a significant difference at each interval between the treated groups and the respective control group. The Simpson's rule method for evaluating the area under a curve was used. Pharmacokinetic parameters were obtained by simulation [13] and graphic approach. [14].

3. Results

3.1. IB plasmatic levels

The plasma level of IB residues was determined by comparison with a calibration curve previously obtained with free IB (correlation level = 0.997). Samples of plasma of the treated animals with the control IB, the acrylic derivative MIA and the polymeric system PolyMIA, gave rise to detectable IB concentration after the analysis by GLC. Fig. 2 shows the variation in the concentration of IB residues detected in the plasma with time after the administration of the corresponding compound in solution, as indicated in Materials and methods. It seems to be clear from the results obtained that both carrier systems, MIA and PolyMIA, give rise to the release of IB in vivo. The diagrams drawn in Fig. 2 indicate that the acrylic derivative MIA presents a kinetic behaviour rather similar to the control IB, with a maximum concentration after 35–40 min after the i.p. administration; and later a decreasing of the concentration from about 31.3 and 38.6 μg/ml up to 5.5 and 12.1 μg/ml, respectively. This seem to indicate that the cleavage of the ester side bond in produced easily, probably through an enzymatic activation of the delivery process, giving rise to the release of free IB. However, the kinetic diagram obtained for the treatment with the polymeric species, PolyMIA, is rather different, reaching a steady state at a level of 20–25 μg/ml, for at least 5 or 6 h after administration. It can also be seen in Fig. 2 that there is no clear maximum and that the concentration of free IB in the plasma increases more slowly than that of the low molecular weight systems IP and MIA, so that the maximum activity is nor reached until 90 min after administration. The real parameters obtained for the three compounds studied are shown in Table 1. The area under the curve, $AUC^{0\rightarrow\infty}$, is 338 μg/ml·h for polymeric form and 143 μg/ml·h for traditional IB. PolyMIA administrated i.p. is capable of releasing IB to plasma, but time was required to reach the steady-state (PolyMIA $K_a = 2.4\ h^{-1}$ and IB $K_a = 1.3\ h^{-1}$).

3.2. In vitro hydrolytic behaviour

Fig. 3 shows the hydrolytic behaviour of films prepared from copolymers of MIA with HEMA. The hydrolysis in alkaline medium (pH = 10) was followed measuring the concentration of IB released from the films, which are not soluble in the buffered solution. Therefore, the model is not comparable with the in vivo experiments, but reveals two important points: first, it is not free IB as an impurity of the polymeric systems, since this would have to give a higher concentration of IB than those found in the experiments; second, the heterogeneous process is strongly dependent on the hydrophilic character of the film, which in turn changes with the composition of the copolymer system. In any case, it is clearly seen in Fig. 3 than the concentration of free IB in the solution increases with the time of treatment but much slower than that found in vivo experiments. It is necessary to take into consideration that the in vivo test was carried out with solutions of

2-(4-Is butylphenyl)pr pionic acid (Ibuprofen, IB))

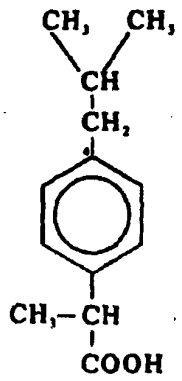

p-Aminophenol

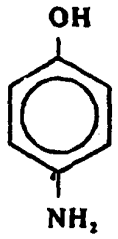

N-(4-(2-(4-Isobutylphenyl) propionyloxy) phenyl) methacrylamide (Monomer, MIA)

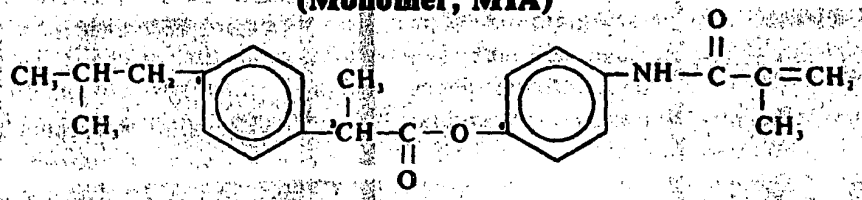

Polymer, PolyMIA (Degree of polymerization = 268)

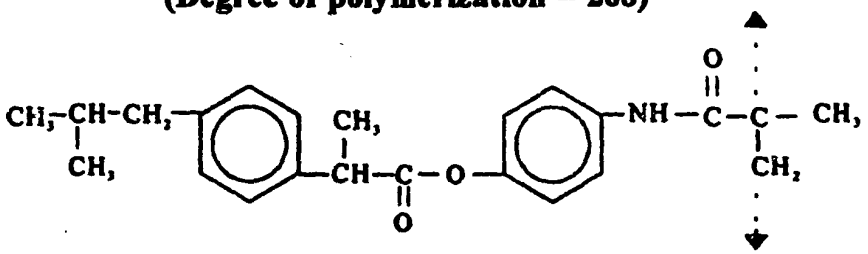

Fig. 1. Chemical structures of IB, MIA, PolyMIA and *p*-aminophenol. The *p*-Aminophenol group, which acts as a lateral spacer, could be released from methacrylic basic chain by amidases, and it is the active metabolite from another antinociceptive agent: paracetamol.

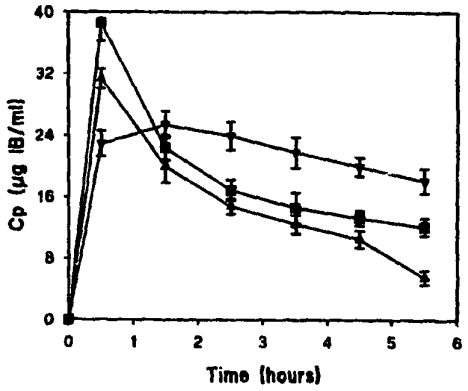

Fig. 2. Average (μg/ml) ± SEM serum Ibuprofen concentration vs. time after single-dose i.p. administration of 5.75 mg/kg of IB, monomeric and polymeric form in mice. ($n=9$ per group). IB (■), MIA (▲), PolyMIA (▼).

Table 1
Pharmacokinetics parameters calculated from each graphic normogram; IB, MIA and PolyMIA

	Ibuprofen	Polymer	Monomer
$t^{1/2}$ (h)	5.6 ± 0.25	7.5 ± 0.30	2.2 ± 0.07
$t_a^{1/2}$ (h)	0.5 ± 0.01	0.3 ± 0.02	0.1 ± 0.02
K_e (1/h)	0.12 ± 0.01	0.09 ± 0.01	0.32 ± 0.06
K_a (1/h)	1.3 ± 0.03	2.4 ± 0.05	6.7 ± 0.14
C_{max} (μgIB/ml)	41 ± 2.34	28 ± 1.88	31 ± 2.02
t_{max} (h)	0.6 ± 0.04	1.6 ± 0.08	0.6 ± 0.04
$AUC^{0\to\infty}$ (μg/ml·h)	143 ± 6.71	338 ± 5.53	92 ± 4.09
CL_t (ml/h)	1.2 ± 0.04	0.5 ± 0.02	1.9 ± 0.04
VD (ml)	10.3 ± 0.07	5.5 ± 0.06	5.7 ± 0.05
VD/kg (ml/kg)	343 ± 3.24	183 ± 2.01	191 ± 3.75

Doses are equivalent to 5.75 mg/kg of IB i.p. in one-compartment model.

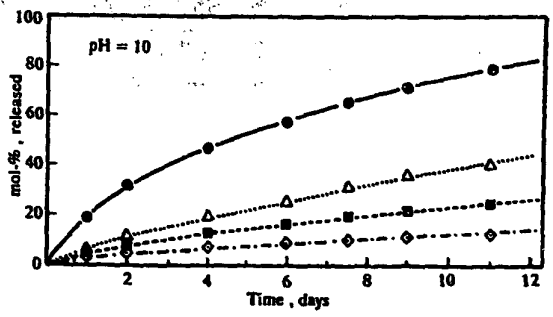

Fig. 3. Heterogeneous hydrolytical behaviour of MIA-HEMA copolymer films in buffered solution (pH = 10) at 37°C. Average composition of copolymer films: (●) 1.0 wt% MIA, (△) 5.0 wt% MIA, (■) 10.0 wt% MIA and (◇) 30.0 wt% MIA.

compounds instead of the insoluble film of copolymer used in vitro.

3.3. Acetic acid test

The i.p. administration of acetic acid 10 min after the treatment with IB, MIA and PolyMIA, significatively reduced the number of abdominal constrictions (65.2%, 71.7% and 74.9%, respectively) ($p<0.01$ vs control) (Fig. 4(a)). Nociception response was delayed 7.9 min (IB, $p<0.01$), 8.1 min (MIA, $p<0.01$) and 6.2 min (PolyMIA, $p<0.05$) (Fig. 4(b)). The IB and PolyMIA pretreatments 40 min prior to acetic acid injection gave rise to a decrease in nociception reaching 40.4% and 45.4%, respectively, with statistical significance $p<0.01$), and delayed its appearance by 2.3 min for IB ($p<0.05$) and 3.2 min for PolyMIA ($p<0.01$) vs control. When IB and PolyMIA were administered 70 min prior to the algesic agent, the number of abdominal constrictions decreased only in animals pretreated with PolyMIA (59.1%, $p<0.01$). PolyMIA showed activity (22.3%, $p<0.05$) even at 100 min of pretreatment.

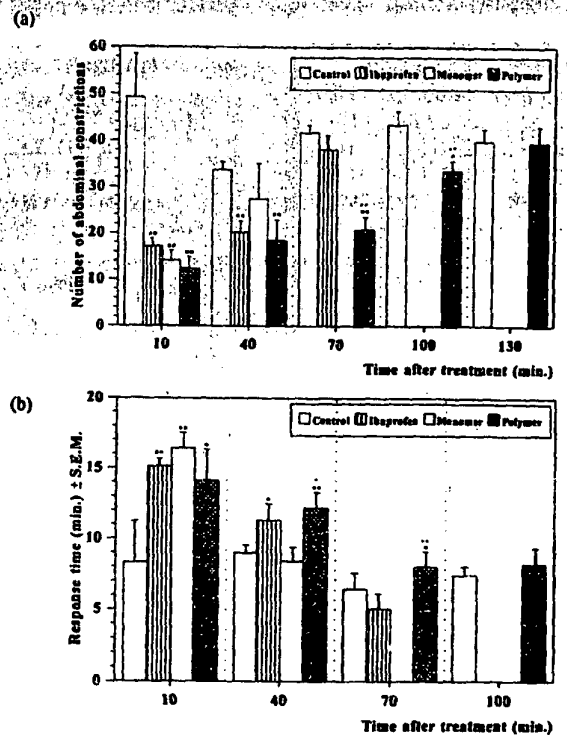

Fig. 4. (a) Average ± SEM number of abdominal constrictions and stretchings and (b) average ± SEM response time (b) in min after time pretreatment, in min. $^{*}p<0.05$, $^{**}p<0.01$ vs. control. $\#p<0.05$, $\#\#p<0.01$ vs. IB. ($n=10$ per group).

Table 2
Effects f compounds on carrageen-induced hyperalgesia

	Time ± S.E.M. (s)	Inhibition (%)	t-Student vs. Control	Newman-Keuls vs. Ibuprofen
Control	11.2 ± 1.5	–	–	–
Ibuprofen	4.8 ± 0.2	58.9	$p<0.01$	–
Monomer	3.5 ± 0.7	65.6	$p<0.01$	$p<0.05$
Polymer	3.3 ± 0.1	70.9	$p<0.01$	$p<0.01$

Time represents mean ± SEM, in seconds, difference in response time between same individual's hind paws. ($n=15$ per group)

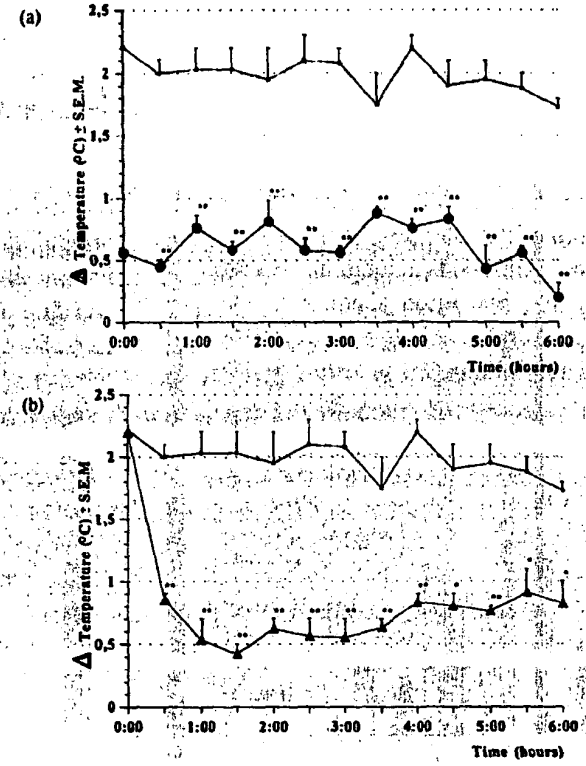

Fig. 5. (a) Positive (■) and negative (●) groups in yeast-induced hyperthermia test and (b) influence of i.p. administration of traditional IB at 5.72 mg/kg (▲) on fever. Average increase of temperature (°C) ± SEM, positive control group (■). $^{*}p<0.05$, $^{**}p<0.01$ vs. control. ($n=9$ per group).

3.4. Carrageen induced hyperalgesia in mice

In the modified Randall-Sellito assay (Table 2) and 10 min treatment, the administration of IB, MIA and PolyMIA caused a decrease in the nociception threshold when pressure was applied to the painful paws related to the internal control paws. Nociception inhibition in (%) was calculated according t the relationship:

$$\text{Inhibition}(\%) = \frac{\text{Control}_{\text{Time}} - \text{Problem}_{\text{Time}}}{\text{Control}_{\text{Time}}} \times 100$$

The values obtained amounted 59% (IB), 65.6% (MIA) and 71% (PolyMIA), $p<0.01$ vs. control). Results were comparable to those from the 10 min pretreatment in the acetic acid assay. The relative power with respect to IB (IB = 1) was: MIA = 1.1 and PolyMIA = 1.2, but a multidimensional Newman-Keuls t-test was not significant.

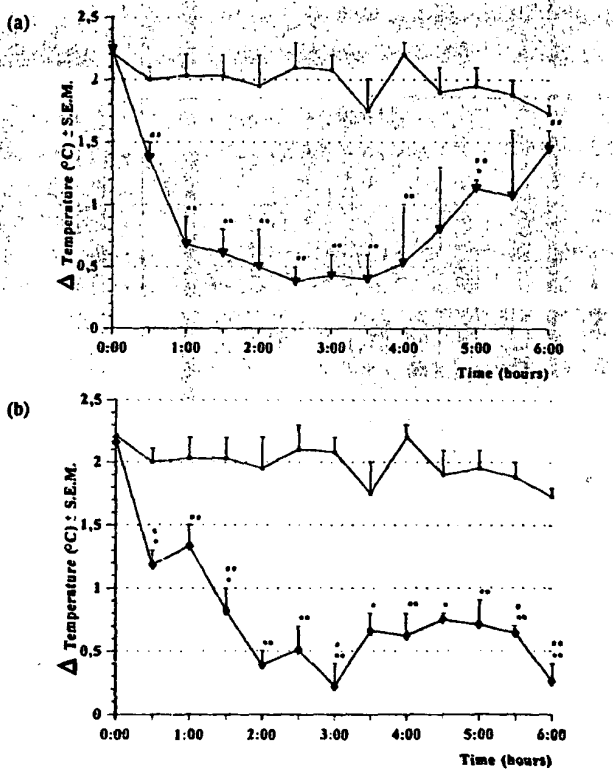

Fig. 6. Influence of monomeric (a) and polymeric forms (b) of IB on yeast-induced hyperthermia. Average increase in temperature (°C) ± SEM, after administration of MIA (▼) and PolyMIA (◆) vs. control group (■). $^{*}p<0.05$, $^{**}p<0.01$ vs. control. $\#p<0.05$, $\#\#p<0.01$ vs. IB. ($n=9$ per group).

3.5. Yeast-induced hyperthermia

Traditional, monomeric and polymeric forms showed antipyretic activity (Figs. 5 and 6): MIA and PolyMIA latency periods, respect to IB, were 1 and 2 h respectively. 60 min after starting the pharmacological treatments, fever inhibition was 73.9% (IB, $p<0.01$), 66.5% (MIA, $p<0.01$) and the anti-pyretic activity of PolyMIA was not significant vs. control (34.5%). From time $t=2$ to $t=5$, MIA and PolyMIA activities were higher than IB. At $t=5$, the activities of the compounds were 61% (IB, $p<0.01$), 42% (MIA, $p<0.05$) and 66% (PolyMIA, $p<0.01$). At $t=5$, MIA activity decreased, as did IB after the sixth hour. PolyMIA was the only compound which increased its activity beyond the sixth hour (84.8% $p<0.01$), doubling the IB activity.

4. Discussion

IB coupled to polymeric compounds seems to preserve the non-steroidal antinociceptive and anti-pyretic activities of the original molecule (IB) [15]. Thus, both monomeric and polymeric methacrylic derivates of IB, presented not only similar but higher antinociceptive activity than IB.

The appearance of analgesic activity shortly after administration of both MIA and PolyMIA seems to indicate that PolyMIA could be active as a 'macromolecular drug'; in other words, in its polymeric form even before the IB has been released. Moreover, in the antipyretic test, in which it is necessary to reach a systemic circulation of the active molecule, no short response time was obtained. This result is in good agreement with the behaviour of macromolecular systems that acts a 'macromolecular drugs'. [16,17]

In addition, the results shown in Fig. 4a and b indicate a noticeable difference between IB, which is not able to counteract the nociceptive effects of acetic acid over 40 min, and the polymeric delivery system, which displays a noticeable antinociceptive activity beyond 100 min after administration.

On the other hand, after 1 h (MIA) or 2 h (PolyMIA) of their administration, both of them show more effectiveness than the traditional IB on fever. The time-extended effect observed in antinociceptive tests, when PolyMIA was administered, is reproduced in the yeast-induced hyperthermia assay.

The pharmacokinetics of new compounds would explain this pharmacological behaviour, so t_{max} and C_{max} obtained were, respectively, 0.6 h and 41 μg/ml (IB), 1.6 h and 28 μg/ml (PolyMIA) and 0.65 h and 31 μg/ml (MIA). The polymeric form acts as a controlled delivery system of IB ($t^{1/2}$ polymer and IB are 7.5 and 5.6 h, respectively), with prolonged activity with respect to the traditional IB form.

Acknowledgements

Financial support from the Comision Interministerial de Ciencia y Tecnología, CICYT is gratefully acknowledged.

References

[1] H. Nozu, Ibuprofen: highly potent inhibitor of prostaglandin. Biophys. Acta. 529 (1978) 493.
[2] G. Thomas, M.D. Kantor, Diagnosis and Treatment: Drugs Five Years Later. Ibuprofen, Ann. Int. Med. 91 (1979) 877–882.
[3] R.F.N. Mills, S.S. Adams, E.F. Clife, W. Dickinson, J.S. Nicholson, The metabolism of ibuprofen, Xenobiotica 3 (1973) 589.
[4] A. Gallardo, J. San Roman, Synthesis and characterization of a new poly(methacrylamide) bearing side groups of biomedical interest, Polymer 34 (1993) 394–400.
[5] A. Gallardo, Polímeros acrílicos biocompatibles con actividad farmacológica, Ph.D. thesis, Facultad CC.QQ., Madrid, 1993, pp. 163–170.
[6] L.J. Davis, Drug evaluation data: Ibuprofen. Drug Intell. Clin. Pharm. 9 (1975) 501–503.
[7] J.E. Pettersen, G.A. Ulsaker, E. Jellum, Studies on the metabolism of 2,4′-isobutylphenylpropionic acid (Ibuprofen) by gas chromatography and mass spectrometry, J. Chromatogr. 145 (1978) 143–146.
[8] M.R. Wright, S. Sattari, D.R. Brocks, F. Jamali, Improved HPLC assay method for the enantiomers of Ibuprofen, J. Chromatogr. 583 (1992) 259–265.
[9] D. Romer, Pharmacological evaluation of mild antinociceptive, Br. J. Clin. Pharmacol. 10 (1980) 2475–2477.
[10] L.O. Randall, J.J. Sellito, A method for measurement of antinociceptive activity on inflamed tissue, Arch. Int. Pharmacodyn. 111 (1957) 409–419.
[11] N.S. Doherty, B.V. Robinson, The inflammatory response to carrageen, J. Pharm. Pharmacol. 27 (1975) 701–703.
[12] M. Colot, Notions Techniques de Pharmacologie Générale. Masson et Cie., Paris (1972) pp. 21–23.

[13] R.J. Tallarida, R.B. Murray, Manual of Pharmacological Calculations with Computer Programs, 2nd. ed., Springer-Verlag, New York, 1987.

[14] W.A. Ritschel, Graphic Approach to Clinical Pharmacokinetics, 2nd ed., J.R. Prous, Barcelona, 1984.

[15] P.A. Liso, M. Rebuelta, A.M. Villar, A. Gallardo, J. San Roman, V. Darias, Ibuprofen polimérico: avances en la terapia de la inflamación, Rev. Farmacol. Clin. Exp., Spec. Iss. (1993) 228.

[16] P. Sinko, J. Kohn, P lymeric drug delivery systems, an overview, in: M.A. El-Nokay, D.M. Piatt, B.A. Charpentier, (Eds.), Polymeric Delivery Systems, Properties and Applications, ACS Series 520. Washington DC, 1993 pp. 18–41.

[17] S. Dumitriu, M. Dumitriu, Polimeric drug carriers, in: S. Dumitriu (Ed.), Polymeric Biomaterials, Marcel Dekker, New York, 1994, pp. 435–689.

STIC-ILL

A61K201.84 J6

From: Schnizer, Richard
Sent: Wednesday, March 26, 2003 3:18 PM
To: STIC-ILL
Subject: 09/627,787

Please send me a copy of:

Sugiyama, Kazuo, J. Macromol. Sci. Chem. (1986), A23(10): 1155-64
102 for broad claims

Lu et al, Bioconjugate Chem. (2000) 11(1): 3-7
Poss interveneing reference

Liso et al J. Controlled Release (1995) 33(3): 429-436)
102 for broad claims?

Rihoiva et al, J. Controlled Release (1985) 2:289-310

Not sure what this is

Omelyanko et al Controlled Release (1998) 53(1-3): 25-37)
Could have fluorescine attached to HPMA

Richard Schnizer, Ph.D.
Patent Examiner
Art Unit 1635
CM1 12E17
703-306-5441
Mail Box CM1 11E12

Journal of Controlled Release, 2 (1985) 289–310
Elsevier Science Publishers B.V., Amsterdam — Printed in The Netherlands

BIOLOGICAL PROPERTIES OF TARGETABLE POLY[*N*-(2-HYDROXYPROPYL)-METHACRYLAMIDE]–ANTIBODY CONJUGATES*

Blanka Říhová
Institute of Microbiology, Czechoslovak Academy of Sciences, CS-142 20 Prague (Czechoslovakia)
and Jindřich Kopeček
Institute of Macromolecular Chemistry, Czechoslovak Academy of Sciences, CS-162 06 Prague (Czechoslovakia)

Conjugates of copolymers of N-*(2-hydroxypropyl)methacrylamide (HPMA) with anti FITC or anti θ antibodies have been synthetized. Although partial inactivation of the antibodies does take place in the course of their binding onto the polymer, the polymer–antibody conjugates retain their specific binding activity both* in vitro *and* in vivo. *It has been shown that copolymers containing a quarternary ammonium group and a bound anti θ antibody are seventy times more effective against T lymphocytes, expressing θ alloantigen, than an analogous polymer bound to nonspecific gamma globulin. The activities of daunomycin–anti θ antibody–copolymer HPMA complexes, one containing a degradable and the other a nondegradable oligopeptidic sequence in the side chain, have been compared. In the case that daunomycin was bound to the end of a sequence degradable with lysosomal enzymes, the killing of T lymphocytes* in vivo *was hundred times more efficient than of those with the conjugate containing a nondegradable sequence. In spite of the many still unresolved problems, the application of such conjugates as drug delivery systems is certainly promising.*

INTRODUCTION

Cytotoxic drugs which are used for treatment of tumors, autoimmune disease and in transplanted patients are not specific enough in the sense that not only the pathological process is affected by the therapy, but the suppressive activity also affects other normal cellular systems. These side effects are therefore factors limiting the use of the most effective cytotoxic substances.

This dilemma, that is, the search for more effective cytotoxic drugs with a weaker cytotoxic general effect, could best be solved by finding a targeting system which would ensure that the drug will reach and act only on the pathological process itself. Such treatment is called affinity therapy.

To find a generally applicable delivery system which could be used in most cases where affinity therapy is indicated, a carrier has to be used which can change its targeting specificity according to the character of the pathological process. Many different targeting moieties are under study now but it seems that so far the only system which fulfils the requirement of high specificity has been represented by the antibody–antigen reaction, where due to the high specificity of the antibody, precisely specified sites in the organism could be reached.

*Paper presented at the Second International Symposium on Recent Advances in Drug Delivery Systems, February 27, 28 and March 1, 1985, Salt Lake City, UT, U.S.A.

0168-3659/85/$03.30

Antibodies as such are usually unsuitable for the therapy as it is extremely difficult to use them in a way which would not harmfully disturb the already existing balance between the immune and the pathological process without weakening the immunity.

The problems connected with the use of antibodies for treatment of a pathological situation are reduced if antibodies are used not as a regulatory but as a targeting system. The main problem involved in the preparation of such antibody–drug complexes is the fact that the chemical treatment necessary for the attachment of the drug to the antibody often destroys the antibody activity or results in the formation of an insoluble complex [1]. As a solution to this problem the use of soluble polymers, either natural or synthetic, as a bridge between the drug and the targeting moiety was suggested.

Synthetic polymers are advantageously used as drug carriers since they could be modified in a defined way in contrast to natural macromolecules. Among them *N*-(2-hydroxypropyl)methacrylamide (HPMA) copolymers have been prepared and intensively studied [2, 3]. HPMA copolymers are based on the *N*-(2-hydroxypropyl)methacrylamide backbone with variable oligopeptide side chains terminated in reactive *p*-nitrophenyl ester groups which allow to bind by aminolysis biologically active compounds containing aliphatic NH_2 groups, e.g., cytotoxic drugs. Different oligopeptidic side chains were studied with respect to their susceptibility to cleavage by a number of proteolytic enzymes [4] such as trypsin [5], chymotrypsin [6], papain [7] and lysosomal thiol proteinases such as cathepsin B, H and L [8, 9].

In this study basic conditions have been examined which should be followed for binding antibodies to polymers in order to attain maximal binding with the least possible inactivation of the antibody. Furthermore, the activities of polymers containing degradable (Gly–Phe–Leu–Gly) and nondegradable (Gly–Gly) oligopeptide sequences in side chains have been compared in *in vivo* and *in vitro* systems. A drug bound onto a n ndegradable sequence is not released from the polymer neither during its transport in peripheral blood nor in the target tissue. On the contrary, the bond between the drug and a degradable side sequence of the polymer — though stable in plasma and serum [10] — is degraded by lysosomal enzymes [8, 9] which allows a selective release of the pharmacologically active drug in the target tissue only.

The drugs tested were daunomycin and the pharmacologically active copolymer of HPMA with methacryloyloxyethyltrimethylammonium chloride. As targeting structures two types of antibodies were examined. In a model system *in vitro*, the antibodies against a defined chemical group (hapten), e.g., fluorescein isothiocyanate (FITC) were used, while in *in vivo* experiments antibodies aimed against the surface structure of immunocompetent T lymphocytes, the so-called θ alloantigen, served as a test system. The degree of depletion of T lymphocytes reflected in a decrease of the immune response is directly related to the activity of the drug–polymer–antibody complexes.

For the preparation of polymer-modified antibodies two types of polymer precursors were used:

(a) Copolymers of *N*-(2-hydroxypropyl)-methacrylamide (1) with *p*-nitrophenyl (ONp) esters of *N*-methacryloylated oligopeptides (2 and 3)

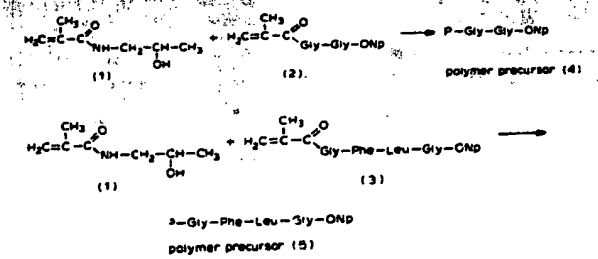

(b) Copolymer of HPMA with *N*-methacryloylglycylglycine *p*-nitrophenyl ester and methacryloyloxyethyltrimethylammonium chloride

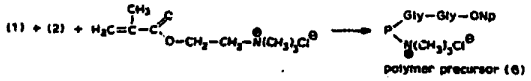

polymer precursor (6)

To polymer precursors 4 and 5 daunomycin (DNM) was bound:

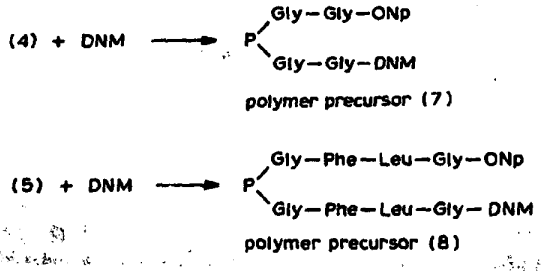

To these polymer precursors 4–8, anti FITC antibodies (9), anti θ antibodies, ATS (10), monoclonal anti θ antibodies, ATS monoclonal (11) or nonspecific rabbit γ-globulin, RGG (12) were bound:

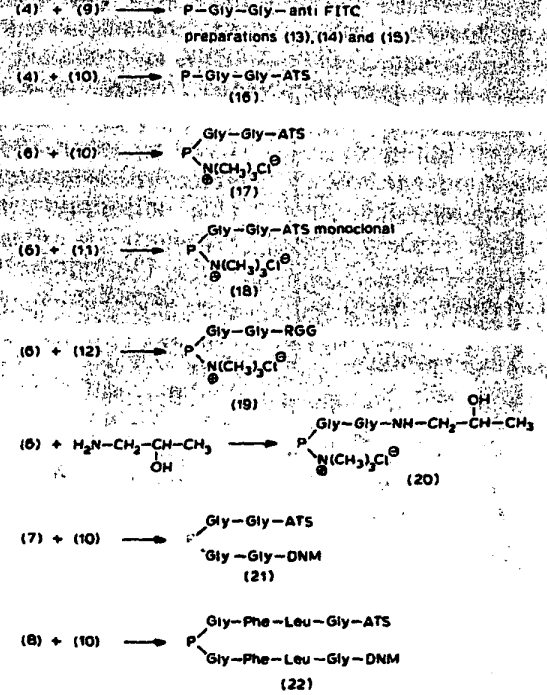

For the sake of comparison, a daunomycin–anti θ antibody conjugate was also prepared

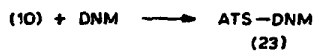

MATERIALS AND METHODS

Cytotoxic agents

Daunomycin was obtained from Rhone-Poulenc, France, Batch 87.

The HPMA copolymer containing quarternary ammonium groups (6), i.e., copolymer of HPMA, *N*-methacryloylglycylglycine *p*-nitrophenyl ester and methacryloyloxyethyltrimethylammonium chloride, was prepared as described in Ref. 11. The structure of the polymer precursor was as follows:

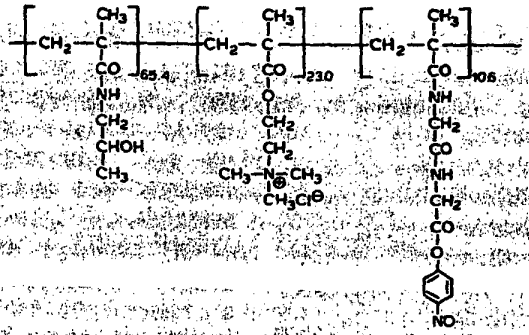

(6)

The copolymer contained 10.6 mol.% of reactive ONp groups and 23.0 mol.% of charged groups. Binding of antibodies was performed by aminolysis. Before determining the biological properties of the carrier itself, the reactive ONp groups were deactivated by aminolysis with 1-amino-2-propanol to yield polymer 20, $\bar{M}_w$ = 13,000.

Preparation of anti FITC and anti θ antibodies

Antibodies against fluorescein isothiocyanate (anti FITC) were prepared by injecting inbred mice C57L/J with 100 μg of FITC–BGG (bovine gamma globulin) antigen, three times in a two-week interval, incorporated in complete Freund's adjuvant (CFA). Seven days after the last immunization the serum was collected and the immunoglobulin frac-

tion was prepared by precipitation of sera with $(NH_4)_2SO_4$ (40% saturation).

Rabbit anti θ serum was prepared according to the method of Levey and Medawar [12]. The immunoglobulin fraction was prepared by precipitation of sera with $(NH_4)_2SO_4$ (40% saturation).

Monoclonal antibodies anti Thy-1.2 (laG4/C5) were provided by Production Unit of Institute of M lecular Genetics, Czechoslovak Academy of Sciences, Prague [13].

Rabbit gamma gl bulin (RGG) was prepared by DEAE cellulose column chromatography.

Binding of antibodies

Copolymers of *N*-(2-hydroxypropyl)-

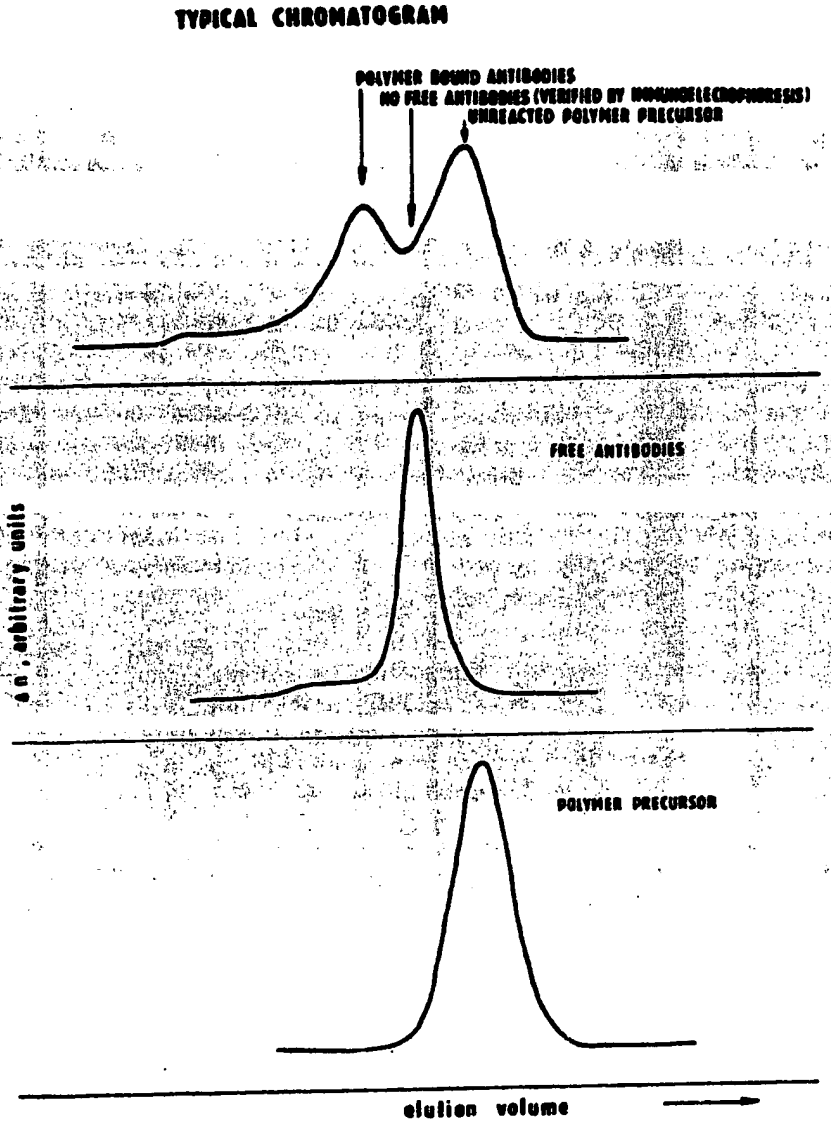

Fig. 1. Typical chromatogram of free antibodies, polymer precursor and polymer-bound antibodies. The mixture was applied to a GPC column packed with Sepharose 6B:4B (1:1) and eluted with Tris buffer (0.05 *M*, pH 8.0) containing 0.5 *M* NaCl.

methacrylamide with *p*-nitrophenyl esters of *N*-methacryloylated oligopeptides [11] were used as polymer carriers. The binding reaction was aminolysis of *p*-nitrophenyl ester (ONp) groups of synthetic polymer molecules by NH_2 groups of immunoglobulins. It was possible to find such binding conditions (ratio of ONp:NH_2 groups; concentration of macromolecular components in the reaction mixture) that after the binding reaction no free antibodies were present. The necessary condition is the presence of a high concentration of reactive ONp groups in the polymer precursor — the optimal concentration is 8—12 mol.%. The analysis of reaction products was performed by gel permeation chromatography (Fig. 1) and immunoelectrophoresis (sensitivity 10 μg/ml of free antibodies) (Fig. 2).

Other binding methods were also used. We have tried to bind antibodies to HPMA copolymers using the following reagents: *N*-cyclohexyl-*N'*-(morpholinoethyl)carbodiimide methyl-4-toluenesulfonate, Woodwards reagent K and 3-(2-pyridyldithio)propionic acid *N*-hydroxysuccinimide ester. However, in all cases the reaction mixtures contained both free and polymer-bound antibodies, even if polymers with a high concentration of COOH or NH_2 groups were used. For this reason we have performed all biological experiments described in this work on samples prepared by aminolysis. A typical procedure is described later.

Preparation of anti θ antibody (A[illegible]) polymer–drug conjugates

Two conjugates, 21 and 22, were prepared (P = polymer and DNM = daunomycin). These polymers were prepared in three steps:

(a) Preparation of polymer precursors by copolymerization of HPMA with *N*-methacryloylglycylglycine *p*-nitrophenyl ester (polymer precursor 4) or *N*-methacryloylglycylphenylalanylleucylglycine *p*-nitrophenyl ester [14] (polymer precursor 5).

(b) Binding of daunomycin by partial aminolysis to the polymer precursor (polymer precursors 7 and 8).

(c) Binding of anti θ antibody to the drug–polymer conjugate (conjugates 21 and 22). The synthetic procedure is demonstrated on the preparation of conjugate 21 in the following paragraphs.

Preparation of anti θ antibody–copolymer of HPMA–daunomycin conjugate (21)

(a) Preparation of polymer precursor 4

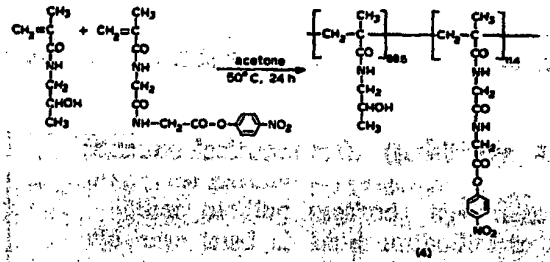

(4)

The copolymer of *N*-(2-hydroxypropyl)-methacrylamide and *N*-methacryloylglycylglycine *p*-nitrophenyl ester was prepared by radical precipitation copolymerization as described earlier [11]. The polymer precursor contained 11.4 mol.% of reactive ONp groups, $\bar{M}_w$ = 20,000.

(b) Binding of daunomycin (DNM—NH_2); synthesis of 7

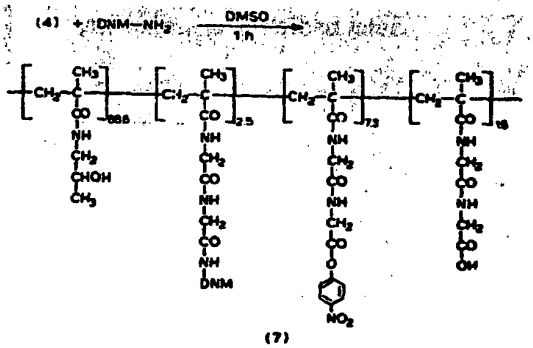

(7)

An amount of 0.388 g of polymer precursor (2.7×10^{-4} mol of ONp groups) was dissolved in 1.5 ml dimethylsulfoxide (DMSO).

To this solution, a soluti n of 0.044 g daunomycin hydrochloride (7.8×10^{-5} m l) in 0.1 ml DMSO was added. After thorough mixing an equivalent (7.8×10^{-5} mol) of triethylamine was added. The mixture was stirred 1 h in the dark. The resulting polymer was precipitated by pouring into a mixture of 400 ml acetone and 100 ml diethyl ether. The precipitate was filtered off, washed with the same mixture of solvents and dried *in vacuo*. The content of daunomycin was 2.5 mol.% (7.7 wt.%); the content of ONp groups was 7.3 mol.%.

(c) Binding of anti θ antibody; synthesis of 21

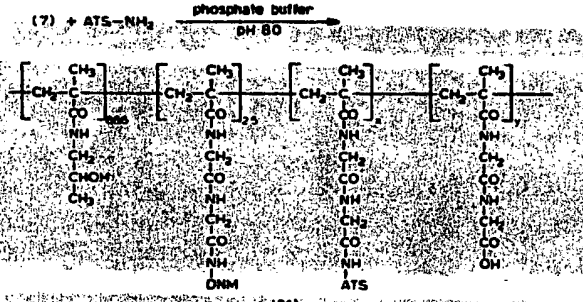

The binding of anti θ antibody was performed in Sørensen's phosphate buffer (1/15 *M* KH_2PO_4; 1/15 *M* Na_2HPO_4), pH 8, containing 0.15 *M* NaCl. The ratio of ONp groups of the polymer precursor and NH_2 groups of the antibody was 2:1 (assuming that 90 NH_2 groups are present in one IgG molecule); the weight concentration of macromolecules in the reaction mixture was 4 wt.%.

An amount of 0.122 g of polymer–daunomycin conjugate (5.2×10^{-5} mol of ONp groups) was dissolved in 1 ml of diluted hydrochloric acid (pH 3) at 5°C. To this solution, 2.27 ml of Sørensen's buffer (pH 8) was added, followed by 0.81 ml of the solution of anti θ antibody (46.2 mg) in the same buffer. After 10 min the temperature of the reaction mixture was slowly increased to 25°C. After one hour a solution of 20 μl of 1-amino-2-propanol) in 0.2 ml of Sørensen's buffer (pH 8) was added. After 10 min the reaction mixture was transferred into Visking dialysis tubing and dialyzed against phosphate buffered saline (pH 7.2).

Binding of daunomycin to anti θ antibody; synthesis of 23

The binding method was an adaption of the method of Yeh and Faulk [15]. Three milligrams of daunomycin hydrochloride were dissolved in 0.5 ml of PBS, pH 7.0. Very slowly a solution of 10 mg of rabbit ATS in 0.5 ml of PBS, pH 7.0, was added. After thorough mixing 0.5 ml of 0.25% glutaraldehyde was added. The reaction proceeded in the dark at room temperature for 2 h. After that the solution was cooled to 4°C and 0.5 ml of 1 *M* ethanolamine solution, pH 7.4, was added, and the reaction mixture was kept overnight at 4°C. The mixture was applied to a GPC column packed with Sepharose 6B and 4B (1:1) and eluted with Tris buffer (0.05 *M*, pH 8.0), containing 0.5 *M* NaCl. The fraction containing daunomycin (as detected at 480 nm) was pooled and dialyzed against PBS.

Inbred strains of mice

Immunization and transplantation reactions were performed in 10–12 weeks old females of inbred strains A/J (immunization), A/J and CBA/J (transplantation); the plaque assay on 8-week old females of strain A/J (Institute of Physiology, Czechoslovak Academy of Sciences, Prague). During experiments the mice were kept under standard conditions.

Immunization, preparation of antigens, immunoelectrophoresis, and cytotoxicity assay

Antigen (16) or ATS were injected i.p. three times in a two-week interval either as a solute or incorporated in complete Freund's adjuvant. Serum was collected 7 days after the last injection and was analyzed for antibodies.

The preparation of FITC–BGC and FITC–

HSA antigens was performed by the method of The and Feltkamp [16].

Immunoelectrophoresis was performed according to Grabar and Williams [17] (Fig. 2).

Cytotoxicity assay was performed with spleen target cells of A/J mice. The two-stage dye-exclusion microcytotoxic test was carried out as previously described [18]. A schematic

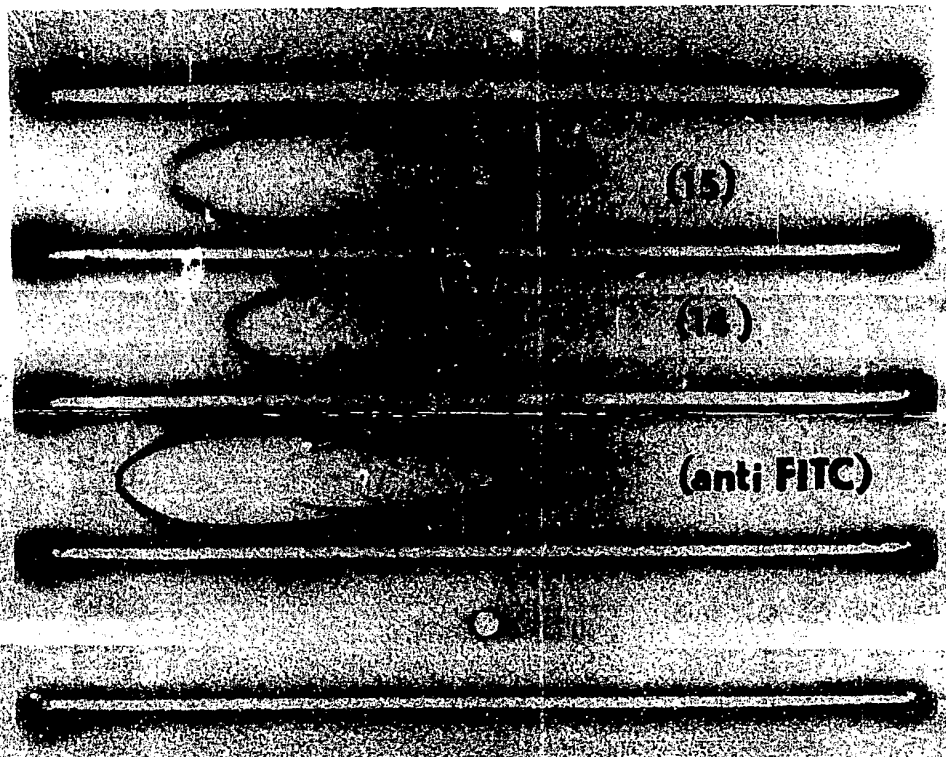

Fig. 2. Immunoelectrophoresis of the samples tested. The wells were filled with samples 14 or 15, or with anti FITC serum; troughs with anti mouse gamma globulin serum.

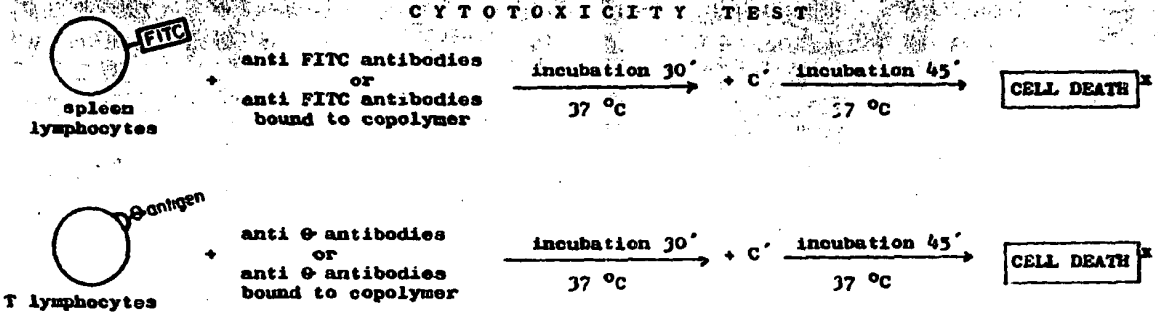

x Detected in vitro by trypan blue exclusion test.

Fig. 3. Schematic diagram of the cytotoxicity test.

diagram f the cytotoxicity test is presented in Fig. 3. The cytotoxicity index (CI) was calculated as

$$\frac{\%\text{ of dead cells with antiserum} - \%\text{ of dead cells in control}}{100 - \%\text{ of dead cells in control}} \times 100$$

Detection of antibodies by the ELISA

Detection of antibodies was performed according to Engvall [19]. Adsorption of the antigen to microplates (Koh-i-noor, Dalečín, Czechoslovakia) proceeded overnight at 4°C. Wells were filled with aliquots of 50 μl (500 μg/ml). Next day the microplates were rinsed with PBS, pH 7.2, and incubated at room temperature for 1 h in PBS containing 0.02% gelatine and 1% BSA (bovine serum albumin). After five more rinsings with PBS and PBS with 0.2% Tween 20 the wells were filled with 50 μl of different dilutions of the tested samples and the plates were kept overnight at 4°C. On the next day the microplates were rinsed and horseradish peroxidase-conjugated swine anti mouse IgG diluted 1:500 was added. The tested samples and the conjugate were diluted in PBS with 1% BSA. After 1 h of incubation at room temperature the conjugate was removed, microplates rinsed and 0.015% H_2O_2 with 1,2,-phenylenediamine (5 mg/10 ml substrate) was added. The reaction was stopped after 10 min with 20 μl 2 *M* H_2SO_4 and absorbance was determined using the ELISA reader (Minireader MR 590, Dynatech) at 492 nm.

For detection of anti FITC antibodies FITC—HSA (human serum albumin) antigen was used; for detection of antibodies against ATS the immunoglobulin fraction of ATS prepared by precipitation with $(NH_4)_2SO_4$ (40% saturation) was used.

Detection of antibodies by passive hemagglutination

Sheep red blood cells (SRBC) were sensitized with fluorescein isothiocyanate (FITC) by the method of Möller and Coutinho [20] and used as a 1% suspension in PBS with 1% fetal calf serum. Hemagglutination was carried out in the micromodification using plastic trays. The indirect hemagglutination (IgG antibodies) with anti gamma globulin serum (Coomb's test) was carried out after reading the direct titres (IgM antibodies). Supernatants were removed and replaced by swine anti mouse polyvalent gamma globulin serum diluted 1:100 in PBS. The plates with resuspended erythrocytes were stored at 4°C and again read after 3—4 h.

Plaque assay

Mice were injected i.p. on day 4, 3, 2 and 1 before antigen stimulation with different samples was tested. On day 0 they were immunized with 0.5 ml of 1×10^8 SRBC i.p. (Fig. 4). On day 5 after immunization their spleens were removed and homogenized in a tissue homogenizer in medium 199 (Sevac, Prague, Czechoslovakia). The cells were washed three times in an ice-cold medium 199 and their viability was estimated by the trypan blue exclusion test. The number of plaque-forming cells (PFC) was estimated by the method of Sterzl and Mandel [21].

Skin transplantation

Recipient mice weighing betwee 20—25 g were injected i.p. with 0.5 ml of rabbit anti mouse thymocyte serum (ATS) 2 days and 1 day prior to skin grafting and 1, 2, 3, 5 and 7 days following skin grafting. Samples 17 (ATS conjugated with polymer containing positively charged groups) and 16 (ATS conjugated to polymer without positively charged groups) were injected in the same time schedule in doses of 5 mg of ATS per mouse per injection.

Skin grafting was performed by the technique of Billingham and Medawar [22]. The skin grafts were prepared from the tail skin of A/J donor mice (about 0.5 cm^2 size) and transplanted onto the back of the CBA/J recipient mice; both donors and recipients

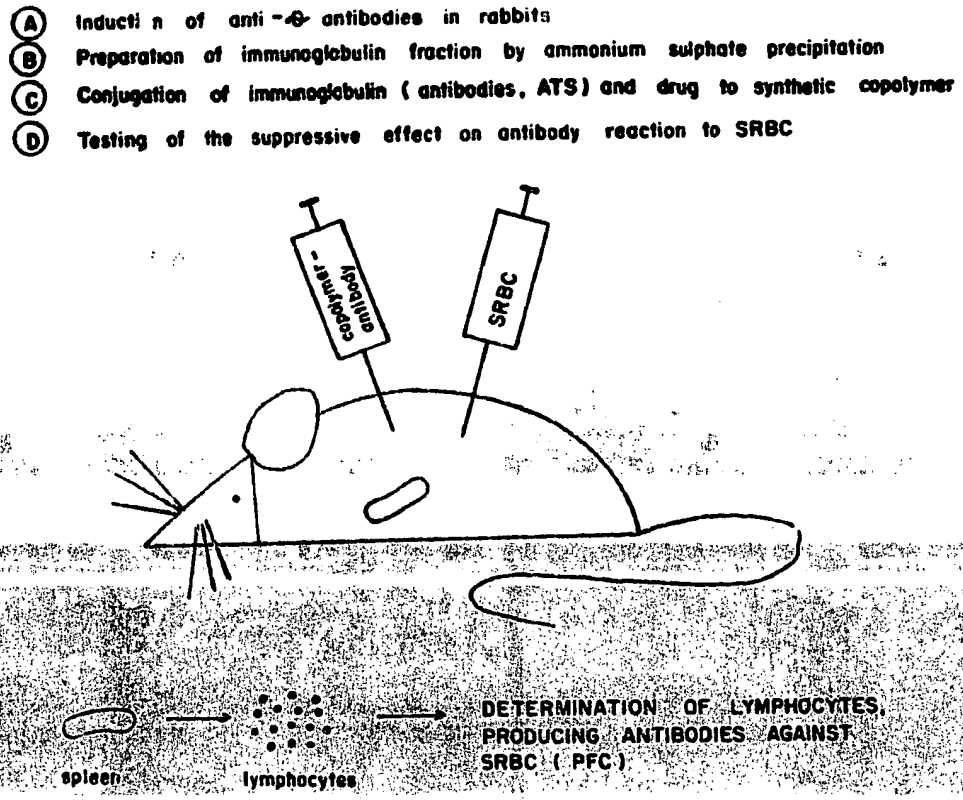

Fig. 4. Schematic diagram of the plaque assay.

were females. Plaster bandages were removed 7 days after transplantation and the grafts were scored daily during the first 3 weeks. Rejection was judged to be complete when only a trace or no surviving epithelium remained (Fig. 5).

RESULTS

The effect of methods and conditions of binding on th activity of polymer-bound antibodies

Covalent binding of antibodies to various carriers, either soluble or corpuscular, is always accompanied by their partial inactivation, the extent of which depends on the conditions of binding. In a model system of antibodies against fluorescein isothiocyanate (anti FITC) we have investigated the effect of the conditions of conjugation on the inactivation of bound antibodies. The activity and specificity of the antibodies were tested *in vitro* by ELISA, passive hemagglutination and by the cytotoxicity test. In the latter test, spleen

TABLE 1

Effect of different conditions of conjugation on the activity of the HPMA copolymer–anti FITC antibody complex: ELISA (enzyme-linked immunoassay)

Sample No.	Structure	[ONp]/[NH_2]	Antibody titer[a]
13	P–Gly–Gly–anti FITC	6:1	1: 8,000
14	P–Gly–Gly–anti FITC	3:1	1: 32,000
15[b]	P–Gly–Gly–anti FITC	1:8	1: 65,000
	anti FITC	—	1:520,000

[a]Expressed as the last sample dilution with detectable antibody activity.
[b]Nonconjugated free antibodies were detected in the sample.

lymphocytes of A/J mice with the bound FITC group were used as target cells.

The results are summarized in Tables 1, 2 and 3. It can be seen that under all conditions of binding (various ratios of the ONp and NH_2 groups) a partial inactivation of the antibodies took place, as is reflected in the decrease in the antibody titer (Tables 1 and 2) or in the lower cytotoxic index (Table 3), i.e., in a lower percentage of the killed target cells. The *in vitro* detected decrease in the antibody activity was smaller in the case of the conjugate with fewer polymer groups bound to the antibody molecule. This result is obviously related to the fact that at a low molecular weight of the polymer ($\bar{M}_w$ 20,000) the relatively small distance between the large molecules of the antibodies ($\bar{M}_w$ 160,000) leads to steric blocking of their combining sites and/or conformational changes of the antibody molecule, which both decrease their activity in classical immunochemical tests.

Only in sample 15 (which contained a considerable initial concentration of the antibodies) a high antibody activity was detected, comparable with the original antibodies. However, this activity was due to the presence of free unconjugated antibodies, as had been demonstrated by immunoelectrophoresis (Fig. 2).

TABLE 2

Effect of different conditions of conjugation on the activity of the HPMA copolymer–anti FITC antibody complex: Passive hemagglutination of FITC–SRBC

Sample No.	Structure	[ONp]/[NH_2]	Antibody titer[a]	
			IgM antibodies	IgG antibodies
13	P–Gly–Gly–anti FITC	6:1	1: 250	1: 2,000
14	P–Gly–Gly–anti FITC	3:1	1:1,000	1: 16,000
15[b]	P–Gly–Gly–anti FITC	1:8	1:1,000	1:260,000
	anti FITC	—	1:2,000	1:520,000

[a] Expressed as the last sample dilution with detectable antibody activity.
[b] Nonconjugated free antibodies were detected in the sample.

TABLE 3

Effect of different conditions of conjugation on the activity of the HPMA copolymer–anti FITC antibody complex: Cytotoxicity test

Sample No.	Structure	[ONp]/[NH_2]	Concentration (μg/ml)	Cytotoxicity index
13	P–Gly–Gly–anti FITC	6:1	800	34
			400	21
14	P–Gly–Gly–anti FITC	3:1	800	39
			400	27
15[a]	P–Gly–Gly–anti FITC	1:8	700	88
			350	62
	anti FITC	—	800	95
			400	67

[a] Nonconjugated free antibodies were detected in the sample.

In vitro cytotoxicity of HPMA copolymers containing pharmacologically active compound and targeting antibody

In this series of tests, anti θ antibodies (ATS) were used as the targeting structure. It can be seen in Table 4 that, similarly to the case of anti FITC antibodies, anti θ antibodies are also partly inactivated by their binding to HPMA copolymers, leading to a decrease of their cytotoxicity. If the binding has destroyed or blocked the binding site of the antibodies, such molecules lose their targeting capacity. If, on the other hand, the binding site is still intact and the low value of the cytotoxic test is due to the fact that the antibody molecules are oriented on the polymer so that they cannot activate the complement system (C') they may still be valuable as a targeting structure where for the effector function the bound drug is responsible. Such a polymer, containing both the targeting antibody and the drug, should be more cytotoxic than the polymer containing only the antibody or the free pharmacologically active compound.

The targeting effect of the antibodies can be seen in Table 5. The table shows a comparison between the pharmacologically active HPMA copolymer [23] alone (20), the pharmacologically active HPMA copolymer conjugated to immunoglobulins isolated from a rabbit anti θ serum (17) or to monoclonal anti Thy-1.2 antibody (18) or to nonspecific rabbit gamma globulin (19). As a control of the pharmacological activity of copolymer 20, copolymer 16 with a bound anti θ antibody but without positively charged groups was used. It can be seen that the cytotoxicity of copolymers 17 or 18 containing both ATS and positively charged groups greatly exceeds that of the nontoxic HPMA copolymer (16) bound to antibody only or that of the sample in which instead of specific antibodies nonspecific gamma globulin was used (19). Copolymer 17, which carries ATS antibodies as the targeting structure, is 2.5 times more active in a system without complement and 70 times more active in a system with complement against T lymphocytes than a similar copolymer containing normal rabbit gamma globulin instead of specific antibodies (19). The toxicity of the copolymer with positively charged groups decreases after binding to immunoglobulin molecules, obviously due to a limited interaction with the cell surface.

The conjugate containing monoclonal antibodies (18) possesses a lower cytotoxicity than that containing conventional antibodies. This result can be attributed to the fact that the conjugate contains a lower quantity of the polymer with positively charged groups, and also that because of their monospecificity monoclonal antibodies react with a smaller percentage of cells than conventional antibodies.

The effect of degradability of side chain oligopeptidic sequences of the HPMA copolymer on the cytotoxicity of the sample is demonstrated in Table 6. In the table the activities of daunomycin bound to the copolymer containing sequences degradable (22) or nondegradable (21) by lysosomal enzymes are compared. The toxicity of the sample with degradable sequences considerably exceeds that of the sample with nondegradable sequences. The copolymer containing sequences Gly—Phe—Leu—Gly—DNM still possesses some cytotoxicity even at a concentration of 3 μg of antibodies and 0.4 μg of daunomycin, while that containing nondegradable sequences is toxic only at a concentration of 1250 μg of antibodies and 250 μg of daunomycin and higher. A

TABLE 4

Cytotoxicity of anti θ antibody bound to HPMA copolymer

Sample No.	Structure	Concentration of ATS (μg/ml)	Cytotoxicity index
	ATS	1,500	94
		150	50
16	P—Gly—Gly—ATS	1,600	46
		320	36
		160	21

TABLE 5

Cytotoxicity of HPMA copolymers containing positively charged groups and/or anti θ antibody

Sample No.	Structure	Concentration (μg/ml) copolymer	Concentration (μg/ml) ATS (RGG)	Cytotoxicity index with C′	Cytotoxicity index without C′
16	P—Gly—Gly—ATS	5,000	2,500	61	5
		2,500	1,250	54	3
		1,000	500	46	3
		500	250	39	3
		100	50	21	3
		50	25	13	3
		25	5	3	3
17	P < Gly—Gly—ATS; $N(CH_3)_2Cl^-$	7,500	4,500	96	43
		3,750	2,250	79	33
		1,500	900	67	29
		750	450	50	17
		150	90	28	5
		75	45	20	7
		25	15	15	5
18	P < Gly—Gly—ATS (monoclonal); $N(CH_3)_2Cl^-$	3,750	2,250	73	32
		1,875	1,125	65	27
		750	450	57	20
		375	225	46	10
		75	45	34	4
		37	22	22	2
		10	6	17	5
19	P < Gly—Gly—RGG; $N(CH_3)_2Cl^-$	3,600	2,250	22	28
		1,800	1,125	11	14
		720	450	12	15
		360	225	8	5
		72	45	6	8
		36	22	7	7
20	P < Gly—Gly—aminopropanol; $N(CH_3)_2Cl^-$	5,000	—	—	70
		2,500	—	—	68
		1,000	—	—	60
		500	—	—	45
		250	—	—	40
		200	—	—	32
		150	—	—	20
		100	—	—	0
		50	—	—	0
		25	—	—	0

comparison with the results in Table 3, where the toxicity of free daunomycin is presented, reveals that daunomycin in the copolymer with nondegradable sequences is obviously inactive and that for the toxicity of the sample the antibody activity is responsible. It can be also seen, by comparing the cytotoxicity of the copolymer with degradable sequences containing daunomycin and that of free daunomycin, that to produce the same cytotoxic effect the cell culture must contain twice the amount of free daunomycin compared with the polymer carrying the targeting structure.

TABLE 6

Cytotoxicity of HPMA cop lymers containing daunomycin and/or anti θ antibody

Sample No.	Structure	Concentration (μg/ml) polymer	ATS	DNM	Cytotoxicity index with C'	without C'
21	P < Gly–Gly–DNM; Gly–Gly–ATS	6,500	2,500	500	43	0
		3,250	1,250	250	40	0
		1,300	500	100	7	0
		650	250	50	5	0
		130	50	10	6	0
		65	25	5	2	0
22	P < Gly–Phe–Leu–Gly–DNM; Gly–Phe–Leu–Gly–ATS	4,800	2,500	355	99	99
		2,400	1,250	177	99	72
		960	500	71	99	43
		480	250	35.5	99	30
		96	50	7.1	70	11
		48	25	3.5	56	0
		24	12	1.8	39	0
		12	6	0.9	30	0
		6	3	0.4	23	0

In vivo cytotoxicity of HPMA copolymers containing pharmacologically active compound and targeting antibody

Effect on the antibody reaction determined by the number of plaque-forming cells (PFC) in the spleen of immunized mice

After immunization with sheep red blood cells in the spleen of the immunized organism lymphatic cells can be detected which release antibodies against this antigen. These cells can be enumerated by a technique which detects the individual anti SRBC antibody producing cells as plaque forming cells (PFC). By the injection of anti θ antibodies (ATS) into an organism, those immunocompetent cells are eliminated which carry the corresponding surface antigen (θ alloantigen). The decrease in the number of θ positive lymphocytes impairs the immune capacity f the organism and reduces the number of PFC. In Table 7 the effects of the activity of the whole ATS, its immunoglobulin fraction and of ATS bound to a copolymer with side sequence Gly–Gly are compared. Similarly to the tests *in vitro*, the covalent binding f antibodies to the copolymer brings about their partial inactivation so that the copolymer with the same amount of ATS is less active in suppressing the immune reaction than whole ATS or its immunoglobulin fraction.

In Table 8, we compare the effect of degradable (22) and nondegradable (21) sequences in the daunomycin containing copolymers on the antibody reaction *in vivo*. For comparison three more groups of mice were included. One group was injected with the pharmacologically active copolymer conjugated to anti θ monoclonal antibody (18), another group received the ATS coupled with the pharmacologically inert HPMA copolymer (16) and the third group was injected with ATS alone. Mice which received a corresponding quantity of normal rabbit serum served as controls. It was found that all samples tested were active and had affected cellular cooperation of the immune system, as reflected in the reduced number of PFC. The copolymer containing ATS and daunomycin on degradable sequences was the most active, being approximately four times more active than the whole ATS serum. On the contrary, daunomycin bound to the copolymer with nondegradable

TABLE 7

The suppressive effect of anti θ antibody bound to HPMA copolymer on antibody response to SRBC

Sample No.	Structure	Total dose of immunoglobulin per mouse (mg)	Application	Number of injections	IgM PFC/10^6 spleen cells
	ATS[a]	12.0	i.p.	4	740
	ATS	12.0	i.p.	4	1,700
16	P–Gly–Gly–ATS	12.0	i.p.	4	29,000
	Control	12.0	i.p.	4	41,000
16	P–Gly–Gly–ATS	6.8	i.p.	5	3,600
		6.8	i.v.	5	4,000
	Control	6.8	i.p.	5	18,000
		6.8	i.v.	5	22,000
16	P–Gly–Gly–ATS	3.2	i.p.	5	43,000
		3.2	i.v.	5	25,000
	Control	3.2	i.p.	5	44,000
		3.2	i.v.	5	44,000

[a] Anti θ serum without fractionation.

TABLE 8

The suppressive effect of HPMA copolymers containing anti θ antibody and daunomycin or positively charged groups on antibody response to SRBC

Sample No.	Structure	Total dose of immunoglobulin per mouse (mg)	DNM	IgM PFC/10^6 spleen cells
	ATS	12.0	–	800
16	P–Gly–Gly–ATS	12.0	–	17,300
18	P < Gly–Gly–ATS (monoclonal) / $N(CH_3)_2Cl$	2.5	–	17,700
21	P < Gly–Gly–DNM / Gly–Gly–ATS	12.0	2.5	16,000
22	P < Gly–Phe–Leu–Gly–DNM / Gly–Phe–Leu–Gly–ATS	3.0	0.4	1,100
	Control	–	–	51,600

sequences appeared to be inactive, similarly to the case *in vitro*, because suppression of the immune response was the same as with the copolymer carrying only ATS antibodies. The polymer with monoclonal antibodies in which instead of daunomycin the toxicity was carried out by the copolymer with positively charged groups, was 16 times less active.

The effect of HPMA copolymers containing positively charged groups and anti θ antibody on the survival of skin allografts in mice

In order to compare the effects of the

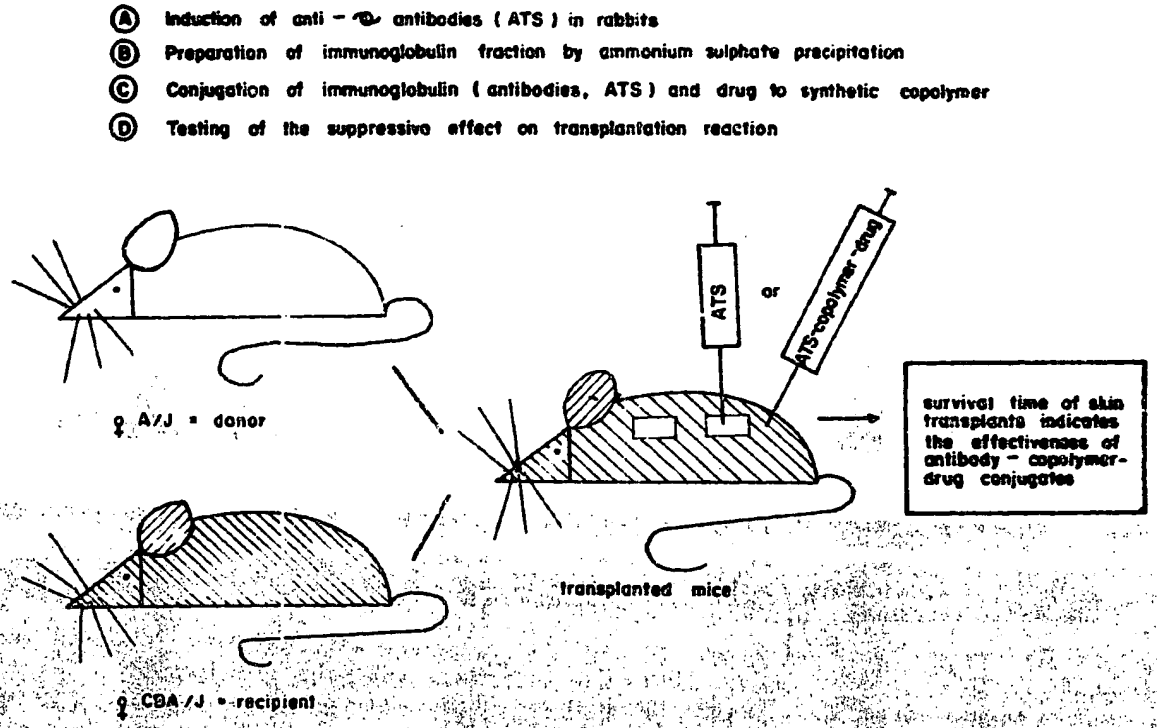

Fig. 5. Schematic diagram of skin transplantation.

pharmacologically active HPMA copolymer alone (20), of the same copolymer with ATS antibodies attached (17) and of the pharmacologically inactive copolymer bound to ATS antibodies (16), we used also the transplantation reaction as the second *in vivo* model (Fig. 5). In the test, skin allografts were transplanted to mice differing in the strong histocompatibility locus (donors: an inbred strain A/J, histocompatibility locus H-2^a; recipients: an inbred strain CBA/J, histocompatibility locus H-2^k). All animals were females of the same age. Figure 6 shows that all mice of the control group rejected the skin grafts within 8 days after transplantation, similarly to mice which were treated only with the copolymer 20, administered in the total dose of 58 mg. On the contrary, the group of mice which received ATS did not show any signs of rejection until the 19th day after the transplantation, when the experiment was terminated. Compared with this finding, the group which received ATS on the copolymer with the Gly—Gly side sequence (16) rejected the

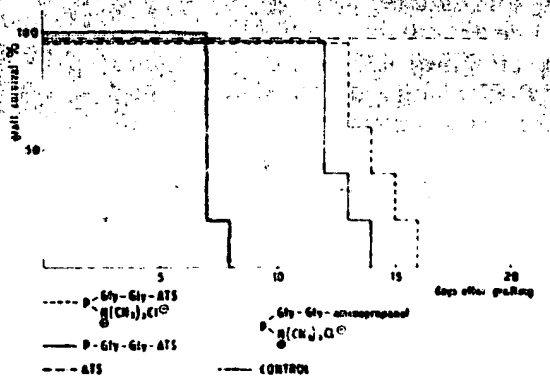

Fig. 6. The effect of HPMA copolymers containing positively charged groups and anti θ antibody on the survival of skin allografts in mice.

grafts within 14 days after the transplantati n and the group in which ATS was bound to the copolymer with positively charged groups (17) rejected grafts within 16 days. None of the administered polymer conjugates was more active than the whole anti θ serum. It should be pointed out, however, that the difference in the rejection of the skin grafts between the controls and test groups seems to indicate that also *in vivo* the antibodies bound to the copolymer may exert their targeting effect in transplantation reaction, and that the activity of the samples should be strengthened by choosing more effective drugs for binding.

Cytotoxicity of DNM attached directly to the antibody molecule without a polymer spacer

We have compared the activity of daunomycin bound via a polymer spacer with that of daun mycin bound directly to anti θ antibodies. Although the binding conditions were not the same, since daunomycin was bound to the antibody molecule by glutaraldehyde and not by aminolysis as previously used for binding daunomycin to the polymer, a comparison of the effect of the two samples underlines the advantages of using the polymer spacer. Direct binding of daunomycin on the antibody results in a poorly soluble complex in which both the antibodies and daunomycin lose their activity (Table 9). To obtain the same effect, i.e., the same cytotoxic index, the daunomycin–antibody complex must contain an almost ten times higher concentration of daunomycin and a 200 times higher concentration of ATS than the complex daunomycin–polymer–ATS (cf. Tables 6 and 9).

TABLE 9

Cytotoxicity of daunomycin–antibody conjugate

Sample No.	Structure	Concentration (μg/ml)		Cytotoxicity index
		ATS	daunomycin	
	ATS	2,500	—	100
		1,250	—	99
		500	—	66
		250	—	60
		100	—	42
		50	—	29
		25	—	15
	DNM	—	17.5	99
		—	8.8	77
		—	3.5	39
		—	1.8	28
		—	0.9	31
		—	0.4	18
		—	0.2	17
23	ATS–DNM	2,500	17.5	40
		1,250	8.8	35
		500	3.5	32
		250	1.8	29
		100	0.9	15
		50	0.4	8
		25	0.2	3

TABLE 10

Immunogenicity of anti θ antibodies (ATS) bound to HPMA copolymer: ELISA (enzyme-linked immunoassay)

Sample No.	Structure	Injected dose of ATS (μg)	Antigen form	Antibody titer against ATS
16	P—Gly—Gly—ATS	100	soluble	1: 8,000
		100	in CFA[a]	1: 32,000
		10	soluble	1: 4,000
		10	in CFA	1: 16,000
		1	soluble	1: 2,000
		1	in CFA	1: 8,000
	ATS	100	soluble	1: 32,000
		100	in CFA	1:130,000
		10	soluble	1: 8,000
		10	in CFA	1: 16,000
		1	soluble	1: 500
		1	in CFA	1: 4,000

[a] Complete Freund's adjuvant.

Immunogenicity of anti θ antibodies bound to the HPMA copolymer

For the use of HPMA copolymers in medicine it is essential to test their immunogenicity, as to be sure that their administration does not lead to allergic reactions. The experiences concerning the immunogenicity of HPMA copolymers alone, which have been already studied (cf. Discussion) were extended by experiments for testing the effect of antibodies bound to these copolymers on the immunogenicity of the complex. The antibody response was tested in inbred mice of strain A/J immunized with a soluble sample, i.e. with a form which can potentially be employed in therapy or with a sample incorporated in complete Freund's adjuvant (CFA). The results presented in Table 10 document that the immunogenicity of ATS free or bound to the HPMA copolymer (16) is similar. Very small differences were observed in response to high (100 μg) and to low (1 μg) doses. In the range of high doses ATS alone induces a higher response than ATS bound to the copolymer (16). This result is obviously due to the fact that after binding to the polymer some epitopes (antigen determinants) become inaccessible to immunocompetent cells, and do not lead to their stimulation. The opposite is true when a very low amount of antigen is administered: in this case ATS on the polymer appears to be more immunogenic than ATS alone.

DISCUSSION

The effectiveness of affinity therapy is predominantly a question of the specificity and of the effectiveness of the "targeting" moiety of the drug complex [24]. In this respect the most promising are antibodies which are able to distinguish specific antigen determinants (epitopes) of the target tissue and to react exclusively with them. However, their wide application, especially in antitumor therapy, is still limited by the fact that in many tumors the expression of a specific antigen has not yet been described.

Even while the idea of affinity therapy is essentially a simple one, it nevertheless calls for caution and detailed knowledge of

many technical problems. We therefore have chosen a well defined model which allows us to study the activity of the antibody—polymer—drug complex not only *in vitro*, but mainly *in vivo*, sensitively and, above all, quantitatively. The anti θ antibodies used as the targeting structures react *in vivo* with immunocompetent cells carrying θ alloantigen (T lymphocytes). This leads to activation of the complement system and consequently to the death of the cells expressing θ alloantigen. As a result of T lymphocyte elimination the antibody reaction decreases. The intensity of the antibody reaction can be tested either by the serum antibody level or by estimation of antibody releasing (so-called plaque forming) cell number. In addition to theoretical advantages we believe that such model can be applied in medical practice. In the post-transplantation period patients are treated with cytostatic immunosuppressive drugs, the toxic action of which on tissues other than lymphatic is as undesirable as are the toxic side effects in the treatment of tumors.

One of the problems of affinity therapy is the fact that due to binding both the antibody and the drug often lose some part of their original activity. We have therefore tested various procedures and conditions of binding of antibodies to soluble HPMA copolymers which would guarantee that after binding no free antibodies will remain in the system, and at the same time their inactivation will be as small as possible.

It was found that by the methods we have used covalent binding of antibodies to the polymer carrier always leads to their partial inactivation. However, inactivation demonstrated by serological tests need not always mean that the antibody binding site is affected. For all classical serological tests not only the antibody binding site (Fab fragment of the immunoglobulin molecule) is necessary but also the effector part of the antibody molecule (Fc fragment) has to be intact and able to activate complement (C') for cytotoxicity, bind the secondary antibody (RIA, ELISA) or be capable of such steric orientation which makes agglutination possible. In the case of Fc fragment blocking the serological reaction is characterized as negative, although binding between the antibody combining site and the antigen determinant (epitope) has taken place. For the purposes of affinity therapy the effector function is taken over mainly by the bound drug. This is why apparent inactivation of antibody molecules (if not too strong) demonstrated by serological tests does not always mean that the complex is unsuitable for affinity therapy.

We have compared the *in vitro* targetable activity of ATS conjugated to the two different copolymers, copolymer 16, which is nontoxic to cells, or copolymer 17, which along with the Gly—Gly sequences in side chains also contains quarternary ammonium groups and possesses a pronounced surface activity against spleen lymphocytes. Although the toxicity of the polymer containing quarternary ammonium groups (17) has been decreased by more than a half due to binding with the antibodies, the targeting ATS antibodies have raised toxicity of the complex 70 times compared to the complex with nonspecific gamma globulin.

The high cytotoxicity of the conjugate (17) carrying positively charged (and hence pharmacologically active) groups and the specific antibody confirms the assumption that the antibodies which in serological tests appear as inactive may still preserve their targeting activity.

If the compound bound to the polymer itself acts upon the cell surface (is surface-active) or if the copolymer itself exerts such an effect, the problem of degradability of side chains is not the essential one. On the other hand, it assumes greater importance if the drug to be bound acts only intracellularly. Such a drug must penetrate into the cells by endocytosis and must be released there from the polymer by lysosomal enzymes to become active [2, 3].

The toxicity of polymers containing

daunomycin bound at the ends f ligopeptide sequences which are either degradable (22) or nondegradable (21) by lysosomal enzymes were compared *in vitro* and *in vivo*. *In vitro*, with 12 μg ATS and 1.6 μg daunomycin on the polymer 22 a comparable cytotoxic effect was observed as with 1250 μg ATS and 250 μg daunomycin on the polymer 21. Such a considerable difference suggests that daunomycin on the polymer with nondegradable sequences is inactive and the cytotoxicity is ensured only by means of bound antibodies. It is also interesting that the conjugate tested is more active in the presence of complement (C′) although the increase in cytotoxicity cannot be explained merely by the effect of bound antibodies. This result suggests that the C′ enhances (via some mechanism as yet unknown) the toxic effect of the daunomycin–polymer–antibody complex.

Similar results as *in vitro* were also obtained *in vivo* in experiments in which the effect on the immune response against SRBC was tested. Daunomycin and ATS bound to a polymer with degradable sequences (22) are four times more active than ATS alone, and sixty times more active than DNM and ATS bound to a polymer with nondegradable sequences (21).

The results reported show the importance of the drug being bound to a sequence from which it could be released in a controlable way at the site of the assumed effect. A random and insufficiently defined bond between the drug and the carrier may easily lead to inactivity of the whole complex. Another important finding which ensues from the *in vivo* experiments is that also under the conditions of an intact organism the antibodies (and the drug) bound to soluble HPMA copolymers may reach the target tissue and act upon it. A similar finding, i.e., the accessibility of target tissues under *in vivo* conditions, was shown by transplantation experiments. In the latter, however, we did not succeed in achieving the same result as in experiments with the inhibition of antibody f rmation. While th administration of wh le ATS resulted in skin graft survival throughout the period under observation (19 days), ATS bound to a pharmacologically active copolymer (17) put the rejection of the skin grafts off only by 6 days compared with controls. This result can be best explained by the low toxicity of the copolymer used. So the results of this experiment should be taken as an example how the choice of a pharmacologically active compound is essential for a successful application *in vivo*. In addition to a suitable drug, the quality of the antiserum used is also of a great importance. Transplantation reaction is a complex immunological process in which a number of cell subpopulations differing in their surface structures take part. For this reason, unlike in tumor diseases, where the monospecificity of the antibodies selected for affinity therapy is the main clue to a successful intervention into the course of the disease, antibodies used to control transplantation reactions should possess a wide range of specificities aimed against all cell components which are involved. Results obtained so far with such models are contradictory. While Beatty et al. [25] and Hilgert et al. [26] did not prove prolongation of the survival of skin grafts after the administration of antilymphocytic serum with the bound drug, Papachristou et al. [27] reported an extended survival of both skin and graft transplants in rats after the administration of chlorambucil bound to antilymphocytic globulin. In all those experiments drugs were bound directly to the antibody without a polymer spacer. At present methods of direct conjugation of antibodies with different drugs are studied in many laboratories and aimed chiefly at antitumor therapy [28–35].

We have also compared the activity of daunomycin bound directly to the antibody (23) with that of daunomycin bound to the antibody through a polymer spacer (22). Even bearing in mind that two different chemical approaches were used in the binding (glutaraldehyde in binding the drug directly

to the antibody; amin lysis in the binding to the polymer spacer), differences between the two preparations are still considerable. To achieve the same effect, i.e., the same cytotoxic index, the complex of daunomycin and antibody must contain a ten times higher concentration of daunomycin and a two hundred times higher concentration of antibodies than the complex in which a polymer spacer has been used.

To consider the soluble HPMA copolymers in connection with their possible application in human medicine, it is absolutely necessary to have sufficient information about the defense reaction which their administration might induce in the recipient. For this reason, great attention has been devoted to the immunogenicity of these compounds. Although a number of factors, such as molecular weight, composition of oligopeptidic sequences, effect of different structures of the bound drug, antigen doses and genetic dispositions of the immunized organism have been studied in great detail, it has not been proved that the copolymers in question give rise to a significant immune response [36—38].

Experiments involving binding of complement showed that these polymers activate complement only at very high concentrations (20 mg/ml) which for therapeutical use do not come into consideration. Lower concentrations (2 mg and 0.2 mg/ml) did not affect the activity of the complement system [39].

It may be said, in conclusion, that the results reported above justify the concept of using soluble copolymers of HPMA as a transport molecule suitable for affinity therapy. It has been demonstrated that targeting antibodies are highly active compared with nonspecific gamma globulin and that it is absolutely essential that the drug should be bound to a defined oligopeptidic sequence which would guarantee a controlled release in the target tissue [14]. It was found that the synthesized drug—polymer—antibody complexes are active not only *in vitro* but also *in vivo*. Since the conjugates investigated in this study not only allow us to reduce the doses of cytostatics, but also to restrict their effects to a certain tissue only, their application as drug delivery systems is promising, in spite of many problems as yet unsolved.

CONCLUSIONS

1. By binding to soluble copolymers of *N*-(2-hydroxypropyl)methacrylamide the bound antibodies lose approx. 40% of their original activity.

2. The pharmacologically active copolymer of HPMA (with positively charged side chains) conjugated to anti-θ antibody is seventy times more active against T lymphocytes carrying θ alloantigen than a similar copolymer carrying nonspecific gamma globulin.

3. The drug (daunomycin) bound to the copolymer of HPMA through a degradable sequence (Gly—Phe—Leu—Gly) and at the same time carrying anti-θ antibodies kills T lymphocytes a hundred times more effectively than the copolymer with the drug bound to a nondegradable sequence (Gly—Gly).

4. The tested drug—polymer—antibody complexes are active not only *in vitro* but also *in vivo*.

ACKNOWLEDGEMENTS

The authors are indebted to Dr. P. Rejmanová, Mr. J. Strohalm and Mrs. D. Plocová for valuable discussions and synthesis of some of the polymer precursors, to Dr. P. Rossmann for morphological studies, to Mrs. H. Semorádová for excellent technical assistance, and to Rhone-Poulenc, France for the generous gift of daunomycin hydrochloride.

REFERENCES

1 R. Arnon and M. Sela, Targeted chemotherapy:

Drugs conjugated to antitumor antibodies, Cancer Surv., 1 (1982) 429—446.
2 J. Kopeček, Synthesis of tailor-made soluble polymeric drug carriers, in: J.M. Anderson and S.W. Kim (Eds.), Recent Advances in Drug Delivery Systems, Plenum Press, New York, NY, 1984, pp. 41—62.
3 R. Duncan and J. Kopeček, Soluble synthetic polymers as potential drug carriers, Adv. Polym. Sci., 57 (1984) 51—101.
4 J. Kopeček, Biodegradation of polymers for biomedical use, in: H. Benoit and P. Rempp (Eds.), IUPAC Macromolecules, Pergamon Press, Oxford, 1982, pp. 305—320.
5 K. Ulbrich, J. Strohalm and J. Kopeček, Polymers containing enzymatically degradable bonds. III. Poly[*N*-(2-hydroxypropyl)metacrylamide] chains connected by oligopeptide sequences cleavable by trypsin, Makromol. Chem., 182 (1981) 1917—1928.
6 J. Kopeček, P. Rejmanová and V. Chytrý, Polymers containing enzymatically degradable bonds. I. Chymotrypsin catalyzed hydrolysis of *p*-nitroanilides of phenylalanine and tyrosine attached to side-chains of copolymers of *N*-(2-hydroxypropyl)methacrylamide, Makromol. Chem., 182 (1981) 799—809.
7 K. Ulbrich, E.I. Zacharieva, B. Obereigner and J. Kopeček, Polymers containing enzymatically degradable bonds. V. Hydrophilic polymers degradable by papain, Biomaterials, 1 (1980) 199—204.
8 R. Duncan, H.C. Cable, J.B. Lloyd, P. Rejmanová and J. Kopeček, Degradation of side-chains of *N*-(2-hydroxypropyl)methacrylamide copolymers by lysosomal thiol-proteinases, Biosci. Rep., 2 (1982) 1041—1046.
9 P. Rejmanová, J. Pohl, M. Baudyš, V. Kostka and J. Kopeček, Polymers containing enzymatically degradable bonds. 8. Degradation of oligopeptide sequences in *N*-(2-hydroxypropyl)methacrylamide copolymers by bovine spleen cathepsin B, Makromol. Chem., 184 (1983) 2009—2020.
10 P. Rejmanová, J. Kopeček, R. Duncan and J.B. Lloyd, Stability in rat plasma and serum of lysosomally degradable oligopeptide sequences in *N*-(2-hydroxypropyl)methacrylamide copolymers, Biomaterials, 6 (1985) 45—48.
11 P. Rejmanová, J. Labský and J. Kopeček, Aminolyses of monomeric and polymeric *p*-nitrophenyl esters of methacryloylated amino acids, Makromol. Chem., 178 (1977) 2159—2168.
12 R.H. Levey and P.B. Medawar, Some experiments on the action of antilymphoid antisera, Ann. N.Y. Acad. Sci., 129 (1966) 164—177.
13 P. Dráber, J. Zikán and M. Vojtíšková, Establishment and characterization of permanent murin hybridomas secreting monoclonal anti-Thy-1 antibodies, J. Immunogenet., 7 (1980) 455—474.
14 J. Kopeček, P. Rejmanová, J. Strohalm, R. Duncan and J.B. Lloyd, unpublished results (Czechoslovak Patent Appl. 97—85, Jan. 4, 1985).
15 C.-J.G. Yeh and W.P. Faulk, Killing of human tumor cells in culture with adriamycin conjugates of human transferin, Clin. Immunol. Immunopathol., 32 (1984) 1—11.
16 T.H. The and T.E.W. Feltkamp, Conjugation of fluorescein isothiocyanate to antibodies. I. Experiments on the conditions of conjugation, Immunology, 18 (1970) 865—873.
17 P. Grabar and C.A. Williams, Jr., Méthode permettant l'étude conjugueé des propriétés électrophorétiques et immunochimiques d'un mélange de protéines. Application au sérum sanguin, Biochim. Biophys. Acta, 10 (1953) 193—194.
18 C.S. David, C.D. Shreffler and J.A. Frelinger, New lymphocyte antigen system (Lna) controlled by the Ir region of the mouse H-2 complex, Proc. Natl. Acad. Sci. U.S.A. 70 (1973) 2509—2514.
19 E. Engvall, Enzyme immunoassay ELISA and EMIT, Methode Enzymol., 70 (1980) 419—439.
20 G. Möller and A. Coutinho, Role of C'3 and Fc receptors in B lymphocyte activation, J. Exp. Med., 141 (1975) 647—663.
21 J. Sterzl and L. Mandel, Estimation of the inductive phase of antibody formation by plaque technique, Folia Microbiol., 9 (1964) 173—176.
22 R.E. Billingham and P.B. Medawar, The technique of free skin grafting in mammals, J. Exp. Biol., 28 (1951) 385—392.
23 L.A. McCormick, L.C.W. Seymour, R. Duncan and J. Kopeček, Interaction of a cationic *N*-(2-hydroxypropyl)methacrylamide copolymer with rat visceral yolks sacs cultered *in vitro* and rat liver *in vivo*, J. Bioactive Compatible Polym., in press (1986).
24 R. Duncan, J. Kopeček, P. Rejmanová and J.B. Lloyd, Targeting of *N*-(2-hydroxypropyl)methacrylamide copolymers to liver by incorporation of galactose residues, Biochim. Biophys. Acta, 775 (1983) 518—521.
25 J.D. Beatty, E. Friesen, J.H. Linford and L.G. Israels, Effects of conjugated and nonconjugated antithymocyte globulin and trenimon on T lymphocytes and skin graft rejection, Transplantation, 25 (1978) 197—203.
26 I. Hilgert, K. Malberg, K. Matthes and H. Ambrosius, Effect of 6-mercaptopurine-rabbit-anti mouse lymphocyte globulin on the survival of skin allografts in mice, Folia Biol. (Prague), 28 (1982) 22—27.

27 D. Papachristou, A.F. Zaki and J.G. Fortner, Chlorambucile-carrying ALG as an immunosuppressive agent in the rat, in: F.T. Rapaport and J.M. Converse (Eds.), Transplantation Today IV, Grune Stratton, New York, 1977, pp. 1059—1065.
28 F.L. Moolten, N.J. Capparell and S.R. Cooperband, Antitumor effects of antibody—diphteria toxin conjugates: Use of hapten-coated tumor cells as an antigenic target, J. Natl. Cancer Inst., 49 (1972) 1057—1062.
29 D.A.L. Davies and G.-J. O'Neill, *In vivo* and *in vitro* effects of tumour specific antibodies with chlorambucil, Br. J. Cancer, 28 Suppl. I (1973) 285—298.
30 J.D. Everall, P. Dowd, D.A.L. Davies, G.-J. O'Neill and G.F. Rowland, Treatment of melanoma by passive humoral immunotherapy using antibody drug synergism, Lancet, I (1977) 1105—1106.
31 V. Raso, Antibody-mediated delivery of toxic molecules to antigen bearing target cells, Immunol. Rev., 62 (1982) 93—117.
32 D.M. Neville and R.J. Youle, Monoclonal antibody—ricin or ricin A chain hybrids: Kinetic analysis of cell killing for tumor therapy, Immunol. Rev., 62 (1982) 75—91.
33 E.S. Vitetta, K.A. Krolick and J.W. Uhr, Neoplastic B cells as targets for antibody—ricin A chain immunotoxins, Immunol. Rev., 62 (1982) 159—183.
34 P.E. Th rpe and W.C.J. Ross, Th preparation and cytotoxic properties of antibody—toxin conjugates, Immunol. Rev., 62 (1982) 119—158.
35 F.K. Jansen, H.E. Blythman, D. Carriére, P. Casellas, P. Gros, J.C. Laurent, F. Paolucci, B. Pau, P. Poncelet, G. Richer, H. Vidal and G.A. Voisin, Immunotoxins: Hybrid molecules combining high specificity and potent cytotoxicity, Immunol. Rev., 62 (1982) 185—216.
36 Б. Říhová, K. Ulbrich, J. Kopeček and P. Mančal, Immunogenicity of *N*-(2-hydroxypropyl)methacrylamide copolymers — Potential hapten or drug carriers, Folia Microbiol., 28 (1983) 217—227.
37 B. Říhová, J. Kopeček, K. Ulbrich, M. Pospíšil and P. Mančal, Effect of the chemical structure of *N*-(2-hydroxypropyl)methacrylamide copolymers on their ability to induce antibody formation in inbred strains of mice, Biomaterials, 5 (1984) 143—148.
38 B. Říhová, J. Kopeček, K. Ulbrich and V. Chytrý, Immunogenicity of *N*-(2-hydroxypropyl)methacrylamide copolymers, Makromol. Chem., Suppl. 9 (1985) 13—24.
39 J. Šimečková, D. Plocová, B. Říhová and J. Kopeček, Activity of complement in the presence of *N*-(2-hydroxypropyl)methacrylamide copolymers, J. Bioactive Compatible Polym., in press (1986).

Mic/Main
QD 380.113

STIC-ILL

From: Schnizer, Richard
Sent: Wednesday, March 26, 2003 1:27 PM
To: STIC-ILL
Subject: 09/627,787

Please send me a copy of:

Chen et al (Macromolecules (1990) 23(24): 5055-5058

~~Tadao et al JP 43008958, issued 4/11/68~~

Both of these for c8

Thank you

Richard Schnizer, Ph.D.
Patent Examiner
Art Unit 1635
CM1 12E17
703-306-5441
Mail Box CM1 11E12

New Thermotropic Chiral Nematic Copolymers Using (1*S*,2*S*,3*S*,5*R*)-(+)- and (1*R*,2*R*,3*R*,5*S*)-(−)-Isopinocampheol as Building Blocks

S. H. Chen* and M. L. Tsai

Department of Chemical Engineering and Laboratory for Laser Energetics, University of Rochester, Rochester, New York 14627

Received January 30, 1990; Revised Manuscript Received May 21, 1990

ABSTRACT: Thermotropic chiral nematic side-chain copolymers were synthesized and characterized by using (1*S*,2*S*,3*S*,5*R*)-(+)- and (1*R*,2*R*,3*R*,5*S*)-(−)-isopinocampheol as the chiral building blocks. The helical twisting power was found to correlate with the volume swept out by the chiral pendant group via rotation for a given nematogenic monomer. However, the enhanced mesomorphic order introduced in both the nematogenic and chiral monomers as a result of an increased extent of conjugation or a shortened spacer length was found to reduce the helical twisting power of the resultant copolymer. Hence, both factors have to be taken into account as the helical twisting power of a copolymer system is to be optimized for a specific application. The present work also generalized our previous observation that the inversion of chirality of the pendant group results in helical sense reversal, although the role of the absolute configuration of the chiral moiety is not yet clearly understood.

I. Introduction

Thermotropic chiral nematic polymers are represented by a class of macromolecular structures in which chiral moieties contribute to the formation of the cholesteric mesophase.[1,2] From the molecular structure point of view, one would expect that a copolymer comprising a nematogenic and a chiral monomer should exhibit cholesteric mesomorphism in view of the common practice in which a chiral nematic material is routinely prepared by mixing a low molar mass nematogen with a chiral dopant.[3,4] Although there exist several empirical rules[5-8] formulated for low molar mass chiral nematics in terms of the helical sense and twisting power in relation to molecular structures, the applicability of these rules to polymeric counterparts has remained inconclusive. In recognition of the tremendous potentials of chiral nematic polymers in emerging optical technologies[9-12] and in view of the scarcity of information[1,2] relating macromolecular structures to relevant optical properties, we have conducted a series of studies on fundamental issues involving helical sense and twisting power in thermotropic side-chain copolymers containing chiral groups other than commonly encountered cholesterol. Cholesterol is known to possess adequate helical twisting power for giving rise to selective reflection wavelength, λ_R, in the visible region; however, it is possible to generate only the left-handed supramolecular structure presumably because of the given set of absolute configurations in naturally occurring cholesterol. Our strategy was to identify pairs of enantiomers that would give rise to strong enough helical twisting power in the yet to be optimized macromolecular structural setting and that would result in both left- and right-handed helical structures, as defined by the sense of the reflected circularly polarized light, to meet the demands of practical applications.

In a recent communcation,[13] we have demonstrated that the inversion of chirality in the side group of a copolymer does lead to the reversal of helical sense using (*R*)-(+)- and (*S*)-(−)-1-phenylethylamine as the chiral building blocks. Furthermore, it was found that the helical twisting power is influenced by the structures of both comonomers, namely, by the consequence of the interplay between the two. These observations have raised the need for systematic investigations of optical property–macromolecular structure relationships with an aim to formulating an empirical basis for molecular design as specific applications arise. With these objectives in mind, we have synthesized and characterized three series of copolymers based on (1*S*,2*S*,3*S*,5*R*)-(+)- and (1*R*,2*R*,3*R*,5*S*)-(−)-isopinocampheol varying in the extent of conjugation (and hence the length of the rigid core) in the chiral monomer structure. The helical twisting power of these new chiral nematic polymers is interpreted in terms of the configurational as well as conformational characteristics and the mesomorphic order of both the chiral and the nematogenic monomers; relevance is also made to the classical cholesterol-containing copolymers.

II. Experimental Section

The chemical structures and phase transition temperatures of the methacrylate monomers employed in the present work are summarized in Table I; literature values for the mesophase transition temperatures are also included for comparison wherever possible. All the monomers were synthesized following the procedures reported in the literature[14-17] except those containing commercially available, optically pure isopinocampheol. Figure 1 sketches the reaction scheme for the synthesis of chiral monomers containing isopinocampheol. All of the following reagents were used as received from Aldrich Chemical Co.: 4-hydroxybenzoic acid (99%), 4-hydroxycinnamic acid, predominantly trans (98%), (1*S*,2*S*,3*S*,5*R*)-(+)-isopinocampheol (99%), (1*R*,2*R*,3*R*,5*S*)-(−)-isopinocampheol (98%), and cholesterol (98%). The four-step procedure of Gray et al.[18] was followed to synthesize 4-(4-hydroxyphenyl)benzoic acid.

Copolymerization of a nematogenic and a chiral monomer was accomplished in anhydrous tetrahydrofuran in the presence of azobis(isobutyronitrile) at 333 K for 48 h in a nitrogen atmosphere. The copolymers were isolated and repeatedly precipitated from acetone or methanol until the monomers were completely removed and then dried in a vacuum oven for several days prior to analysis. The structures of the copolymers synthesized for the present investigation are summarized in Figure 2.

The chemical structures of both monomers and copolymers were elucidated with IR (710B, Perkin-Elmer) and proton NMR (QE-300, GE) spectroscopy. The mesophase transition temperatures were determined with a differential scanning calorimeter (DSC-4, Perkin-Elmer) at a scan rate of 20 °C/min while continuously purged either with nitrogen for normal operations or helium for low-temperature runs; the inflection point was taken

* Author to whom correspondence should be addressed.

0024-9297/90/2223-5055$02.50/0

Table I
Chemical Structures and Phase Transition Temperatures (K) for Monomers[a]

Nematogenic component

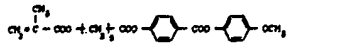

(i) K 327.2 I (308.6 N)

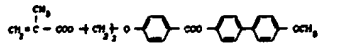

(ii) K 381.0 N 483.0 I [K 381.0 N 484.0 I][b]

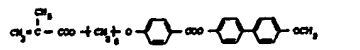

(iii) K 356.5 N 451.0 I [K 358.0 N 456.0 I][c]

Chiral component

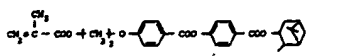

(iv) K 349.0 I

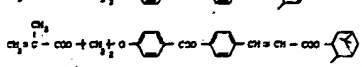

(v) K 372.0 I

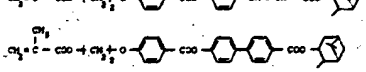

(vi) K 384.0 Ch 411.0 I

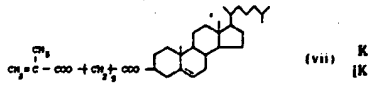

(vii) K 320.0 Ch 330.5 I (299.0 S) [K 321.2 Ch 330.3 I (298.0 S)][d]

[a] Symbols for mesophase transitions: K, crystalline; N, nematic; S, smectic; Ch, cholesteric; I, isotropic. Monotropic transitions represented by parentheses. [b] Finkelmann, H.; Ringsdorf, H.; Wendorff, J. H. *Makromol. Chem.* **1978**, *179*, 273. [c] Finkelmann, H.; Portugall, M.; Ringsdorf, H. *Polym. Prepr.* **1978**, *19* (2), 183. [d] Shannon, P. J. *Macromolecules* **1983**, *16*, 1677.

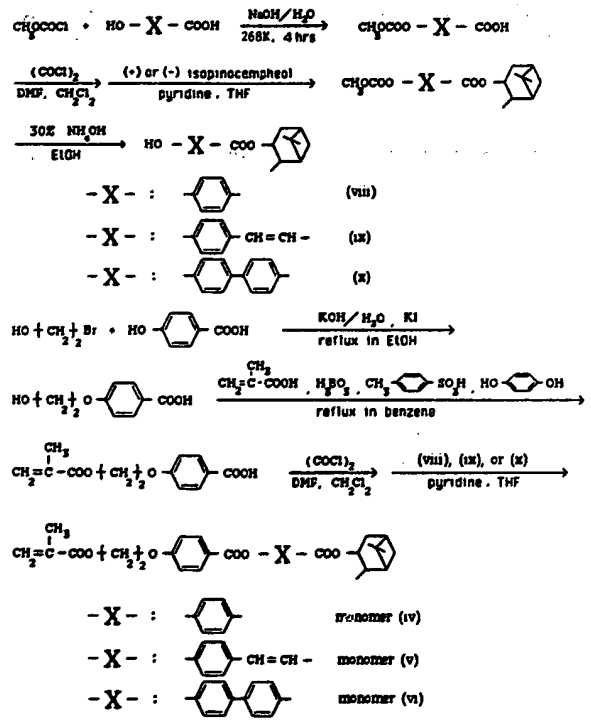

Figure 1. Reaction scheme for the synthesis of the chiral monomers containing (1*S*,2*S*,3*S*,5*R*)-(+)- and (1*R*,2*R*,3*R*,5*S*)-(−)-isopinocampheol.

as T_g. A polarizing optical microscope (Leitz Orthoplan-Pol) equipped with a programmable hot stage (FP52, Mettler) was used to identify mesomorphism upon heating or cooling. Normally, thermal annealing at selected elevated temperatures for 2 days or so was required to increase the domain size for mesophase identification of copolymers.

The determination of molecular weight distribution, from which both $\bar{M}_n$ and $\bar{M}_w$ could be calculated, was accomplished in a size exclusion chromatography system constructed with an HPLC metering pump (Constametric III, Milton Roy), two PLgel columns in series (500 and 10 000 Å, Hewlett-Packard) housed in a column oven (Jones Chromatography), and a UV differential absorbance detector (UV III Monitor, Milton Roy) set at 254 nm. The selective reflection wavelength λ_R was determined on a UV-vis-near-IR spectrophotometer (Lambda 9, Perkin-Elmer). Prior to the spectrophotometric measurements, optical elements (prepared by placing about 20 mg of copolymer products between a pair of soda lime glass substrates separated with 13-μm-thick Kapton spacers) were annealed at temperatures close to $0.95T_I$, T_I being the isotropic transition temperature, for a day or two before quenching to room temperature. The determination of λ_R was found to be reproducible to within ±5% of the mean on repeated measurements. The handedness of the chiral nematic copolymers was further determined by spectrophotometric measurements of the so-prepared optical elements placed in series with those made of a commercially available low molar mass nematic host and a chiral dopant mixed at a rati that gives rise to the desired value f r λ_R with known handedness. For example, low molar mass chiral nematics containing nematogen E-7 and chiral additive CB-15 (both from BDH Ltd.) are known to exhibit a right-handed helical structure. The determinati n of

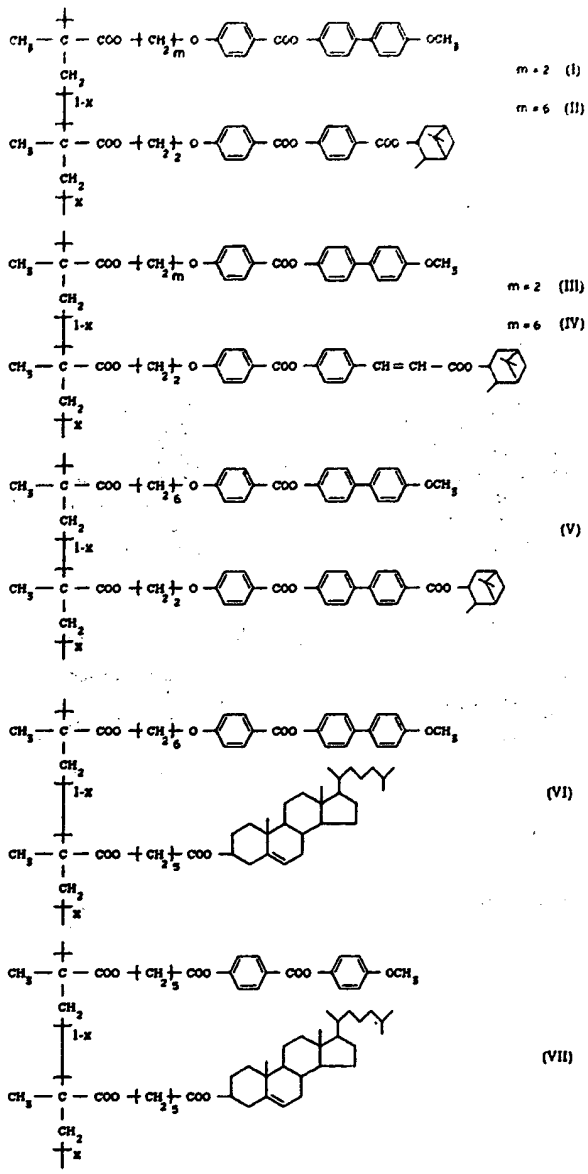

Figure 2. Structures of the thermotropic chiral nematic copolymers synthesized for the present study.

Table II
Structural Characteristics and Thermal Properties of Copolymers I and II

x^a	T_g,[b] K	$T_{Ch\rightarrow I}$,[c] K	$10^{-3}\bar{M}_w$	$\bar{M}_w/\bar{M}_n$
Copolymer I with (1*S*,2*S*,3*S*,5*R*)-(+)-Isopinocampheol				
0.17	363	514	12.5	1.44
0.28	345	475	13.6	1.65
0.38	366	460	22.2	2.74
0.49	367	443	37.2	2.62
0.59	362	424	36.3	2.50
0.70	374	417	41.8	2.09
0.75	364	380	32.1	1.92
Copolymer II with (1*R*,2*R*,3*R*,5*S*)-(-)-Isopinocampheol				
0.41	331	439	22.2	2.49
0.48	338	421	22.0	2.26
0.59	349	420	19.0	2.20
0.69	355	404	23.2	2.12

[a] Mole fraction of chirality; determined with integration on proton NMR spectra. [b] Glass transition temperature. [c] Mesomorphic transition.

Table III
Structural Characteristics, Thermal Properties, and the Observed Values of λ_R for Copolymers III, IV, and V

x^a	T_g,[a] K	$T_{Ch\rightarrow I}$,[a] K	λ_R, nm	$10^{-3}\bar{M}_w$	$\bar{M}_w/\bar{M}_n$
Copolymer III with (1*S*,2*S*,3*S*,5*R*)-(+)-Isopinocampheol					
0.16	360	504	*b*	11.0	1.45
0.26	357	488	2817	15.3	1.84
0.38	364	463	2176	26.2	2.38
0.46	353	451	1735	19.4	1.76
0.49	380	amorph		29.1	2.44
Copolymer IV with (1*R*,2*R*,3*R*,5*S*)-(-)-Isopinocampheol					
0.35	326	428	1936	23.1	2.19
0.44	336	411	1511	24.4	2.23
0.54	342	398	1151	26.4	2.26
Copolymer V with (1*S*,2*S*,3*S*,5*R*)-(+)-Isopinocampheol					
0.31	345	520	*b*	21.3	1.90
0.40	352	513	2908	19.7	1.80
0.51	348	512	1996	23.3	1.65
0.60	356	519	1572	28.4	1.88

[a] See Table II footnotes. [b] λ_R outside of the wavelength region on a Lambda 9 spectrophotometer although the cholesteric mesophase was observed under a polarizing optical microscope.

handedness was further assisted by the polysiloxane series[19] furnished by Dr. F. H. Kreuzer of the Consortium für Elektrochemische Industrie (West Germany). The polysiloxane samples provided a wide range of λ_R from 442 to 2200 nm with left-handed helical sense.

III. Results and Discussion

The chemical structures of the copolymers as summarized in Figure 2 should permit one to address the following questions:

(1) How does the extent of conjugation as well as the attendant configurational characteristics built in the chiral monomer affect the helical twisting power for a given nematogenic comonomer?

(2) How does the mesomorphic order of the nematogenic and chiral monomers influence the helical twisting power of the resultant copolymer?

(3) Does the spacer length in the nematogenic monomer play any role in the determination of the helical twisting power?

(4) Is there any correlation between the chirality of one of the pendant groups and the helical sense in a copolymer?

The structural characteristics, the thermal properties, and the observed values of λ_R for copolymer series I–VII are presented in Tables II–IV. To address the first question raised above, it is noted that the increased anisotropy (the length to the diameter ratio) and the increased extent of conjugation contribute to the enhanced clearing

Table IV
Structural Characteristics, Thermal Properties, and the Observed Values of λ_R for Copolymers VI and VII

x^a	T_g,[a] K	$T_{S\rightarrow Ch\rightarrow I}$,[a] K		λ_R, nm	$10^{-3}\bar{M}_w$	$\bar{M}_w/\bar{M}_n$
Copolymer VI						
0.10	316	393	515	1659	21.7	1.74
0.18	313	411	500	905	14.5	1.48
0.26	313	424	497	648	22.9	1.58
Copolymer VII						
0.08	313		379	1244	14.0	1.13
0.17	323		393	642	16.5	1.18
0.21	314		386	534	14.2	1.12

[a] See Table II footnotes.

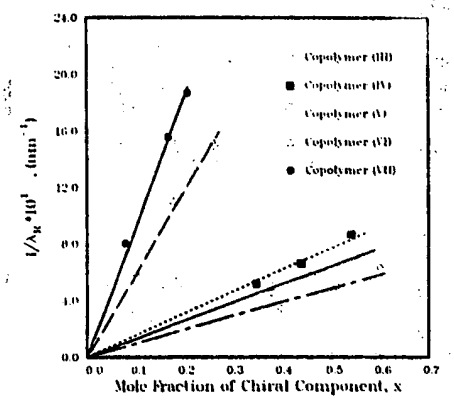

Figure 3. $1/\lambda_R$ as a function of x for copolymers III–VII.

temperature and to the formation of the cholesteric mesophase as one examines the thermal behaviors of monomers iv, v, and vi as presented in Table I. The copolymers comprising the nematogenic monomer ii or iii and chiral comonomers iv and v with an increasing extent of conjugation were found to exhibit a higher helical twisting power. For instance, although the cholesteric mesophase could be identified on optical elements prepared with copolymers I and II with polarizing optical microscopy, the λ_R values appear to have fallen beyond the long-wavelength limit of 3200 nm on the Lambda 9 spectrophotometer. The pitch of a cholesteric mesophase is essentially a measure of the angular displacement between adjacent nematic layers. With increased volume swept out by the *trans*-4-hydroxycinnamic acid moiety via rotation in chiral monomer v as compared to iv, copolymers III and IV give rise to λ_R in the range from 2817 to 1151 nm as shown in Table III. Following this line of argument, one would have expected that copolymer V should possess a helical twisting power intermediate between those of copolymers II and IV because of the linear character of the biphenyl moiety, which is consistent with what is shown in Figure 3, where the slope of $1/\lambda_R$ vs x represents a measure of the helical twisting power.

An alternative argument is that for a given nematogenic monomer, the chiral comonomer that possesses higher mesomorphic order would yield a copolymer with reduced helical twisting power as one compares copolymer V with copolymer IV. It is suspected that the reduced helical twisting power with copolymer V might have originated from what Shibaev and Freidzon[2] referred to as the tendency toward smectogenicity suppressing the helical twisting power although no smectic mesophase was observed in addition to the cholesteric mesophase as reported in Table III. The failure to detect the smectic mesophase prior to the cholesteric mesophase in the

temperature scale with the DSC technique is not surprising in view of the observation made by Freidzon et al.[20] on methacrylate copolymers. It remains to be verified if the same argument applies to situations in which a given chiral monomer is copolymerized with two nematogenic comonomers with different mesomorphic order. A case in point is chiral monomer vii copolymerized with nematogenic monomer iii vs i, the former showing a regular nematic to isotropic transition upon heating while the latter a monotropic isotropic to nematic transition upon cooling. In other words, a nematogenic monomer with enhanced mesomorphic order is expected to yield copolymers with a reduced helical twisting power for a given chiral comonomer. This prediction is borne out in Figure 3 in which copolymer VII is found to possess a higher helical twisting power than copolymer VI. Thus, one could answer the second question by concluding that the higher the mesomorphic order of either nematogenic or chiral monomer, the lower the helical twisting power of the resulting copolymer. Such a conclusion does not seem to contradict the observation made above for copolymers III and IV as opposed to copolymers I and II for the reason that neither monomer iv nor v possesses mesomorphic character. As a matter of fact, the volume swept out by the chiral pendant group seems to play a predominant role in helical twisting power in this case.

The effect of the spacer length in the nematogenic monomer on the helical twisting power for a given chiral comonomer is revealed in Figure 3 in terms of the slopes of $1/\lambda_R$ vs x for copolymers III and IV. It is clearly demonstrated that the longer spacer length yields the higher helical twisting power, an observation consistent with the conclusion reached above in terms of the role of mesomorphic order of monomers in the determination of helical twisting power. Simply put, monomer ii possesses a more stable nematic mesophase than monomer iii as indicted in Table I. Hence, for the given chiral comonomer v, monomer ii is expected to form a copolymer, i.e., III, possessing a lower helical twisting power than copolymer IV synthesized from monomer iii. However, an exception to this general observation was reported by Finkelmann and Rehage[21] on siloxane-based copolymers. Finally, it was found that (1*S*,2*S*,3*S*,5*R*)-(+)-isopinocampheol yields right-handed helices in copolymers III, IV, and V and that (1*R*,2*R*,3*R*,5*S*)-(−)-isopinocampheol yields left-handed counterparts in copolymers with otherwise identical structures. In a recent communication,[13] we have also reported that (*R*)-(+)- and (*S*)-(−)-1-phenylethylamine yield right- and left-handed helixes, respectively. However, none of these observations appear to constitute a sound basis for the correlation between the absolute configuration of the chiral moiety and the handedness of the copolymer on the supramolecular scale. It is noted in passing that the sense of the specific optical rotation of the chiral moiety has been demonstrated to play no role in the helical sense of the cholesteric mesophase.[13] Nevertheless, that the inversion of chirality leads to opposite handedness does seem to have a solid empirical foundation.

IV. Summary

Using (1*S*,2*S*,3*S*,5*R*)-(+)- and (1*R*,2*R*,3*R*,5*S*)-(−)-isopinocampheol, we have synthesized a series of thermotropic chiral nematic copolymers with a varying extent of conjugation built into the chiral monomer. Along with the observations made for the classical cholesterol-containing copolymers, we summarize the present study in what follows:

(1) With a given nematogenic monomer, an increased volume swept out by the chiral pendant group via rotation contributes to the enhanced helical twisting power.

(2) Enhanced mesomorphic order as a result of an increased length of the rigid core or a shortened spacer length of both the nematogenic and chiral monomers tends to suppress the helical twisting power.

(3) It is a general observation that the inversion of chirality in the side group does lead to opposite handedness in the helical sense of the cholesteric mesophase. The question of how the helical sense correlates with the absolute configuration of the pendant chiral moiety has yet to be carefully addressed.

Acknowledgment. We acknowledge helpful discussions with S. D. Jacobs and K. L. Marshall and technical assistance of T. Pfuntner of the Laboratory for Laser Energetics, University of Rochester. We appreciate reviewers' comments that were included to help enhance the readability of the paper. We also thank Dr. F. H. Kreuzer of the Consortium für Elektrochemische Industrie (West Germany) for furnishing a series of left-handed polysiloxane samples for the determination of handedness of some of the copolymers reported here. This work was supported by Kaiser Electronics in San Jose, CA. Partial support was also furnished by the U.S. Department of Energy Division of Inertial Fusion under agreement No. DE-FCO3-85DP40200, the U.S. Army Research Office under Contract DAAL 03-86-K-0173, and the Laser Fusion Feasibility Project at the Laboratory for Laser Energetics, which has the following sponsors: Empire State Electric Energy Research Corp., New York State Energy Research and Development Authority, Ontario Hydro, and the University of Rochester. Such support does not imply endorsement of the content by any of the above parties.

References and Notes

(1) Chiellini, E.; Galli, G. In *Recent Advances in Liquid Crystalline Polymers*; Chapoy, L. L., Ed.; Elsevier Applied Science Publishers: New York, 1985; Chapter 2.
(2) Shibaev, V. P.; Freidzon, Ya. S. In *Side Chain Liquid Crystal Polymers*; McArdle, C. B., Ed.; Chapman and Hall: New York, 1989, Chapter 9.
(3) Finkelmann, H.; Stegemeyer, H. *Ber. Bunsen-Ges. Phys. Chem.* 1978, *82*, 1302.
(4) Vill, V.; Fischer, F.; Thiem, J. *Z. Naturforsch.* 1988, *43a*, 1119.
(5) Hiebert, M.; Solladie, G. *Mol. Cryst. Liq. Cryst. Lett.* 1981, *64*, 211.
(6) Leder, L. B. *J. Chem. Phys.* 1971, *55*, 2649.
(7) Tsukamoto, M.; Ohtsuka, T.; Morimoto, K.; Murakami, Y. *Jpn. J. Appl. Phys.* 1975, *14*, 1307.
(8) Gray, G. W.; McDonnell, D. G. *Mol. Cryst. Liq. Cryst.* 1976, *37*, 189; *Mol. Cryst. Liq. Cryst. Lett.* 1977, *34*, 211.
(9) Tsai, M. L.; Chen, S. H.; Jacobs, S. D. *Appl. Phys. Lett.* 1989, *54*, 2395.
(10) Ortler, R.; Brauchle, C.; Miller, A.; Riepl, G. *Makromol. Chem., Rapid Commun.* 1989, *10*, 189.
(11) Eich, M.; Wendorff, J. H. *Makromol. Chem., Rapid Commun.* 1987, *8*, 467.
(12) Nakamura, T.; Ueno, T.; Tani, C. *Mol. Cryst. Liq. Cryst.* 1989, *169*, 167.
(13) Tsai, M. L.; Chen, S. H. *Macromolecules* 1990, *23*, 1908.
(14) Finkelmann, H.; Ringsdorf, H.; Wendorff, J. H. *Makromol. Chem.* 1978, *179*, 273.
(15) Rodriguez-Parada, J. M.; Percec, V. *J. Polym. Sci., Polym. Chem. Ed.* 1986, *24*, 1363.
(16) Decobert, G.; Soyer, F.; Dubois, J. C. *Polym. Bull.* 1985, *14*, 179.
(17) Shannon, P. J. *Macromolecules* 1983, *16*, 1677.
(18) Gray, G. W.; Hartley, J. B.; Jones, B. *J. Chem. Soc.* 1955, *55*, 1412.
(19) Pinsl, J.; Brauchle, C.; Kreuzer, F. H. *J. Mol. Electron.* 1987, *3*, 9. Kreuzer, F. H.; Gawhary, M. E. U.S. Patent 4410570, Oct 18, 1983.
(20) Freidzon, Ya. S.; Boiko, N. I.; Shibaev, V. P.; Plate, N. A. *Eur. Polym. J.* 1986, *22*, 13.
(21) Finkelmann, H.; Rehage, G. *Makromol. Chem., Rapid Commun.* 1980, *1*, 733.

STIC-FPAS
From: STIC-ILL
Sent: Wednesday, March 26, 2003 1:55 PM
To: STIC-FPAS
Subject: RE: 09/627,787

-----Original Message-----
From: Schnizer, Richard
Sent: Wednesday, March 26, 2003 1:27 PM
To: STIC-ILL
Subject: 09/627,787

Please send me a copy of:

Chen et al (Macromolecules (1990) 23(24): 5055-5058

~~Tadao et al JP 43008956, issued 4/11/68 **********~~

Both of these for c8

Thank you

Richard Schnizer, Ph.D.
Patent Examiner
Art Unit 1635
CM1 12E17
703-306-5441
Mail Box CM1 11E12

23 E 0 ①～③(26 B 121)
(23 A 0)
(26 B 1)
(26 B 131)
(26 B 151)

特　許　庁

特　許　公　報

特許出願公告
昭43－8956
公告　昭43．4.11
（全7頁）

新規なるキサンテン系高分子着色料の製法

特　　願　昭　39－45218
出　願　日　昭　39．8．8
発　明　者　伊田忠夫
西宮市枝川町33
同　高橋省二
西宮市枝川町30
同　橋本武之
大阪市東淀川区加島町1070
同　松崎重之
大阪市城東区放出町中3の75
出　願　人　田辺製薬株式会社
大阪市東区道修町3の21
代　表　者　平林忠雄
代　理　人　弁理士　赤岡迪夫

発明の詳細な説明

本発明は一般式

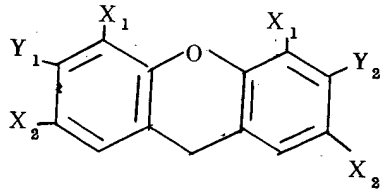

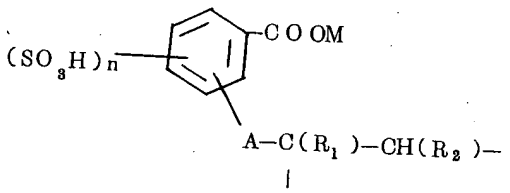

（ただし、R_1およびR_2は水素または低級アルキル基、Aは－NHCO－，－O－CO－，－

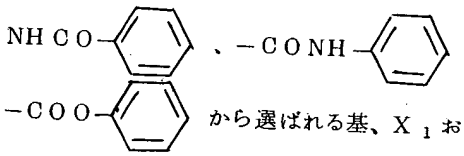

から選ばれる基、X_1およびX_2は水素またはハロゲン、Mは1価の金属イオン、nは整数0または1を表わし、Y_1およびY_2はY_1が－OMを表わすときY_2がオキソ基を表わし、Y_1がモノまたはジアルキルアミノ基を表わすときY_2はモノまたはジアルキルイムモニウム基を表わす）

で示される基本単位からなる新規なるキサンテン系高分子着色料の製法に関する。

すなわち、本発明によれば一般式

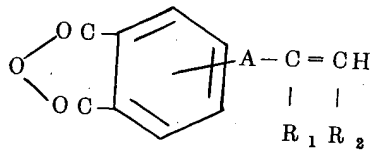

（ただし、記号は前記と同一意味を有する）

で示される無水フタル酸誘導体を一般式

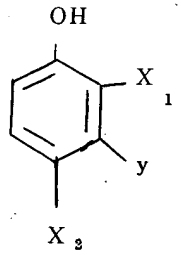

（ただし、X_1およびX_2は前記と同一意味を有し、yは水酸基、モノアルキルアミノ基またはジアルキルアミノ基を表わす）

で示されるフエノール誘導体と縮合反応させて一般式

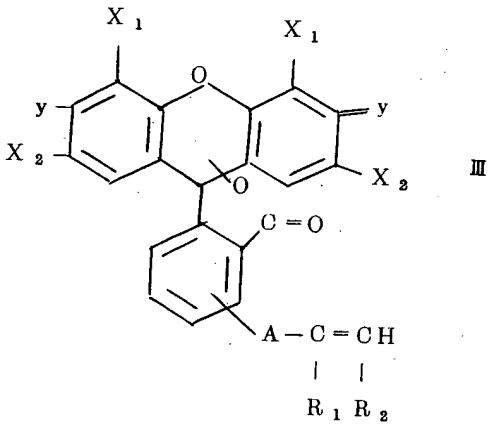

（ただし、記号は前記と同一意味を有する）で示されるキサンテン誘導体を製しこれを単独重合させるかあるいはこれと共重合しうる他のビニール単量体と共重合させて高分子化した後、さらにこの生成重合体の置換基yが水酸基である場合はアルカリ処理し、また置換基yがアルキル置換アミノ基である場合は酸で処理することにより新規な

るキサンテン系高分子着色料が製造される。

化合物ⅠおよびⅡの縮合反応は常法により、そのままもしくは適当な溶媒中に加熱するか、あるいはたとえば塩化第二水銀、塩化亜鉛、三フッ化ホウ素、塩化アルミニウム、硫酸のごとき触媒の存在下に加熱することにより遂行できる。反応溶媒としてはたとえばベンゼン、トルエン、キシレン等の芳香族炭化水素溶媒が適当である。かくして得られた化合物Ⅲの単独重合または共重合反応は、ラジカル重合あるいはイオン重合等いずれの重合反応にしたがつても行うことができる。すなわちラジカル重合による場合はたとえばα，α′－アゾビスイソブチロニトリル、過酸化ベンゾイル、過硫酸カリウム、過硫酸アンモニウム、過酸化水素のごとき触媒の存在下、塊重合、溶液重合、乳化重合あるいは懸濁重合法のいずれかの方法によつても実施することができる。またイオン重合による場合はベンゼン、トルエン、エーテルのごとき溶媒中、たとえばn－ブチルリチウム、チグラー触媒、グリニヤー試薬等の存在下に反応させるのが適当である。

本発明において使用される共重合可能な他のビニール単量体としてはたとえばアクリル酸、メタクリル酸、これらのアルキルエステル、アクリロニトリル、酢酸ビニール、スチレン、アルキルビニール、酢酸ビニール、スチレン、アルキルビニールピリジン等のビニール単量体のごときが好適である。しかして、共重合させるビニール単量体の種類、使用量等を変化させることによりその溶解性、色調、その他の物理的性質を適宜に調整することも可能となる。

なお、一般式Ⅲにおいて置換基X_1およびX_2の少くともいずれか一方が水素である場合はこの高分子化工程の後必要に応じて、生成重合体をハロゲン化することによりハロゲンに変えることができる。

ハロゲン化は常法にしたがい、たとえば氷酢酸のごとき溶媒中加温ないし加熱してハロゲンと反応させることにより行う。この際塩化第2銅、塩素酸ソーダのごとき触媒が存在すれば一層好適である。

またかかるハロゲン化反応にかえて当該生成重合体をさらにスルホン化してキサンテンの9位に結合せるフエニール基にスルホン酸基を導入することもでき、スルホン化の度合を適宜変化させれば得られる高分子着色料の水溶性あるいはアルカリに対する溶解性等を調整することも可能である。スルホン化反応は常法にしたがい、たとえば濃硫酸、発煙硫酸、あるいはクロルスルホン酸と冷時ないし加熱することにより行われる。

かくして得られた生成化合物は置換基yが水酸基である場合はつずいて金属水酸化物で処理してフルオレッセイン型の塩とする。

また置換基yがアルキル置換アミノ基であつて前記したスルホン化反応を行わなかつた場合は、たとえば塩酸のごとき無機酸あるいはしゆう酸のごとき有機酸で処理して3－イソキサンテン－3－イリデン－イムモニウム型塩とする。

重合反応後スルホン化を行つた場合は、スルホン化反応と同時に生成化合物のイムモニウム型塩への変換反応もあわせ行われるため、このような酸処理工程は不要となる。なお、酸処理工程は不要であるが、生成化合物をさらにアルカリ処理してたとえばナトリウム塩とすればその水溶性を一層増加させることができる。

上記本発明により得られる化合物を例示すれば下記のごとくである。

ポリ－〔9－（2′－カルボキシ－4′－パラビニールベンゾイルアミド）－フエニール－6－ヒドロキシ－3－イソキサントン・ジナトリウム塩〕、ポリ－〔9－（2′－カルボキシ－4′－アクリロイルアミド）－フエニール－2，4，5，7－テトラブロム－6－ヒドロキシ－3－イソキサントン・ジナトリウム塩〕、ポリ－〔9－（2′－カルボキシ－4′－アクリロイルオキシ）－フエニール－6－ヒドロキシ－3－イソキサントン・ジナトリウム塩〕、ポリ－〔9－（2′－カルボキシ－4′－メタクリロイルオキシ）－フエニール－2，4，5，7－テトラヨード－6－ヒドロキシ－3－イソキサントン・ジナトリウム塩〕、ポリ－〔9－（2′－カルボキシ－3′－メタブロペニルアニリノカルボニル）－フエニール－2，4，5，7－テトラヨード－6－ヒドロキシ－3－イソキサントン・ジナトリウム塩〕、〔9－（2′－カルボキシ－3′－メタビニールアニリノカルボニル）－フエニール－6－ヒドロキシ－3－イソキサントン・ジナトリウム塩〕・スチレン共重合体、〔9－（2′－カルボキシ－4′－オルトビニールフエノキシカルボニル）－フエニール－6－ヒドロキシ－3－イソキサントン・ジナトリウム塩〕・メタクリル酸共重合体、〔9－（2′－カルボキシ－4′－ビニールオキシ－5′－スルホ）－フエニール－6－ヒドロキシ－3－イソキサントン・トリナトリウム塩〕・2－ビニール－5－エチルピリジン共重合体、ポ

リー〔9－(2′－カルボキシ－4′－アクリロイルアミド)－フエニール－6－メチルアミノ－3－イソキサンテン－3－イリデン－N－メチル－イムモニウムクロリド〕、ポリー〔9－(2′－カルボキシ－4′－メタクリロイルアミド)－フエニール－6－ジメチルアミノ－3－イソキサンテン－3－イリデン－N，N－ジメチル－イムモニウムクロリド〕、ポリー〔9－(2′－カルボキシ－4′－パラビニールフエノキシカルボニル)－フエニール－6－ジエチルアミノ－3－イソキサンテン－3－イリデン－N，N－ジエチル－イムモニウムクロリド〕、ポリー〔9－(2′カルボキシ－4′－ビニールオキシ－5′－スルホ)－フエニール－6－ジエチルアミノ－3－イソキサンテン－3－イリデンN，N－ジエチル－イムモニウム½硫酸塩〕本発明により得られる新規なるキサンテン系高分子着色料は毒性、日光堅牢度、あるいは色調等の点で既存着色料にみられる物理的、化学的欠点がなく、優れた着色料である。特にその内のあるものは水、メタノール、エタノール等の水性溶媒に溶解し、食用色素、染料として極めて有用である。またあるものは溶媒にまつたく不溶性の化※合物として得られ、顔料として使用できる。顔料として使用する場合はこれら化合物が特に塩化ビニール、ポリエチレン等の合成高分子物質とブレンドしやすいためこれらの着色料あるいは塗料として用いるのが最適である。

実施例　1

4－(パラビニールベンゾイルアミド)－無水フタル酸29gおよびレゾルシン22gを混合し、200°に約1時間加熱かくはんする。反応物を冷時希カ性ソーダ水溶液に溶解後この溶液を氷－塩酸中に注加し、析出する沈殿をメタノールから再結晶することにより黄色微細結晶43.5gが得られる。本品をN，N－ジメチルホルムアミド200mlに溶解し、α，α′－アゾビスイソブチロニトリル450mgを加え、窒素置換封管中、70°に20時間反応させた後、反応液をメタノール－エーテル混液(1：1)4l中に注加することにより黄色沈殿38gが得られる。カセイソーダ12gを溶解した水溶液200mlに本品を溶解し、ついでこの溶液を塩析することにより

式

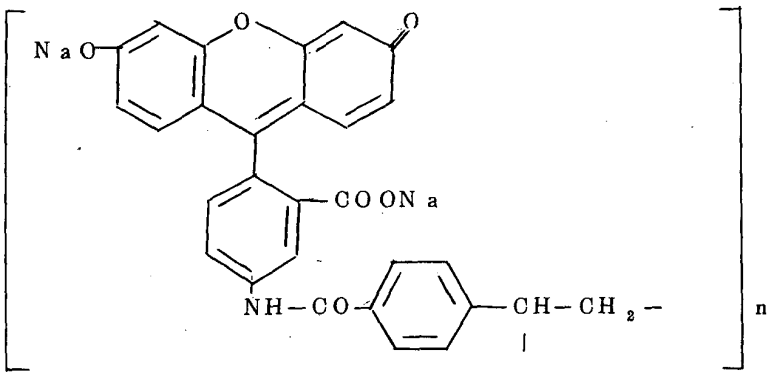

で示される黄褐色粉末状化合物37gが得られる。

実施例　2

4－アクリロイルアミド－無水フタル酸24g、レゾルシン22gおよび塩化第2水銀2gを混合し、120°に2時間加熱溶融する。反応物をメタノールに溶解し、エーテルを加えて析出する沈殿を水洗後メタノールから再結晶することにより黄色結晶38gが得られる。本品をN，N－ジメチルホルムアミド150mlに溶解し、α，α′－アゾビスイソブチロホトリル400mgを加え、窒素置換封管中、70°に20時間反応させた後、反応液をエーテル3lに注加することにより黄褐色粉末沈でん35.5gが得られる。本品を氷酢酸150mlに溶解し、これを臭素60gの氷酢酸溶液250mlとともに2時間加温する。反応液を氷水2lに注加し、析出する沈でんを口取、水洗後、カ性ソーダ12gを溶解した水溶液250mlに冷時溶解する。この溶液を塩析し、析出する沈殿を充分乾燥することにより式

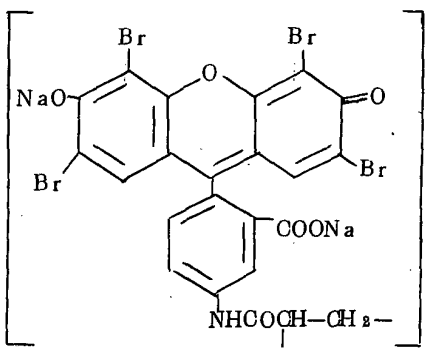

で示される化合物53gが得られる。

実施例　3

4－メタクリロイルオキシー無水フタル酸27gおよび2，4－ジヨードレゾルシン87gを実施例1と同様に反応、処理することにより

式

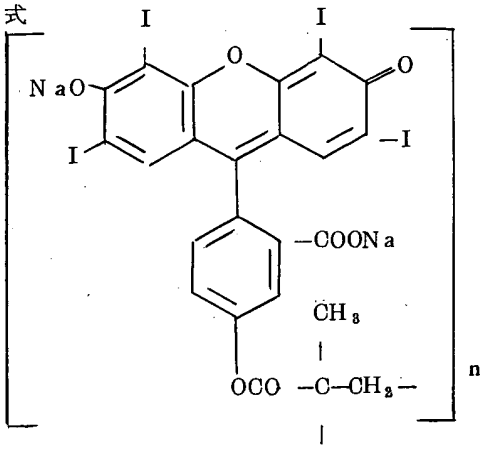

※

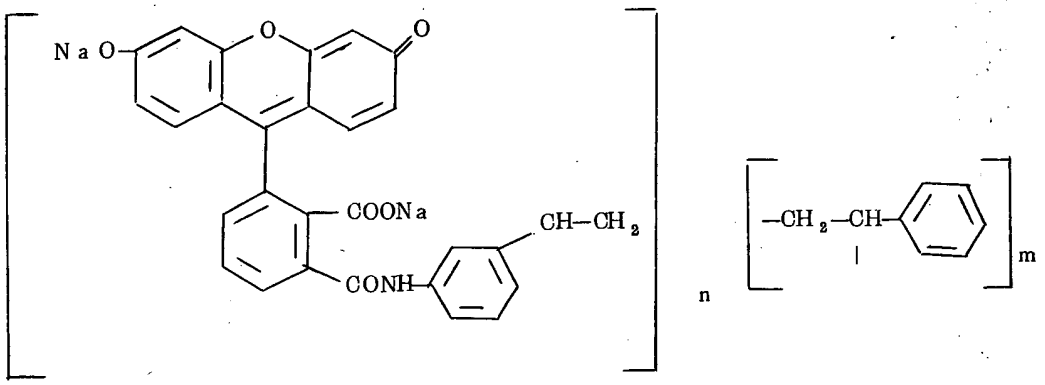

で示される黄色粉末状の化合物55gが得られる。

実施例　5

4－パラビニールフエノキシカルボニル－無水フタル酸29gおよび3－ジエチルアミノフエノール66gを180°に2時間加熱溶融する。反応物をエタノール500mlに溶解後エーテル－石油エーテル（5：1）混液3lに注加する。析出する微細結晶をエタノール300mlに溶解し、α,☆α'－アゾビスイソブチロニトリル1gを加え、窒素気流中70°に10時間反応させる。析出する赤色粉末を濾取してN，N－ジメチルスルホキサイド200mlに溶解し、これに塩化水素5．5gを吸収させた含水メタノール50mlを加える。この溶液を減圧濃縮して約200mlとした後エーテル2lを加えることにより式

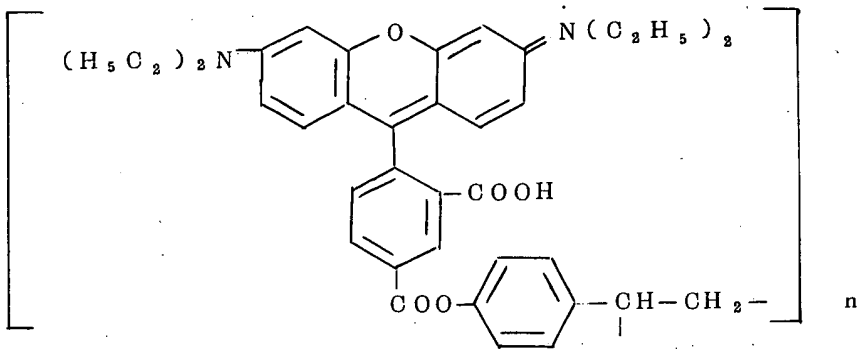

※で示される黒赤色粉末状の化合物93．5gが得られる。

実施例　4

3－メタビニールアニリノカルボニル－無水フタル酸29g、レゾルシン22gおよび塩化亜鉛10gを160°に3時間溶融反応後、以下実施例2と同様に処理することにより黄色微細結晶42．5gが得られる。本品をN，N－ジメチルホルムアミド200mlに溶解し、スチレン18gおよび過酸化ベンゾイル600mgを加え、窒素置換封管中60°に44時間反応させる。反応液をメタノールに注加し、析出する沈殿をカ性ソーダ14gの水溶液300mlに溶解後塩析することにより式

で示される赤黒褐粉末状の化合物61gが得られる。

実施例　6

4－アクリロイルアミドー無水フタル酸18g、3－メチルアミノーフエノール32gおよび塩化第2水銀2gを120°に2時間加熱溶融する。※

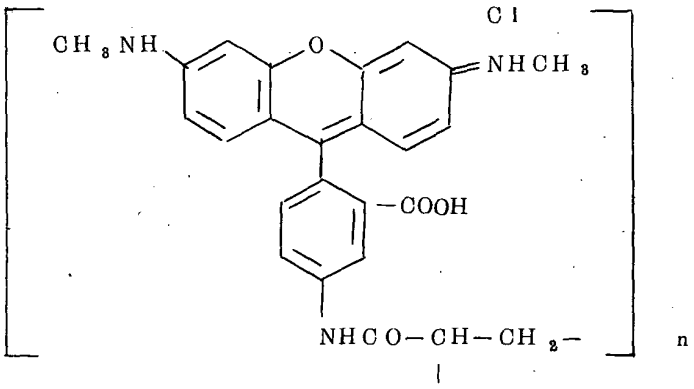

で示される黒赤色粉末状の化合物36.5gが得られる。

実施例　7

4－ビニールオキシ無水フタル酸19g、3－ジエチルアミノフエノール33gおよび3フツ化ホウ素7gをベンゼン100mlに溶解して3時間加熱還流させた後、ベンゼンを留去する。反応残査を少量のエタノールに溶解した後、これを水中にあけ、析出する沈殿をベンゼンーエタノール（1：1）混液で溶出後再結晶することにより赤色結晶39gが得られる。本品をトルエン400☆

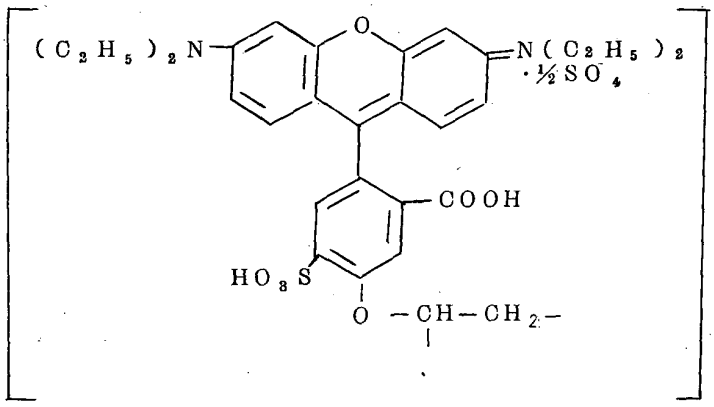

で示される赤色粉末状の化合物37.5gが得られる。

実施例　8

実施例7により得られた赤色粉末状の高分子着

※反応物をメタノールに溶解後、この溶液を水中にあけ、析出する沈殿をエタノールから再結晶することにより赤色微細針晶41gが得られる。本品を以下実施例5と同様にして重合し、塩酸塩とすることにより式

☆mlに溶解し、窒素気流中－10～－20°に冷却下、n－ブチルリチウム0.004モルを含有する石油エーテルを加えながら3時間かくはんする。さらに20時間0°の氷室に放置後、石油エーテル2lを加え、析出する沈殿を濾取、乾燥する。本品を20%発煙硫酸400ml、98%硫酸100mlの混液に少量ずつ加え、60°に10時間加熱する。反応液を冷却後氷水3l中にあけて析出する沈殿を濾取、水洗後乾燥することにより式

色料10gを1規定カ性ソーダ水溶液200mlに溶解し、塩析すると式

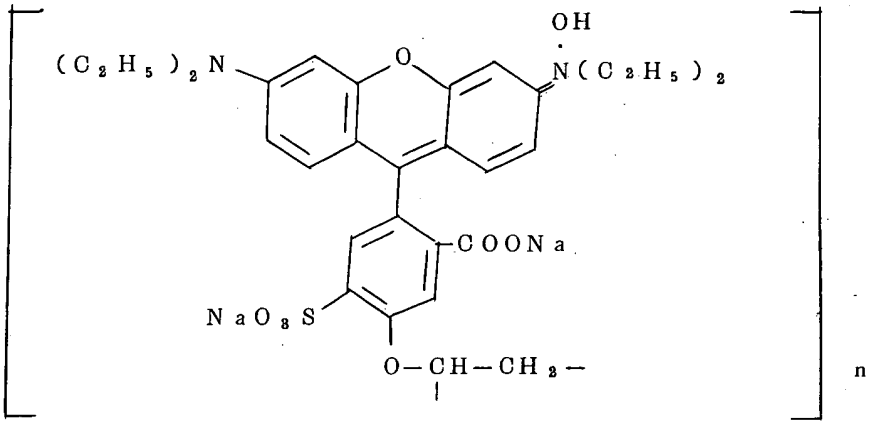

で示される赤黒色粉末状の化合物9．5gが得られる。本品は実施例7で得られた高分子着色料にくらべて、水に対し約3倍の溶解性を有する。

特許請求の範囲

1　一般式

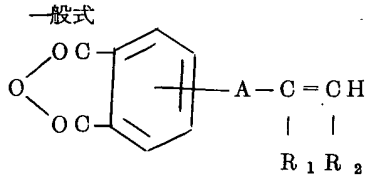

（ただし、R_1およびR_2は水素または低級アルキル基、Aは、－NHCO－、－O－CO－、－O－、－NHCO－  、－CONH－

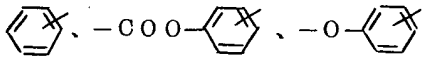

から選ばれる基を表わす）

で示される無水フタル酸誘導体を一般式

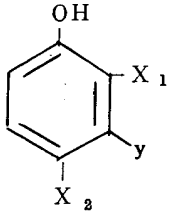

（ただし、X_1およびX_2は水素またはハロゲンyは水酸基、モノアルキルアミノ基またはジアルキルアミノ基を表わす）

で示されるフエノール誘導体と縮合反応させて相当する9－キサンテン誘導体を製した後これを単独重合させるかあるいはこれと共重合しうる他のビニール単量体と共重合させて高分子化し、さらにこの生成化合物を、置換基yが水酸基の場合は金属水酸化物で処理し、置換基yがアルキル置換アミノ基の場合は酸で処理することを特徴とする一般式

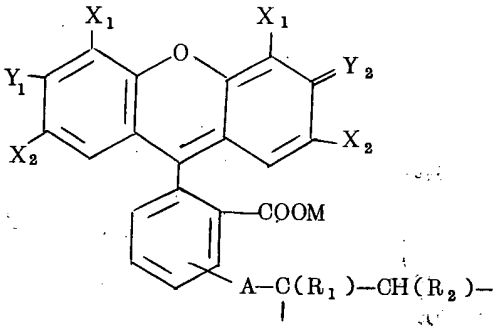

（ただし、記号R_1，R_2，A，X_1およびX_2は前記と同一意味を有し、Mは1価の金属イオン、Y_1およびY_2はY_1が－OM基を表わす時Y_2がオキソ基、Y_1がモノまたはジアルキルアミノ基を表わすときY_2はモノまたはジアルキルイムモニウム基を表わす）で示される基本単位からなる新規なるキサンテン系高分子着色料の製法。

2　一般式

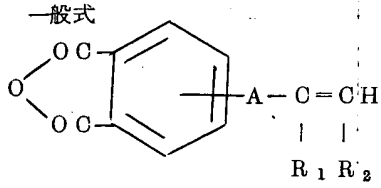

（ただし、R_1およびR_2は水素または低級アルキル基、Aは－NHCO－、－O－CO－、－O－、－NHCO  、－CONH  、

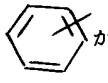

から選ばれる基を表わす）

で示される無水フタル酸誘導体を一般式

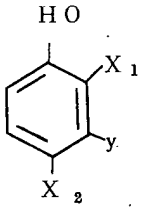

（ただし、X_1およびX_2は水素またはハロゲン、yは水酸基、モノアルキルアミノ基またはジアルキルアミノ基を表わす）

で示されるフエノール誘導体と縮合反応させて相当する9－キサンテン誘導体を製し、これを単独重合させるかあるいはこれと共重合しうる他のビニール単量体と共重合させて高分子化した後、これを常法によりスルホン化し、さらにこの生成化合物を置換基yが水酸基の場合は金属水酸化物で処理することを特徴とする一般式

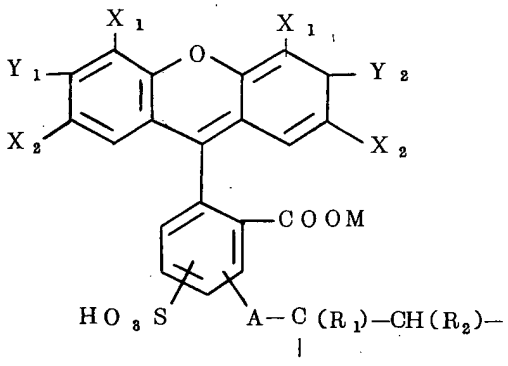

（ただし、記号R_1，R_2，A，X_1およびX_2は前記と同一意味を有し、Mは1価の金属イオン、Y_1およびY_2はY_1が－OM基を表わすときY_2がオキソ基、Y_1がモノまたはジアルキルアミノ基を表わすときY_2はモノまたはジアルキルイムモニウム基を表わす）で示される基本単位からなる新規なるキサンテン系高分子着色料の製法。

3　一般式

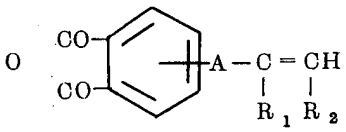

（ただし、R_1およびR_2は水素または低級アルキル基、Aは－NHCO－、－OCO－、－O－、－NHCO 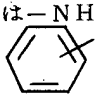 、－CONH 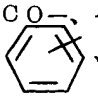 、－

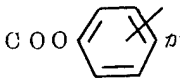 から選ばれる基を表わす）

で示される無水フタル酸誘導体を一般式

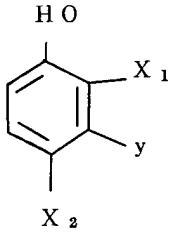

（ただし、X_1およびX_2は一方が水素、他方が水素またはハロゲンを表わし、yは水酸基、モノアルキルアミノ基またはジアルキルアミノ基を表わす）で示されるフエノール誘導体と縮合反応させて相当する9－キサンテン誘導体を製し、これを単独重合させるかあるいはこれと共重合しうる他のビニール単量体と共重合させて高分子化した後、これをハロゲン化し、さらにこの生成化合物を、置換基yが水酸基の場合は金属水酸化物で処理し置換基yがアルキル置換アミノ基である場合は酸で処理することを特徴とする一般式

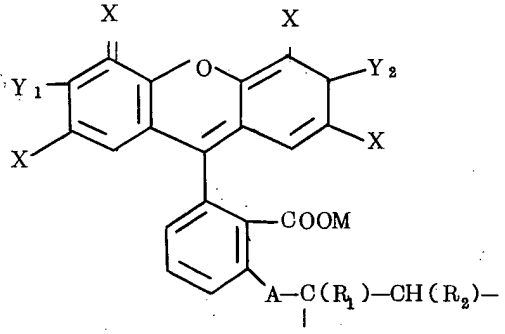

（ただし、記号R_1，R_2およびAは前記と同一意味を有し、Mは1価の金属イオン、Xはハロゲン、Y_1およびY_2はY_1が－OM基を表わすときY_2がオキソ基、Y_1がモノまたはジアルキルアミノ基を表わすときY_2はモノまたはジアルキルイムモニウム基を表わす）

で示される基本単位からなる新規なるキサンテン系高分子着色料の製法。

NOS - BS201.04 J6
Adams ✓

STIC-ILL

From: Schnizer, Richard
Sent: Wednesday, March 26, 2003 3:18 PM
To: STIC-ILL
Subject: 09/627,787

Please send me a copy of:

Sugiyama, Kazuo, J. Macromol. Sci. Chem. (1986), A23(10): 1155-64
102 for broad claims

Lu et al, Bioconjugate Chem. (2000) 11(1): 3-7
Poss interveneing reference

Liso et al J. Controlled Release (1995) 33(3): 429-436)
102 for broad claims?

Rihoiva et al, J. Controlled Release (1985) 2:289-310

Not sure what this is

Omelyanko et al Controlled Release (1998) 53(1-3): 25-37)
Could have fluorescine attached to HPMA

Richard Schnizer, Ph.D.
Patent Examiner
Art Unit 1635
CM1 12E17
703-306-5441
Mail Box CM1 11E12

Article title	Targetable HPMA copolymer-adriamycin conjugates: Recognition, internalization, and subcellular fate
Article identifier	0168365998005480
Authors	Omelyanenko_V Kopeckova_P Gentry_C Kopecek_J
Journal title	Journal of Controlled Release
ISSN	0168-3659
Publisher	Elsevier Netherlands
Year of publication	1998
Volume	53
Issue	1-3
Supplement	0
Page range	25-37
Number of pages	13
User name	Adonis
Cost centre	
PCC	$22.00
Date and time	Thursday, March 27, 2003 4:26:54 AM

ELSEVIER

Journal of Controlled Release 53 (1998) 25–37

journal of controlled release

Targetable HPMA copolymer-adriamycin conjugates. Recognition, internalization, and subcellular fate

V. Omelyanenko, P. Kopečková, C. Gentry, J. Kopeček*

Departments of Pharmaceutics and Pharmaceutical Chemistry/CCCD, and of Bioengineering, University of Utah, Salt Lake City, UT 84112, USA

Received 1 May 1997; received in revised form 30 July 1997; accepted 7 August 1997

Abstract

Recognition, internalization, and subcellular trafficking of *N*-(2-hydroxypropyl)methacrylamide (HPMA) copolymer conjugates containing N-acylated galactosamine (GalN) or monoclonal OV-TL16 antibodies (Ab) have been investigated in human hepatocarcinoma HepG2 and ovarian carcinoma OVCAR-3 cells, respectively. The intrinsic fluorescence of fluorescein or adriamycin (ADR) attached to HPMA copolymers permitted us to follow the subcellular fate of HPMA copolymer conjugates by confocal fluorescence microscopy and fluorescence spectroscopy. The pattern of fluorescence during incubation of HPMA copolymer-ADR-GalN conjugate containing lysosomally degradable tetrapeptide (GFLG) side-chains with HepG2 cells was consistent with conjugate recognition, internalization, localization in lysosomes, followed by the release of ADR from the polymer chains and ultimately diffusion via the cytoplasm into the cell nuclei. A similar pattern was observed in OVCAR-3 cells for Ab targeted HPMA copolymer conjugates. To test our hypothesis that HPMA-copolymer-bound anticancer drugs will be inaccessible to the energy-driven P-glycoprotein efflux pump in multidrug resistant (MDR) cells, we have compared the internalization of the HPMA copolymer-ADR conjugates by sensitive (A2780) and ADR-resistant (A2780/AD) ovarian carcinoma cell lines. Preliminary data on relative retention of ADR in MDR (A2780/AD) cells indicate a higher intracellular ADR concentration after incubation with HPMA copolymer-ADR conjugate when compared to incubation with free (unbound) ADR. © 1998 Elsevier Science B.V.

Keywords: HPMA copolymer; Subcellular trafficking; Drug release; Confocal microscopy

1. Introduction

Use of polymeric drug delivery systems is rapidly becoming an established approach for improvement of cancer chemotherapy [1–3]. The covalent binding of low molecular weight drugs to water soluble polymer carriers offers a potential mechanism to nhance the specificity of drug action. If a drug that rapidly penetrates all cells by random diffusion is associated with a larger carrier molecule, endocytosis becomes its only mode of entry, and this can be a highly cell-specific mechanism [1,2]. The cell specificity could be achieved either by an active targeting of polymer-drug conjugates to cancer cells or passive accumulation of conjugates within solid tumors [3]. The latter is due to the exceptional tumor's tissue biology. The abnormal vasculature of tumors with an increased vessel permeability makes them take up large molecules more efficiently than

*Corresponding author. Tel: +1 801 5817211; e-mail: jindrich.kopecek@m.cc.utah.edu

PII S0168-3659(97)00235-6

normal tissues. At the same time the poor lymphatic drainage of tumors allows high concentrations of polymeric drug to build up in these tissues [3–7]. This phenomenon was referred to as 'enhanced permeability and retention (EPR) effect' [7].

The limit of the cellular uptake of polymer-drug conjugates to the endocytic route has a major impact on the design of polymeric carriers. Anticancer drug conjugates have to be designed in such a way that the spacer between the carrier and the drug should be stable in the blood stream [8] but susceptible to either enzymatically catalyzed or pH-dependent hydrolysis in the lysosomal compartment of the cell [9,10]. The conjugate used would require features enabling it to enter particular cell-types [1,11–13], and ideally the drug would not be released in active form until the macromolecule was inside the target cell.

The prerequisite of a successful design of polymeric anticancer drugs is the detailed knowledge of the relationship between their structure and properties. A detailed study of the subcellular trafficking of new designed conjugates is an important part of polymeric drug's evaluation. Such studies are especially important in the case of conjugates targeted with antibody against cancer-associated antigens. Non-targeted macromolecules can enter cancer cells, which are predominantly epithelial-type cells by pinocytosis. The pinocytosis is a constitutive activity of cells, i.e. it is not substrate-triggered. Any soluble substances present in the ambient fluid will be captured by pinocytosis and delivered to the lysosomes. However, a targetable conjugate recognizable by an antigen at the plasma membrane could be recycled to the plasma membrane [14–16] and escape the exposure to lysosomal enzymes. On the other hand, intra- and intermolecular aggregation of hydrophobic drugs bound to hydrophilic polymeric carriers could influence the rate of release of drugs from polymer chains in the lysosomal compartment due to a steric inaccessibility of the covalent bond between polymer chain and drug to lysosomal enzymes [17]. Thus development of new approaches to study the subcellular trafficking of conjugates and the intracellular release of drugs provides crucial information on the therapeutic potential of the conjugates studied.

During the last decade we have designed, developed, and evaluated, targetable *N*-(2-hydroxypropyl)methacrylamide (HPMA) copolymer-anticancer drug conjugates (reviewed in [1]). Phase I clinical trial data seem to indicate their great potential in cancer therapy [18,19]. Here we report the use of confocal fluorescence microscopy and fluorescence spectroscopy to study the recognition, internalization, and subcellular trafficking of HPMA copolymer conjugates containing N-acylated galactosamine (GalN) or monoclonal OV-TL16 antibodies (Ab) in human hepatocarcinoma HepG2 and ovarian carcinoma OVCAR-3 cells, respectively. The intrinsic fluorescence of fluorescein isothiocyanate (FITC) or adriamycin (ADR) attached to HPMA copolymers permitted us to follow the subcellular fate of HPMA copolymer conjugates and the intracellular release of ADR from the HPMA copolymer carrier. Preliminary experiments on sensitive (A2780) and ADR-resistant (A2780/AD) ovarian carcinoma cell lines were performed to verify the hypothesis that macromolecular drugs may be inaccessible to the energy driven P-glycoprotein efflux pump in multidrug resistant (MDR) cells.

2. Experimental

2.1. Materials

2.1.1. Chemicals

Adriamycin was a kind gift from Dr. A. Suarato, Pharmacia-Upjohn, Milano, Italy; MEM and RPMI 1640 cell culture media and fetal bovine serum were from HyClone Laboratories (Ogden, UT). Protein-A-Sepharose and other chromatographic materials were from Pharmacia (Piscataway, NJ), α_2-macroglobulin was from Calbiochem (San Diego, CA). All other chemicals were of reagent grade or better.

2.1.2. Cell lines

The human cancer cell lines: HepG2 and NIH: OVCAR-3 were purchased from American Type Culture Collection. The A2780, A2780/AD human ovarian cancer cell lines were obtained from Dr. T.C. Hamilton (Fox Chase Cancer Center, Philadelphia,

PA). HepG2 cells were cultured in MEM medium. OVCAR-3, A2780, and A2780/AD cells were cultured in RPMI 1640 medium supplemented with 10 μg/ml insulin. Both media were supplemented with 10% fetal bovine serum, penicillin (100 U/ml), and streptomycin (100 μg/ml). Cells were grown at 37°C in a humidified atmosphere of 5% CO_2 (v/v) in air.

2.1.3. Antibody

The hybridoma cell line which produces the OV-TL16 (IgG_1 subclass) antibody was a kind gift from Dr. L. Poels (University of Nijmegen, Netherlands). The hybridoma cells were grown as ascites in pristained BALB/c mice. The OV-TL16 antibody was isolated by ammonium sulfate precipitation followed by affinity chromatography using Protein A-Sepharose as described in [20]. The Ab was shown to be pure on isoelectric focusing gels using the Phast System (Pharmacia).

2.2. Synthesis of HPMA copolymers

The polymer conjugates were synthesized (Fig. 1) either in a two-step procedure or by a direct copolymerization of corresponding monomers. Radical precipitation copolymerization was performed in an acetone/DMSO mixture at 50°C for 24 h using 2,2'-azobisisobutyronitrile as the initiator as described elsewhere [21]. The characterization of polymers and methods used are shown in Table 1 and Table 2.

P-(GG-ADR)-GalN (**1**). The polymer precursor containing GalN and reactive ONp ester groups was prepared by copolymerization of 10 mol% MA-GG-ONp, 20 mol% MA-GG-GalN [21] and HPMA. The GalN content was determined after hydrolysis of ONp groups, dialysis and freeze drying of a small amount of sample. The ADR was bound to the polymer precursor in DMF solution in the presence of triethylamine. The product was purified by precipitation to acetone followed by separation of free ADR by chromatography on a Sephadex LH-20 column in MeOH (with 5% H_2O). The conjugate was isolated after dialysis by freeze drying.

P-(GFLG-ADR)-GalN (**2**) was prepared from precursor P-(GFLG-ONp)-GalN by a similar procedure as described for conjugate **1**.

P-(GG-ADR)-Ab (**3**). First the polymer precursor containing 12.6 mol% of -GG-ONp was prepared by copolymerization of HPMA and MA-GG-ONp. Then the ADR was bound by aminolysis of part of the reactive groups. In this stage the polymer was carefully purified to remove free (unbound) ADR using a Sephadex LH-20 column with MeOH containing 0.5% acetic acid. The polymer was isolated after evaporation of solvent and reprecipitation into acetone. In the next step the antibody was bound in phosphate buffered saline (PBS). The pH of the reaction was gradually increased from 7.2 to 7.5. The separation and isolation of conjugate was performed as described previously [20].

P-(GFLG-ADR)-Ab (**4**) was prepared from polymer precursor containing 8.5 mol% -GFLG-ONp by a similar procedure as described for conjugate **3**.

P-(AP-FITC)-GalN (**5**). The monomer 5-[3-(methacryloylaminopropyl)thioureidyl] fluorescein (MA-AP-FITC) was synthesized by reacting 3-aminopropylmethacrylamide (0.36 g; 2 mmol) with fluorescein isothiocyanate (isomer I) (0.78 g; 2 mmol) in the presence of triethylamine (0.22 g; 2.2 mmol) and dibutyl dilauryl tin (20 μl) in DMF. After 48 h at room temperature the solvent was partially rotoevaporated, the product acidified and precipitated into water. M.p. 166°C (decomp.). Extinction coefficient 82 000 M^{-1} cm^{-1} (borate buffer pH 9.2, 10% DMF); TLC: R_f 0.58 (AcOEt/AcOH, 9:1). The polymer was prepared by copolymerization of 2 mol% MA-AP-FITC and 10 mol% MA-GG-GalN with HPMA. After precipitation to acetone and dialysis the polymer contained 1.7 mol% -AP-FITC and 9.6 mol% -GG-GalN side chains.

2.3. Subcellular trafficking of conjugates

The intrinsic fluorescence of FITC and ADR were used to monitor the subcellular trafficking of HPMA copolymer conjugates containing the non-degradable (GG) side-chain, namely P-(GG-FITC)-GalN, P-(GG-ADR)-GalN, and P-(GG-ADR)-Ab. The P-(GFLG-ADR)-GalN and P-(GFLG-ADR)-Ab conjugates containing the lysosomally degradable side-chain (GFLG) were suitable to monitor the liberation

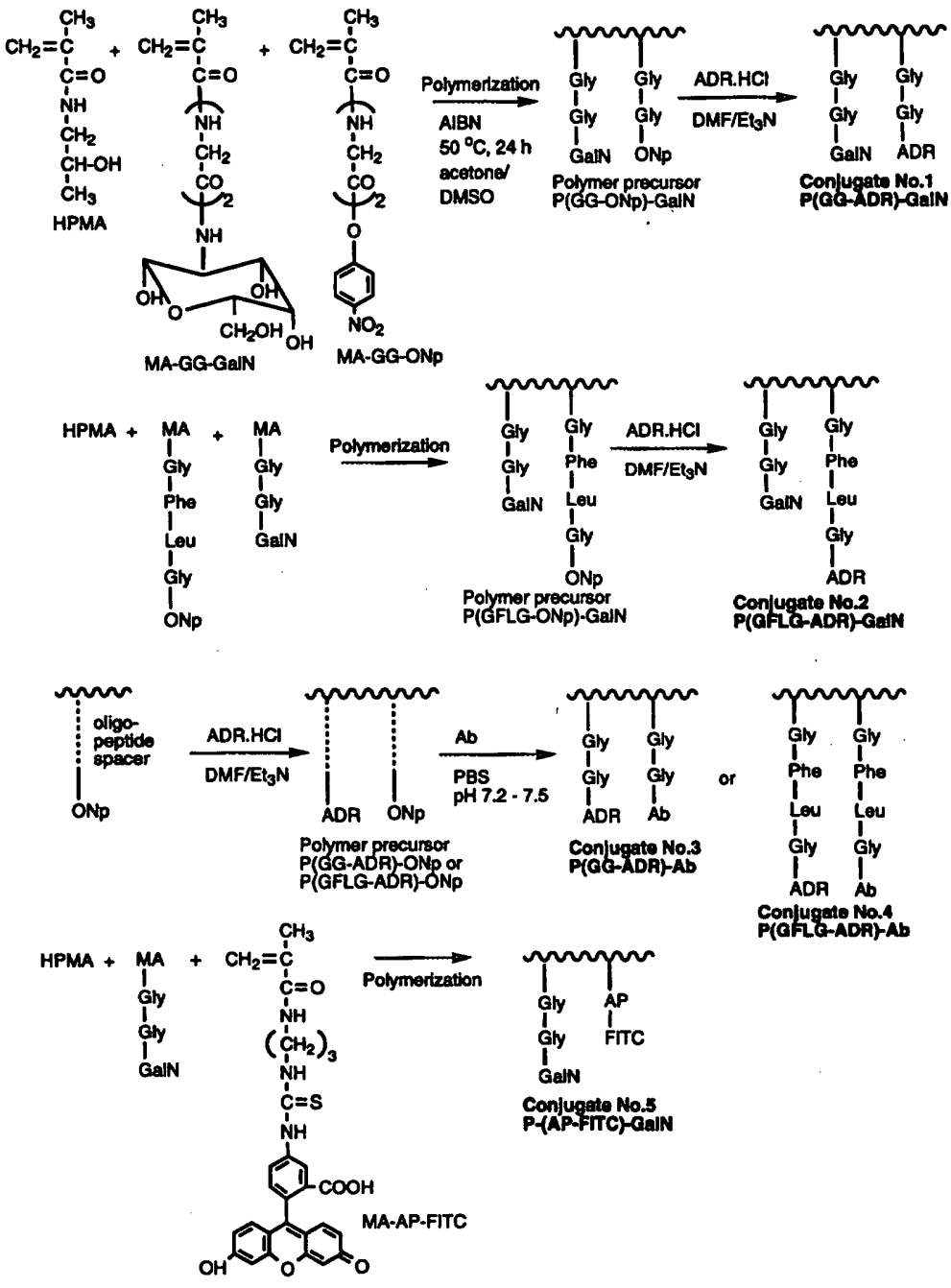

Fig. 1. Synthesis of conjugates.

of ADR from the polymer carrier and the trans-compartmental transport of free ADR from the lysosomes into the nuclei.

After trypsinization, 2×10^4 cells were seeded on an N1 coverslip (Corning) and cultured for 24 h. The culture medium was replaced with medium con-

Table 1
Characteristics of polymer precursors

Structure	Side-chains	Mol %	μmol ligand per mg polymer	M_w^a (M_w/M_n)
P-(GG-ONp)-GalN	-GG-GalN	14.1	0.79	22 000[b]
	-GG-ONp	6.4	0.34	(1.4)
P-(GFLG-ONp)-GalN	-GG-GalN	16.0	0.83	25 000[b]
	-GFLG-ONp	6.3	0.29	(1.5)
P-(GG-ADR)-ONp	-GG-ADR	3.8	0.22	19 000[b,c]
	-GG-ONp	6.0	0.34	(1.3)
P-(GFLG-ADR)-ONp	-GFLG-ADR	2.8	0.15	20 000[b,c]
	-GFLG-ONp	3.2	0.17	(1.4)

[a]Molecular weight averages (M_w) and polydispersity (M_w/M_n) of polymers were estimated by SEC using Superose 12 column, FPLC system, PBS buffer pH 7.3, calibrated with poly(HPMA) fractions.
[b]Determined after aminolysis of ONp groups with 1-amino-2-propanol.
[c]The buffer for SEC contained 20% acetonitrile.

taining conjugates (50 μg/ml). Cells were cultured with the conjugates for time intervals indicated. Unbound conjugates were removed by washing the cell layer three times with PBS. Cells were fixed with 3% paraformaldehyde for 10 min at room temperature and washed again with PBS.

2.4. Staining of acidic organelles

Neutral Red was used as a marker for acidic cell organelles [22]. Cells were cultured with a 20 μM solution of Neutral Red for 30 min, followed by washing with PBS. Cells were fixed with 3% paraformaldehyde for 10 min at room temperature.

2.5. Fluorescence labeling of α_2-macroglobulin

To a solution of α_2-macroglobulin (2 mg/ml in 0.1 M sodium carbonate, pH 9.0) was added 20 μl of rhodamine isothiocyanate — RITC (1 mg/ml in DMSO) at 4°C. The reaction was left for 2 h in the dark. Unbound RITC was separated on a PD-10

Table 2
Characteristics of polymer conjugates

No.	Structure	Composition wt. % (molecular ratio)					Approximate M_w of conjugate (kDa)
		Polymer	:	Fluorescence ligand[a] (ADR, FITC)	:	Targeting moiety[b] (GalN, Ab)	
1	P-(GG-ADR)-GalN	81		6.3		13	22[c]
		(1	:	3	:	19)	
2	P-(GFLG-ADR)-GalN	80		5.6		14	25[c]
		(1	:	3	:	24)	
3	P-(GG-ADR)-Ab	37		4.9		56	245[d]
		(5	:	24	:	1)	
4	P-(GFLG-ADR)-Ab	38		3.3		59	270[d]
		(6	:	16	:	1)	
5	P-(AP-FITC)-GalN	86		3.9		10	46[c]
		(1	:	5	:	30)	

[a]The contents of ADR and FITC were determined spectrophotometrically using ε 11 000 M^{-1} cm^{-1} (ADR, H_2O) and ε 82 000 M^{-1} cm^{-1} (FITC, pH 9.1).
[b]The content of GalN was determined after acid hydrolysis using Carbopac PA-1 anion exchange column and pulsed amperometric detection (Dionex system); the content of antibody was determined by Lowry method (after subtraction of polymer backbone background).
[c]Molecular weight averages (M_w) and polydispersity (M_w/M_n) of polymers were estimated by SEC using Superose 6 column, FPLC system, PBS buffer pH 7.3, calibrated with poly(HPMA) fractions.
[d]Molecular weight was estimated using FPLC system and laser light scattering detection (Wyatt detector).

column and the pooled fractions containing α_2-macroglobulin were dialyzed overnight against PBS.

2.6. Monitoring of subcellular trafficking by steady-state fluorescence

HepG2 cells were grown on a coverslip. To demonstrate the localization of conjugates in lysosomes, cells were cultured in the MEM medium containing P-(GG-ADR)-GalN conjugate for 24 h at 37°C, followed by washing with PBS. Cells were again transferred into the conjugate-free medium and cultured for 2 h at 37°C to allow traces of the uptaken conjugates to be transported to lysosomes. The cells were washed with an ice-cold PBS containing 50 mM of NaN_3 and the coverslip was placed in a device to hold the coverslip in the optical cuvette. The coverslip was aligned at 30° to the excitation beam to minimize the effect of light reflections [23]. Spectra were corrected for scattered light; the extent of the latter was obtained as an average form spectra monitored with several coverslips containing non-treated cells.

To study the localization of the conjugate in the prelysosomal compartments (endosomes), cells were incubated with the P-(GG-FITC)-GalN conjugate at 16°C for 24 h in the medium containing 20 mM of the HEPES buffer. Cells were washed and the coverslip mounted for the fluorescent spectroscopy. Coverslips containing a homogeneous cell monolayer in the place where the excitation light beam was focused were chosen for experiments and placed in a cuvette containing PBS and 50 mM of NaN_3 thermostated at 4°C. The fluorescence was accumulated via the interference filter 514 nm.

2.7. Flow cytometry

Cells were plated in a 24-well plate (Corning Co.), 1×10^5 per well and grown until 80–90% confluence (48 h). The regular cell culture medium was changed to medium containing the conjugates (20 μM ADR equivalent) and cells were incubated for various time intervals. Cells were harvested by trypsinization with 0.25% trypsin-0.02% EDTA, transferred into PBS containing 15 mM NaN_3 and immediately analyzed by the flow cytometer (Ortho Cytofluorograph IIS). Excitation was at 514 nm. Signals for forward and 90-degree light scatter and fluorescence above 550 nm were collected for 5×10^3 cells using the 90-degree light scatter parameter as the master signal. The flow cytometer was calibrated using rhodamine labeled beads — FluoSpheres™ (Molecular Probes).

2.8. Fluorescence microscopy

A Bio-Rad MRC 600 laser scanning confocal imaging system based on a Zeiss Axioplan microscope and a krypton/argon laser was employed. A plan-apo objective (×60, numerical aperture 1.4, oil) was used. The ADR and FITC fluorescence images were accumulated via the BHS block of filters (excitation at 488 nm and emission through a 515 nm barrier filter) and the rhodamine (RITC) fluorescence image was collected via the GHS block filter (excitation at 514 nm, emission through a 550 nm barrier filter). A coverslip containing fixed cells was mounted on a microscope slide in PBS, 90% glycerol, 50 mM NaN_3 supported on lacquer tiers to prevent the cells from being compressed. The NaN_3 was used to inhibit photobleaching. The microscope was adjusted in such a way that non-stained, control cells did not generate a signal. Fluorescence images were scaled to 256 gray levels.

3. Results and discussion

3.1. Subcellular trafficking of HPMA copolymers targeted by N-acylated galactosamine to HepG2 cells

One of the ways to monitor subcellular trafficking of HPMA copolymer conjugates is to demonstrate their colocalization with known markers of cell organelles. There are two main groups of lysosomal markers. The first group are markers taken up via receptor-mediated endocytosis: asialoglycoproteins, LDL particles, α_2-macroglobulin [24,25]. The second group are low molecular weight compounds containing a weak basic group. These compounds can penetrate cellular membranes. However, once in the lysosomes they become protonated and are rendered impermeable for the lysosomal membrane. Chloroquine, ammonium chloride, acridin orange

[26], and Neutral Red [22] are widely used examples of this set.

We have chosen α_2-macroglobulin to visualize the lysosomes in HepG2 cells and study its colocalization with the P-(AP-FITC)-GalN conjugate. Cells were incubated with RITC-labeled α_2-macroglobulin (10 μg/ml) for 1 h at 37°C following the incubation of cells with the conjugate (100 μg/ml) for 24 h. A short duration of incubation of cells with α_2-macroglobulin-RITC was chosen to minimize the degradation of the protein inside of lysosomes which could lead to staining of the cytoplasm with free fluorescent label. Using the two channel operation mode of the confocal fluorescence microscopy the fluorescence images of FITC and RITC were simultaneously accumulated from the optical section through the bottom part of the cells (Fig. 2). The left image in Fig. 2 is the image collected via the FITC channel. It shows fluorescence from round-shaped organelles centered around the nuclei and a diffusive fluorescence from the basal membrane. The right image is the image collected via the RITC channel. The α_2-macroglobulin-RITC as well as the conjugate were accumulated in round-shaped organelles localized in the perinuclear region of cells. The superposition of images reveals that numerous organelles emit both FITC and RITC fluorescence (some of them are marked with arrows). The FITC was coupled to polymer chain via the non-degradable aminopropyl (AP) spacer. Consequently, the FITC image corresponds to the localization of the macromolecules. The colocalization of the lysosomal marker, α_2-macroglobulin-RITC, and of the P-(AP-FITC)-GalN conjugate indicates the lysosomotropism of HPMA copolymer conjugates.

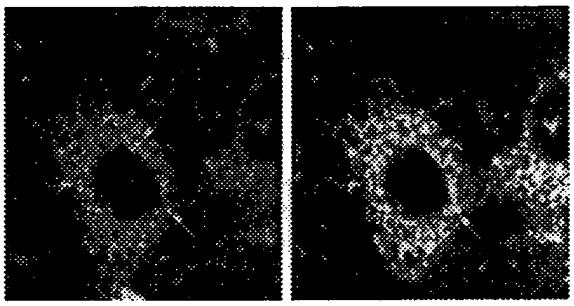

Fig. 2. Confocal fluorescence images of HepG2 cells incubated with HPMA copolymer-FITC-GalN conjugates and α_2-macroglobulin-RITC. The left image was accumulated via an FITC channel (BHS block of filters). The right image was accumulated simultaneously with the left image via an RITC channel (GHS block of filters). Arrows point to some organelles containing both the conjugates and α_2-macroglobulin.

The design of the HPMA copolymer conjugates targetable to hepatocytes and/or hepatocarcinoma cell lines was based on the specificity of the asialoglycoprotein receptor. This galactose/*N*-acetylgalactosamine-recognizing receptor is responsible for the effective clearance of desialated serum glycoproteins in vivo [25]. The data reported here are in agreement with data obtained from subcellular fractionation of rat hepatocytes after intravenous administration of ^{125}I-labeled HPMA copolymer-GalN conjugates. Fractions obtained by centrifugation in a density-gradient showed similar profiles of arylsulfatase activity (marker of lysosome enzymes) and radioactivity (polymer marker) [27].

In addition, we have demonstrated the lysosomotropism of the P-(AP-FITC)-GalN conjugate by monitoring intracellular fluorescence spectra of polymer bound FITC. It is well known that during internalization the substrates are transported in organelles which become continually acidified. This permits the use of the pH sensitivity of fluorescein fluorescence to estimate its intracellular localization. Fluorescein may exist in several different ionic forms: (I) a cation with a positive charge localized in the xanthenone ring, (II) a neutral molecule, (III) a monoanion with a negatively charged phenylcarboxylate group (pK_a=4.4), and (IV) a dianion [28]. The fluorescence emission spectra of all four forms have similar shapes [28], but the dianionic form has a much higher quantum yield of fluorescence than the monoanionic, neutral, and cationic forms. Influence of protonation of the enolic group on the absorption maxima has been used to monitor the pH value of the local environment of fluorescein in solutions as well as inside of cells [23]. The alkaline spectrum is dominated by a large peak at 492 nm. As the pH decreases, this peak gradually disappears and is replaced by two new, lower intensity peaks at 480 and 450 nm. Ratio of fluorescence intensities upon excitation at 492 nm to that with excitation at 450 nm, that is referred to as the 492/450 ratio, is used as a measure of pH. To monitor the pH value of the local environment of internalized HPMA copolymer

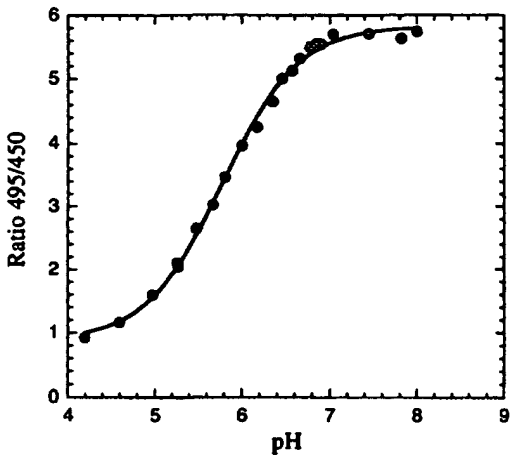

Fig. 3. Dependence of a spectral parameter of FITC fluorescence on pH. The ratio 492/450 is the ratio of intensities of fluorescence upon excitation at 492 nm and 450 nm. Fluorescence was recorded via an interference 514 nm filter. The solid line is a theoretical curve obtained as a result of fitting of experimental points with Eq. (1).

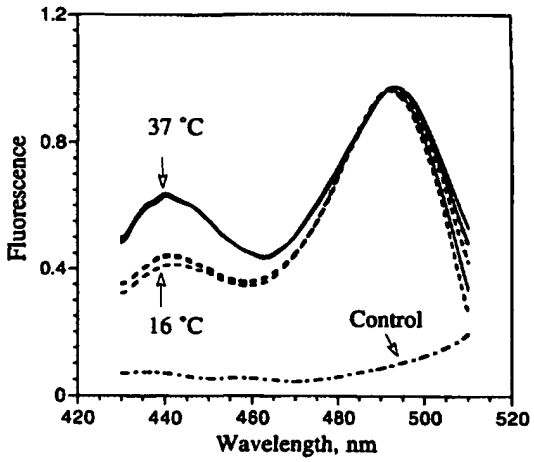

Fig. 4. Representative excitation spectra of a cell monolayer incubated with the P-(AP-FITC)-GalN conjugate for 24 h at 37°C or 16°C. Spectra were corrected on the average light scattered signal obtained from untreated cells (marked as 'control'). The ratio 492/450 of fluorescein fluorescence at 37°C was equal to 1.72±0.03 corresponding to a pH value of 5.09±0.02. After incubation of cell with the conjugate at 16°C the ratio was equal to 2.48±0.07 (pH=5.46±0.05).

conjugates, a calibration curve for the P-(AP-FITC)-GalN conjugate was determined. In Fig. 3 the dependence of the 492/450 ratio for the P-(AP-FITC)-GalN conjugate and free fluorescein on pH value are shown. Experimental points were fitted using the following equation based on ionization equilibria:

$$Y = (\lim_1 + \lim_2 \times 10^{(pH-pK)})/(1 + 10^{(pH-pK)}) \quad (1)$$

where Y is the 492/450 ratio at various pH values, $\lim_1$ is the limiting 492/450 ratio at low pH, and $\lim_2$ is the limiting 492/450 ratio at high pH. The theoretical curve was used to estimate the pH value of a conjugate environment.

Representative excitation spectra of the P-(AP-FITC)-GalN conjugate containing FITC coupled to polymer chain via a non-degradable spacer and incubated with HepG2 cells at 37°C are shown in Fig. 4. The 492/450 ratio was determined to be equal to 1.72±0.03. The value pH of the conjugate microenvironment was calculated according to Eq. (1) by using parameters of fitting experimental points. The calculated pH value was 5.09±0.02.

The conjugate incubated with cells at 16°C is supposed to be localized in endosomes [29]. Representative corrected excitation spectra of the P-(AP-FITC)-GalN conjugate incubated with cells at 16°C are shown in Fig. 4. The ratio 492/450 was determined to be equal to 2.48±0.07. The calculated pH value was 5.46±0.05. Obtained pH values are in general agreement with the pH values found in other cell types for lysosomes and endosomes, respectively [30–32].

3.2. Subcellular trafficking of HPMA copolymer targeted by OV-TL16 antibody to OVCAR-3 cells

Recently, our focus is on the evaluation of the potential of HPMA copolymer-drug conjugates targeted to human ovarian carcinoma cells with a monoclonal OV-TL16 antibody or its fragments [20,33]. The OV-TL16 antibody as well as similar antibodies (OV-TL3, OC125, and Mov18A) are considered tumor markers for epithelial-derived tumors [34,35].

Using the intrinsic fluorescence of ADR the uptake and subcellular localization of HPMA copolymer-ADR-Ab conjugates by OVCAR-3 cells was followed by confocal fluorescence microscopy. Cells were cultured in a medium containing the

P-(GG-ADR)-Ab conjugate for 24 h before fluorescence images were taken. The non-degradable spacer was used so that the images observed correspond to the conjugate and not to free drug. In Fig. 5A an image of ADR fluorescence accumulated upon an optical sectioning of OVCAR-3 cells through the middle part of the nuclei is shown. The ADR fluorescence is detectable in round-shaped organelles predominantly clustered around nuclei. The low molecular weight marker, Neutral Red, which is known to accumulate in acidic organelles was used to visualize the lysosomes in OVCAR-3 cells. The fluorescence image of cells stained with this marker showed organelles having similar morphology and localization to those containing the conjugate (Fig. 5B). So it appears that the Ab targeted conjugates end up within acidic organelles. Similar images of lysosomes containing the conjugates were observed in both cells studied. The lysosomes are centered in the perinuclear region of cells. This appears to be a general phenomenon observed during the subcellular transport of material internalized via endocytosis. Localization of lysosomes around the nuclei was also observed in electron microscopy studies [36].

3.3. Intracellular release of adriamycin from the polymer carrier

Macromolecular anticancer drug conjugates have to be designed in such a way that the spacer between the carrier and the drug is stable in the blood stream [8] but susceptible to an enzymatically catalyzed hydrolysis in the lysosomal compartment of the cells [9,10,37]. We have used confocal fluorescence microscopy to demonstrate the internalization of the HPMA copolymer conjugates, release of ADR from the polymer chain in the lysosomes, followed by the transport of ADR through the lysosomal membrane via the cytoplasm into the nuclei. Cells incubated with free ADR reveal the ADR fluorescence predominantly from nuclei [38,39]. When HepG2 cells are exposed for 30 min to free ADR, an intense nuclear fluorescence is observed by fluorescent microscopy (Fig. 6). Nuclear fluorescence of anthracyclines is likely to be due to binding of the drugs to some components of the nucleus [40] following saturation of DNA binding sites. Quenching of the antracycline's fluorescence by DNA is a known phenomenon, in fact, this quenching has been used to measure intercalation [41].

Similar staining of nuclei with ADR was observed after 24 h incubation of HepG2 cells with the P-(GFLG-ADR)-GalN conjugate (Fig. 7). The confocal fluorescence image was obtained upon localization of the focal plane in the middle of nuclei. Staining of lysosomes as well as nuclei is shown in some cells. It is important to note that cells cultured for 24 h with the P-(GG-ADR)-GalN conjugate containing ADR attached via a non-degradable spacer did not demonstrate staining of nuclei (data not shown). The pattern of ADR fluorescence emitted from lysosomes was similar to the fluorescein fluorescence after incubation of HepG2 cells with the P-(GG-FITC)-GalN conjugate (Fig. 2). This observation is supported with data obtained on ovarian carcinoma cells. ADR fluorescence was not detected in the

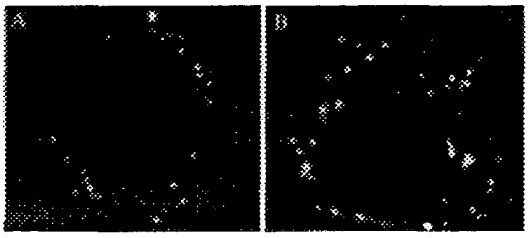

Fig. 5. Fluorescence images of OVCAR-3 cells incubated with Neutral Red (A), and with P-(GG-ADR)-Ab conjugate (B). Organelles containing the conjugate are morphologically similar to organelles containing Neutral Red.

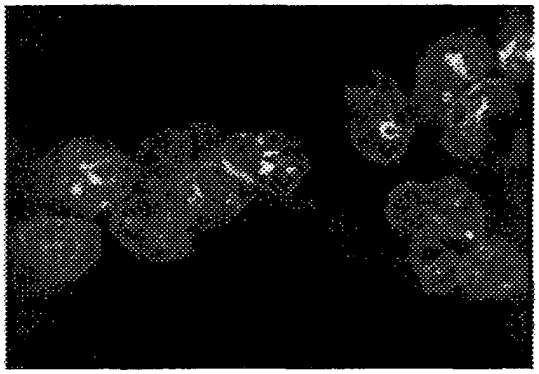

Fig. 6. Fluorescence image of HepG2 cells incubated 30 min with free ADR at 37°C. The ADR fluorescence emitted predominantly from the cell nuclei.

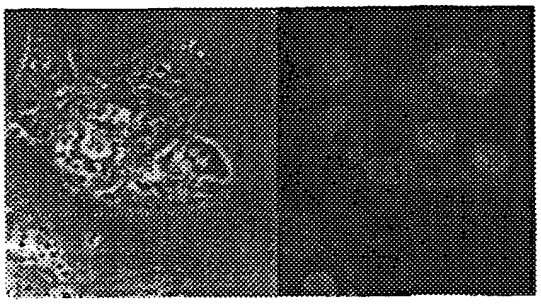

Fig. 7. Confocal images of HepG2 cells incubated with P-(GFLG-ADR)-GalN conjugate. The ADR was bound to polymer chain via the degradable spacer-tetrapeptide (GFLG). The left image is the reflection image accumulated simultaneously with the (right) ADR fluorescence image. The reflection image helps to identify nuclei, which are, as shown by the fluorescence image, stained with ADR.

nuclei of OVCAR-3 cells incubated with the non-degradable spacer-containing conjugate, P-(GG-ADR)-Ab, after 24 h (Fig. 5B); however, the nuclei were stained after incubation with P-(GFLG-ADR)-Ab conjugate (data not shown). These results indicate that the targeted drug conjugates are taken up by cells and transported into the lysosomal compartment. In this compartment ADR is released from the degradable side-chain of the conjugate and ultimately diffuses via the cytoplasm into the cell nuclei. The possibility of the nuclear staining being due to free ADR present as a contaminant in the conjugates can be ruled out since both the conjugate with degradable and with non-degradable spacers undergo identical purification procedures before coupling of targeting moiety to polymer chains.

3.4. Could lysosomal delivery of polymeric drugs overcome the MDR effect?

The ultimate success of the treatment of various carcinomas depends on the successful elimination of multidrug resistant (MDR) cancer cells [42]. Resistance of malignant tumors to chemotherapeutic agents remains the major cause of failure in cancer therapy. A membrane glycoprotein, termed P-glycoprotein, has been shown to be responsible for cross-resistance to a broad range of structurally and functionally distinct cytotoxic agents. This glycoprotein, encoded in humans by the *MDR1* gene, functions as an energy-dependent efflux pump to remove cytotoxic agents from the resistant cells [43]. It was demonstrated that P-glycoprotein overexpression diminishes drug accumulation and cytotoxicity in animal and human cells [44].

We believe that due to the differences in the mechanism of cellular uptake, polymer bound drugs have the potential to remain inside the cancer cells because their intracellular trafficking occurs in membrane limited organelles. The exclusion of the polymer-drug conjugate from the cytoplasm of the cell should render the efflux pump ineffective. Subcellular trafficking along the endocytic pathway from the plasma membrane to the perinuclear region changes the gradient of distribution of drug inside cells. A cartoon of subcellular distribution of drugs which entered cells either by diffusion or by pinocytosis is shown in Fig. 8. Whereas, in the case of the free drug the gradient is directed from the plasma membrane to the perinuclear membrane, in the case of polymer bound drugs the gradient is from the perinuclear region to the plasma membrane. The drug escapes from the lysosomal compartment in the perinuclear region. Consequently, the probability of its interaction with nuclear DNA and/or topoisomerase II is higher than the probability of its recognition by the P-glycoprotein pump.

To test our hypothesis that HPMA-copolymer-bound anticancer drugs will be inaccessible to the energy-driven efflux pump, we have compared the internalization of the HPMA copolymer-ADR conju-

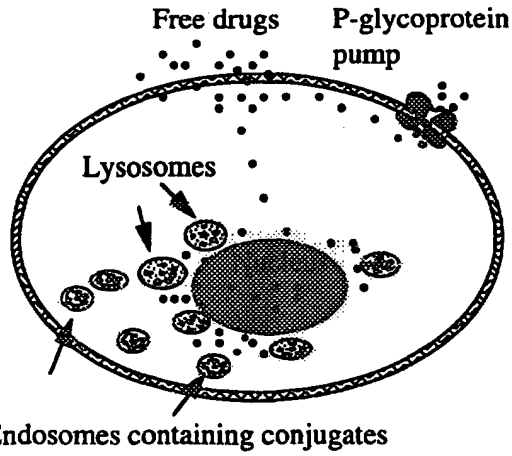

Fig. 8. Schematic drawing of subcellular distribution of drugs which entered cells either by diffusion or by pinocytosis.

gates by normal (sensitive) and ADR-resistant cell lines. Two cell lines, A2780 and A2780/AD, were chosen for these experiments. The A2780/AD cell line is a P-glycoprotein expressing cell line [45]. The ADR IC_{50} dose of the A2780/AD cell line was about 40 times higher when compared to the sensitive A2780 cell line (data not shown).

First, we have studied the accumulation of HPMA copolymer-ADR conjugate by both cell lines. Binding of ADR via a non-degradable (GG) spacer (conjugate P-(GG-ADR)) permitted the comparison of intracellular ADR concentrations by flow cytometry. We found that for the P-(GG-ADR) conjugate both the amount of ADR accumulated and the rate of accumulation were similar for the sensitive and resistant cell lines (Fig. 9). However, to be effective, ADR has to be released from the carrier in the lysosomal compartment and diffuse into the cytoplasm. To mimic a therapeutic situation, we compared the internalization of free ADR and of P-(GFLG-ADR) conjugate containing ADR bound to the HPMA copolymer via a lysosomally degradable bond (GFLG). Concentration of the conjugate used (20 μM of ADR equivalent) inhibited the growth of both resistant and sensitive cells by about 40%.

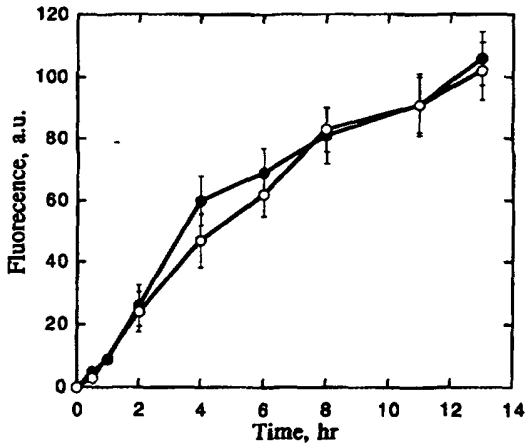

Fig. 9. Kinetics of accumulation of P-(GG-ADR) conjugate by sensitive (A2780) (●) and resistant (A2780/AD) (○) ovarian carcinoma cells. Cells were analyzed by flow cytometry following incubation (37°C, 5% CO_2) in cell culture medium containing the conjugate (20 μM of ADR equivalent) for various time intervals. Excitation was at 514 nm. The sensitive and resistant cells were incubated with the conjugate at 0°C as a control. Under those conditions no fluorescence emission was detected.

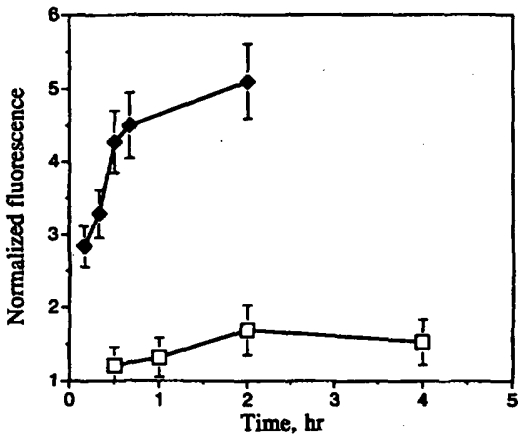

Fig. 10. The ratio of intensities of ADR fluorescence in sensitive (A2780) cells to that in resistant (A2780/AD) cells. Resistant and sensitive cells were cultured with free ADR (♦) or P-(GFLG-ADR) conjugate (□) for various time intervals. The concentration of ADR (free or in conjugate) was 20 μM. For experimental details see Fig. 9.

Following incubation with the conjugate, the ratio of fluorescence in sensitive and ADR resistant cell lines was compared (Fig. 10). The results demonstrated an increased intracellular concentration of polymer bound ADR in MDR (A2780/AD) cells when compared to free drug. After 2 h, the ratio of fluorescence in sensitive (A2780) and resistant (A2780/AD) cells of free ADR was about 5, whereas for P-(GFLG-ADR) it was only about 1.5. The data obtained seem to support our hypothesis that the change in the direction of the gradient of distribution of drug inside cells when bound to a polymer carrier results in an increased intracellular drug concentration in the latter case.

Acknowledgements

The research was supported in part by NIH National Cancer Institute Grant CA51578 and by the University of Utah Research Foundation.

References

[1] D. Putnam, J. Kopeček, Polymer conjugates with anticancer activity, Adv. Polym. Sci. 122 (1995) 55–123.

[2] R. Duncan, Drug-polymer conjugates: potential for improved chemotherapy, Anti-Cancer Drugs 3 (1992) 175–210.

[3] H. Maeda, L.M. Seymour, Y. Miyamoto, Conjugates of anticancer agents and polymers: advantages of macromolecular therapeutics in vivo, Bioconjug. Chem. 3 (1992) 351–362.

[4] L.J. Nugent, R.K. Jain, Extravascular diffusion in normal and neoplastic tissues, Cancer Res. 44 (1984) 238–244.

[5] J. Cassidy, R. Duncan, G.J. Morrison, J. Strohalm, D. Plocová, J. Kopeček, S.B. Kaye, Activity of *N*-(2-hydroxypropyl)methacrylamide copolymers containing daunomycin against a rat tumor model, Biochem. Pharmacol. 38 (1989) 875–879.

[6] F. Yuan, M. Dellian, D. Fukumura, M. Leunig, D.A. Berk, V.P. Torchilin, R.K. Jain, Vascular permeability in a human tumor xenograft: molecular size dependence and cutoff size, Cancer Res. 55 (1995) 3552–3756.

[7] H. Maeda, Polymer conjugated macromolecular drugs for tumor-specific targeting, in: A.J. Domb (Ed.), Polymeric Site-specific Pharmacotherapy, John Wiley, New York, 1994, pp. 95–116.

[8] P. Rejmanová, J. Kopeček, R. Duncan, J.B. Lloyd, Stability in rat plasma and serum of lysosomally degradable oligopeptide sequences in *N*-(2-hydroxypropyl)methacrylamide copolymers, Biomaterials 6 (1985) 45–48.

[9] J.B. Lloyd, R. Duncan, J. Kopeček, Synthetic polymers as targetable carriers for drugs, Pure Appl. Chem. 56 (1984) 1301–1304.

[10] J. Kopeček, Controlled degradability of polymers — a key to drug delivery systems, Biomaterials 5 (1984) 19–25.

[11] L.W. Seymour, R. Duncan, P. Kopečková, J. Kopeček, Potential of sugar residues attached to *N*-(2-hydroxypropyl)methacrylamide copolymers as targeting groups for the selective delivery of drugs, J. Bioact. Comp. Polym. 2 (1987) 97–119.

[12] B. Říhová, P. Kopečková, J. Strohalm, P. Rossman, V. Větvička, J. Kopeček, Antibody directed affinity therapy applied to the immune system: in vivo effectiveness and limited toxicity of DNM conjugated to HPMA copolymers and targeting antibody, Clin. Immunol. Immunopathol. 46 (1988) 100–114.

[13] M. Šťastný, B. Říhová, J. Strohalm, K. Ulbrich, Comparison of binding kinetics of antibody-targeted *N*-(2-hydroxypropyl)methacrylamide (HPMA)-bound doxorubicin in vitro and in vivo, J. Control. Release 42 (1996) 229–236.

[14] S. Mayor, J.F. Presley, F.R. Maxfield, Sorting of membrane components from endosomes and subsequent recycling to the cell surface occurs by a bulk flow process, J. Cell Biol. 121 (1993) 1257–1269.

[15] R.H. Steinman, I.S. Mellman, W.A. Muller, Z.A. Cohn, Endocytosis and the recycling of plasma membrane, J. Cell Biol. 96 (1983) 1–27.

[16] H.S. Wiley, Receptors as models for the mechanism of membrane protein turnover and dynamics, Curr. Top. Membr. Transport 24 (1985) 369–412.

[17] N.L. Krinick, Y. Sun, D. Joyner, J.D. Spikes, R.C. Straight, J. Kopeček, A polymeric drug delivery system for the simultaneous delivery of drugs activatable by enzymes and/or light, J. Biomater. Sci. Polymer. Edn. 5 (1994) 303–324.

[18] P.A. Vasey, R. Duncan, S.B. Kaye, J. Cassidy, Clinical trial of PK1 (HPMA copolymer doxorubicin), Eur. J. Cancer 31A (1995) S193.

[19] L.W. Seymour, D.R. Ferry, C. Boivin, P. Julyan, J. Doran, M. David, D. Anderson, C. Christodoulou, A.M. Young, D.J. Kerr, S. Hesslewood, Preliminary study of distribution of HPMA copolymers bearing doxorubicin and galactosamine, in: 8th International Symposium on Recent Advances in Drug Delivery Systems, Salt Lake City, Utah, February 24–27, 1997, Abstracts, pp. 132–135.

[20] V.G. Omelyanenko, P. Kopečková, C. Gentry, J.-G. Shiah, J. Kopeček, HPMA copolymer-anticancer drug-OV-TL16 antibody conjugates. 1. Influence of the methods of synthesis on the binding affinity to OVCAR-3 ovarian carcinoma cells in vitro, J. Drug Target. 3 (1996) 357–373.

[21] R.C. Rathi, P. Kopečková, B. Říhová, J. Kopeček, *N*-(2-hydroxypropyl)methacrylamide copolymers containing pendant saccharide moieties: synthesis and bioadhesive properties, J. Polym. Sci.: Part A: Polym. Chem. 29 (1991) 1895–1902.

[22] J.K. Burkhardt, F.K. Wiebel, S. Hester, J. Argon, The giant organelles in beige and chediak-higashi fibroblast are derived from late endosomes and mature lysosomes, J. Exp. Med. 178 (1993) 1845–1856.

[23] S. Ohkuma, B. Poole, Fluorescence probe measurement of the intralysosomal pH in living cells and the perturbation of pH by various agents, Proc. Natl. Acad. Sci. USA 75 (1978) 3327–3331.

[24] T.E. McGraw, F.R. Maxfield, Internalization and sorting of macromolecules, in: R.L. Juliano (Ed.), Targeted Drug Delivery, Springer, Berlin, 1991, pp. 10–41.

[25] A.L. Schwartz, The hepatic asialoglycoprotein receptor, CRC Crit. Rev. Biochem. 16 (1984) 207–233.

[26] S. Ohkuma, B. Poole, Cytoplasmic vacuolation of mouse peritoneal macrophages and the uptake into lysosomes of weakly basic substances, J. Cell Biol. 90 (1981) 656–664.

[27] R. Duncan, L.C.W. Seymour, L. Scarlett, J.B. Lloyd, P. Rejmanová, J. Kopeček, Fate of *N*-(2-hydroxypropyl)methacrylamide copolymers with pendent galactosamine residues after intravenous administration to rats, Biochim. Biophys. Acta 880 (1986) 62–71.

[28] M.M. Martin, L. Lindqvist, The pH dependence of fluorescein fluorescence, J. Luminescence 10 (1975) 381–390.

[29] N.H. Salzman, F.R. Maxfield, Fusion accessibility of endocytic compartments along the recycling and lysosomal endocytic pathways in intact cells, J. Cell Biol. 109 (1989) 2097–2104.

[30] B. Tycko, R.R. Maxfield, Rapid acidification of endocytic vesicles containing α_2-macroglobulin, Cell 28 (1982) 643–651.

[31] B. Tycko, C.H. Keith, R.R. Maxfield, Rapid acidification of endocytic vesicles containing asialoglycoprotein in cell of a human hepatoma line, J. Cell Biol. 97 (1983) 1762–1776.

[32] J. Van Renswoude, K.R. Bridges, J.B. Harford, R.D. Klausner, Receptor-mediated endocytosis of transferrin and the uptake in K562 cells: identification of a non-lysosomal

acidic compartment, Proc. Natl. Acad. Sci. USA 79 (1982) 6186–6190.

[33] V. Omelyanenko, P. Kopečková, C. Gentry, J. Kopeček, Performance of HPMA copolymer-drug conjugate targeted to ovarian carcinoma cells, in: Proceedings of 23rd International Symposium on Controlled Release of Bioactive Materials, Kyoto, Japan, 1996, p. 633.

[34] C.C. Van Niekerk, F.C.S. Rameakers, A.G.J.M. Hanselaar, J. Aldeweireldt, L.G. Poels, Changes in expression of differentiation markers between normal ovarian cells and derived tumors, Am. J. Pathol. 142 (1993) 157–177.

[35] O. Boerman, L. Massuger, K. Makkink, C. Thomas, P. Kenemans, L. Poels, Comparative in vitro binding characteristics and biodistribution in tumor-bearing athymic mice of anti-ovarian carcinoma monoclonal antibodies, Anticancer Res. 10 (1990) 1289–1296.

[36] J. Swanson, Fluorescence labeling of endocytic compartments, Methods Cell Biol. 29 (1989) 137–151.

[37] P. Rejmanová, J. Pohl, M. Baudyš, V. Kostka, J. Kopeček, Polymers containing enzymatically degradable bonds. 8. Degradation of oligopeptide sequences in *N*-(2-hydroxypropyl)methacrylamide copolymers by bovine spleen cathepsin B, Makromol. Chem. 18 (1983) 2009–2020.

[38] P.J. Smith, H.R. Sykes, M.E. Fox, I.J. Furlong, Subcellular distribution of the anticancer drug mitoxantrone in human and drug-resistant murine cells analyzed by flow cytometry and confocal microscopy and its relationship to the induction of DNA damage, Cancer Res. 52 (1992) 4000–4008.

[39] J.H.M. De Lange, N.M. Schipper, G.J. Schuurhuis, T.K. ten Kate, Th.H.M. van Heijningen, H.M. Pinedo, J. Lankelma, J.P. Baak, Quantification by laser scan microscopy of intracellular doxorubicin distribution, Cytometry 13 (1992) 571–576.

[40] J.H. Doroshow, Anthracyclines and anthracenediones, in: B.A. Chabner, D.L. Longo (Eds.), Cancer Chemotherapy and Biotherapy, Lippincott-Raven, PA, 1996, pp. 409–434.

[41] E. Calendi, A. Di Marco, M. Reggiani, B. Scarpinato, L. Valentini, On physicochemical interactions between daunomycin and nucleic acids, Biochim. Biophys. Acta 103 (1965) 25–49.

[42] D. Fennelly, Dose intensity in advanced ovarian cancer: have we answered the question?, Clin. Cancer Res. 1 (1995) 575–582.

[43] H.M. Pinedo, G. Giaccone, P-glycoprotein — a marker of cancer-cell behavior, N. Engl. J. Med. 333 (1995) 1417–1419.

[44] C.B. Hendricks, E.K. Rowinsky, L.B. Grochow, R.C. Donehower, S.C. Kaufmann, Effect of P-glycoprotein expression on the accumulation and cytotoxicity of topotecan, a new camptothecin analogue, Cancer Res. 52 (1992) 2268–2278.

[45] E.C. Spoelstra, H. Dekker, G.J. Schuurhuis, H.J. Broxterman, J. Lankelman, P-glycoprotein drug efflux pump involved in the mechanism of intrinsic drug resistance in various colon cancer cell lines. Evidence for a saturation of active adriamycin transport, Biochem. Pharmacol. 41 (1991) 349–359.

STIC-ILL

P Tomaszewski
QD350, F6

From: Schnizer, Richard
Sent: Wednesday, March 26, 2003 3:18 PM
To: STIC-ILL
Subject: 09/627,787

Please send me a copy of:

Sugiyama, Kazuo, J. Macromol. Sci. Chem. (1986), A23(10): 1155-64
102 for broad claims

Lu et al, Bioconjugate Chem. (2000) 11(1): 3-7
Poss interveneing reference

Liso et al J. Controlled Release (1995) 33(3): 429-436)
102 for broad claims?

Rihoiva et al, J. Controlled Release (1985) 2:289-310

Not sure what this is

Omelyanko et al Controlled Release (1998) 53(1-3): 25-37)
Could have fluorescine attached to HPMA

Richard Schnizer, Ph.D.
Patent Examiner
Art Unit 1635
CM1 12E17
703-306-5441
Mail Box CM1 11E12

J. MACROMOL. SCI.–CHEM., A23(10), pp. 1155-1164 (1986)

Synthesis and Hydrolysis of Polymers Having Anesthetic or Amantadine Residues in Sidechains

KAZUO SUGIYAMA

Faculty of Engineering
Kinki University
Hiro-Machi, Kure-shi, Hiroshima 737-01, Japan

ABSTRACT

The polymerizable derivatives of chemotherapeutic agents such as benzocaine, procaine, and amantadine were prepared and free-radical copolymerized with styrene or methyl methacrylate in order to obtain polymers with pharmacological activity and increased duration of action of the drugs. The monomeric and polymeric derivatives were subjected to hydrolysis in vitro in order to measure the release of the active ingredient.

INTRODUCTION

As the retention of drugs in the body can be increased by use of macromolecular controls, much interest has been manifested recently in the synthesis of pharmacologically active macromolecular compounds which are able to release the free drug component by enzymatic degradation or hydrolysis [1, 2]. A hydrolyzable bond between drug and macromolecules is required if the drug is active only in its free form. The macromolecule-drug complex then acts as a reservoir and can be considered a macromolecular prodrug. In such polymers the chemotherapeutic agents are fixed either directly or by means of

0022-233X/86/2310-1155$3.50/0

spacer groups to carrier macromolecules such as starch [3-6], protein [7, 8], and vinyl [9-15] or other [16-19] synthetic polymers. In the present work, benzocaine and procaine, well-known local anesthetics, and amantadine, a known antiviral agent, were modified or provide polymerizable derivatives for making the macromolecular prodrug with possibly prolonged activity.

EXPERIMENTAL

Materials

Benzocaine hydrochloride (ethyl 4-aminobenzoate) and procaine hydrochloride (2-(diethylamine)ethyl 4-aminobenzoate) were commercial products of the highest purity available (Aldrich, Merck). Methacrylyl chloride was prepared from methacrylic acid and benzoyl chloride [20].

Preparation of Monomeric Derivatives Without Spacer Group, 1. 100 mmol of drug was dissolved in 300 mL freshly distilled chloroform and 120 mmol triethylamine. Then 5 mg 1,4-benzoquinone was added with stirring and cooling at 0°C, and 120 mmol methacrylyl chloride was dropped into the solution. After stirring 1.5 h at 0°C, ~200 mL water was added to the reaction mixture. The chloroform layer was washed with water and evaporated to dryness. The sticky residue obtained was left to crystallize for a week at 0°C and recrystallized from ethanol-ether.

1a: mp 106-108°C, yield 88.4%. NMR ($CDCl_3$), δ (ppm): 1.3 (t, 3H,$CH_2\underline{CH_3}$), 2.0 (s,3H,$\underline{CH_3}$), 4.4 (q,2H,$\underline{CH_2}CH_3$), 5.4 (m,1H,H–CH=), 6.7 (m,1H,H–CH=), 7.5-8.2 (q,4H,aromatic), 8.4 (br,1H,CONH). $C_{13}H_{15}NO_3$ = 233.267. Calculated: C:H:N = 66.96:6.48:6.00%. Found: C:H:N = 66.24:6.54:5.86%.

1b: mp 78-80°C, yield 57.2%. NMR ($CDCl_3$), δ (ppm): 1.4 (t, 6H,$CH_2\underline{CH_3}$), 2.0 (s,3H,CH_3), 2.7 (q,4H,$\underline{CH_2}CH_3$), 2.8 (t,2H,$CH_2\underline{CH_2}N$), 4.4 (t,2H,$\underline{CH_2}CH_2N$), 5.5 (m,1H,H–CH=), 6.8 (m,1H,H–CH=), 7.8 (q, 4H, aromatic), 8.3 (br,1H,CONH). $C_{17}H_{24}N_2O_3$ = 304.389. Calculated: C:H:N = 67.08:7.97:9.20%. Found: C:H:N = 67.56:7.75:9.16%.

1c: 104-105°C, yield 53.2%. NMR ($CDCl_3$), δ (ppm): 1.7 (s, 3H,$\underline{CH_3}$), 1.5-2.3 (m,15H, adamantyl), 5.3 (m,1H,H–CH=), 6.5 (m, 1H,H–CH=). $C_{14}H_{21}NO$ = 219.330. Calculated: C:H:N = 76.67:9.65: 6.39%. Found: C:H:N = 76.55:9.45:6.42%.

Preparation of Imine, 3. 50 mmol vanillin and drug in 300 mL dry benzene was heated under reflux for 10 h, during which time

an equimolar quar
After removal of
90% yield by recr
3a: mp 148-14
3.9 (s,3H,OCH3),
8.4 (s,1H,CH=N).
5.72:4.68%. Foun
3b: mp 86-88°
(q,4H,CH2CH3),
CH2N), 7.4 (q,4H
C21H26N2O4 = 3(
C:H:N = 69.30:7.(
3c: mp 147-1
adamantyl), 3.5 (
CH=N). C18H23
Found: C:H:N =
Preparatic
Group, 2. 30
and 36 mmol trie
while stirring an
was slowly adde
mL water was a
was washed with
tained was recry
2a: mp 93-9
CH2CH3), 2.1 (s
(m,1H,H–CH=),
1H,CH=N). C21
3.81%. Found:
2b: mp 86-8
CH2CH3), 2.2 (s
3.9 (s,3H,OCH3
1H,H–CH=), 7.5
1H,CH=N). C25
6.39%. Found:
2c: mp 117-
3H,CH3), 1.6-2.
H–CH=), 6.3 (m

an equimolar quantity of water was collected in a Dean-Stark trap. After removal of the solvent, the pure imine was obtained in above 90% yield by recrystallization from ethanol.

3a: mp 148-149°C. NMR ($CDCl_3$), δ (ppm): 1.4 (t,3H, $CH_2\underline{CH}_3$), 3.9 (s,3H,$OC\underline{H}_3$), 4.2-4.6 (q,2H,$C\underline{H}_2CH_3$), 7.1-8.3 (m,7H, aromatic), 8.4 (s,1H,$C\underline{H}$=N). $C_{17}H_{17}NO_4$ = 299.326. Calculated: C:H:N = 68.22:5.72:4.68%. Found: C:H:N = 67.83:5.53:4.73%.

3b: mp 86-88°C. NMR ($CDCl_3$), δ (ppm): 1.1 (t,6H,$CH_2\underline{CH}_3$), 2.6 (q,4H,$C\underline{H}_2CH_3$), 2.9 (t,2H,$CH_2\underline{CH}_2N$), 3.9 (s,3H,$OC\underline{H}_3$), 4.4 (t,2H,$C\underline{H}_2CH_2N$), 7.4 (q,4H, aromatic), 6.8-8.1 (m,3H, aromatic), 8.3 (s,1H,$C\underline{H}$=N). $C_{21}H_{26}N_2O_4$ = 362.477. Calculated: C:H:N = 69.59:7.23:7.73%. Found: C:H:N = 69.30:7.00:7.95%.

3c: mp 147-148°C. NMR ($CDCl_3$), δ (ppm): 1.3-2.3 (m,15H, adamantyl), 3.5 (s,3H,$OC\underline{H}_3$), 6.4-7.4 (m,3H, aromatic), 7.8 (s,1H, $C\underline{H}$=N). $C_{18}H_{23}NO_2$ = 285.391. Calculated: C:H:N = 75.76:8.12:4.91%. Found: C:H:N = 75.55:7.85:4.90%.

Preparation of Monomeric Derivatives with Spacer Group, 2. 30 mmol of 3 was dissolved in 200 mL dry chloroform and 36 mmol triethylamine. Then 5 mg 1,4-benzoquinone was added while stirring and cooling at 0°C, and 36 mmol methacrylyl chloride was slowly added to the solution. After stirring for 1.5 h at 0°C, 200 mL water was added to the reaction mixture. The chloroform layer was washed with water and evaporated to dryness. The product obtained was recrystallized from ethanol and ether.

2a: mp 93-94°C, yield 33.4%. NMR ($CDCl_3$), δ (ppm): 1.3 (t,3H, $CH_2\underline{CH}_3$), 2.1 (s,3H,$C\underline{H}_3$), 3.8 (s,3H,$OC\underline{H}_3$), 4.4 (q,2H,$C\underline{H}_2CH_3$), 5.6 (m,1H,$\underline{H}$–CH=), 6.4 (m,1H,$\underline{H}$–CH=), 7.0-8.2 (m,7H, aromatic), 8.4 (s, 1H,$C\underline{H}$=N). $C_{21}H_{21}NO_5$ = 367.401. Calculated: C:H:N = 68.65:5.76:3.81%. Found: C:H:N = 68.55:5.90:3.80%.

2b: mp 86-88°C, yield 30.4%. NMR ($CDCl_3$), δ (ppm): 1.3 (t,6H, $CH_2\underline{CH}_3$), 2.2 (s,3H,$C\underline{H}_3$), 2.7 (q,4H,$C\underline{H}_2CH_3$), 3.0 (t,2H,$CH_2\underline{CH}_2N$), 3.9 (s,3H,$OC\underline{H}_3$), 4.5 (t,2H,$C\underline{H}_2CH_2N$), 5.7 (m,1H,$\underline{H}$–CH=), 6.3 (m, 1H,$\underline{H}$–CH=), 7.5 (q,4H, aromatic), 7.1-8.2 (m,3H, aromatic), 8.4 (s, 1H,$C\underline{H}$=N). $C_{25}H_{30}N_2O_5$ = 438.524. Calculated: C:H:N = 68.47:6.90:6.39%. Found: C:H:N = 68.01:6.80:6.50%.

2c: mp 117-119°C, yield 46.2%. NMR ($CDCl_3$) δ (ppm): 1.5 (t, 3H,$C\underline{H}_3$), 1.6-2.3 (m,15H, adamantyl), 3.7 (s,3H,$OC\underline{H}_3$), 5.5 (m,1H, $\underline{H}$–CH=), 6.3 (m,1H,$\underline{H}$–CH=), 6.9-7.5 (m,3H, aromatic), 8.1 (s,1H,

CH=N). $C_{22}H_{27}NO_3$ = 353.467. Calculated: C:H:N = 74.76:7.70:3.96%. Found: C:H:N = 74.55:7.81:3.75%.

Polymerization Procedure

15 mL dimethylsulfoxide solution containing the required amounts of monomeric drug derivative, comonomer, and 0.01 g azobisisobutyronitrile (AIBN) in a glass tube was degassed by the freeze-thaw technique using a Dry-Ice/methanol bath and sealed in vacuo. The sealed tube was shaken at 60°C. After polymerization for 3.5-6 h, the content of the tube was poured into a large amount of methanol (or petroleum ether) to precipitate the polymer. The intrinsic viscosities $[\eta]$ of the polymer were determined in dimethylformamide (DMF) at 30°C with an Ubbelohde viscometer after recrystallization from DMF-methanol. The composition ratios of the copolymers were calculated from the nitrogen content as obtained by elemental analyses.

Hydrolysis Procedure

A known amount of sample was sealed in a small packet made of filter paper (Toyo No. 5C). The packet was then placed in a 100-mL Erlenmeyer flask containing 30 mL of an aqueous solution with a specific pH. The flask was shaken in a thermostat maintained at 37°C. After hydrolysis for a given time, the aqueous layer was made basic and extracted with chloroform. The degree of hydrolysis was followed by the determination of the amount of drug in the chloroform, using calibration curves obtained independently against an internal standard, with a Shimadzu LC 5A HPLC (Column Zorbax sil 4.6 mm × 25 cm P.N.). The calibrations were as follows:

$y = 0.1859x + 0.0113$ for benzocaine (internal standard: thianthrene)

$y = 0.000952x - 0.01779$ for procaine (internal standard: thianthrene)

$y = 0.0102x - 0.0025$ for amantadine (internal standard: p-aminoethylbenzoate)

where x and y are the molar ratio in the feed (drug/standard) and the ratio of the area obtained from HPLC, respectively.

POLYMERS WI

Preparation
Derivatives

Polymerizab
acylation of the
Unsaturated der
vanillin as a sp
the effect on the
In order to o
drug, hydrolysi

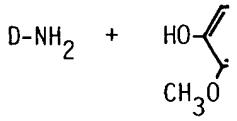

SCHEME 1.

74.76:7.70:3.96%.

quired amounts
; azobisisobutyro-
eze-thaw tech-
uo. The sealed
5-6 h, the con-
hanol (or petro-
viscosities [η]
: (DMF) at 30°C
rom DMF-meth-
calculated from

cket made of
d in a 100-mL
ion with a spe-
ined at 37°C.
is made basic
is was followed
oform, using
ernal standard,
nm × 25 cm

ard:

dard:

ard:

ndard) and

RESULTS AND DISCUSSION

Preparation and Hydrolysis of Monomeric Derivatives

Polymerizable derivatives of the drugs, 1, were prepared by direct acylation of the amino groups of the drugs with methacrylyl chloride. Unsaturated derivatives containing the drug covalently fixed through vanillin as a spacer group, 2, were also synthesized in order to study the effect on the rate of release of the drug (Scheme 1).

In order to obtain basic information for the macromolecular prodrug, hydrolysis of monomeric derivatives 1 and 2 was first carried

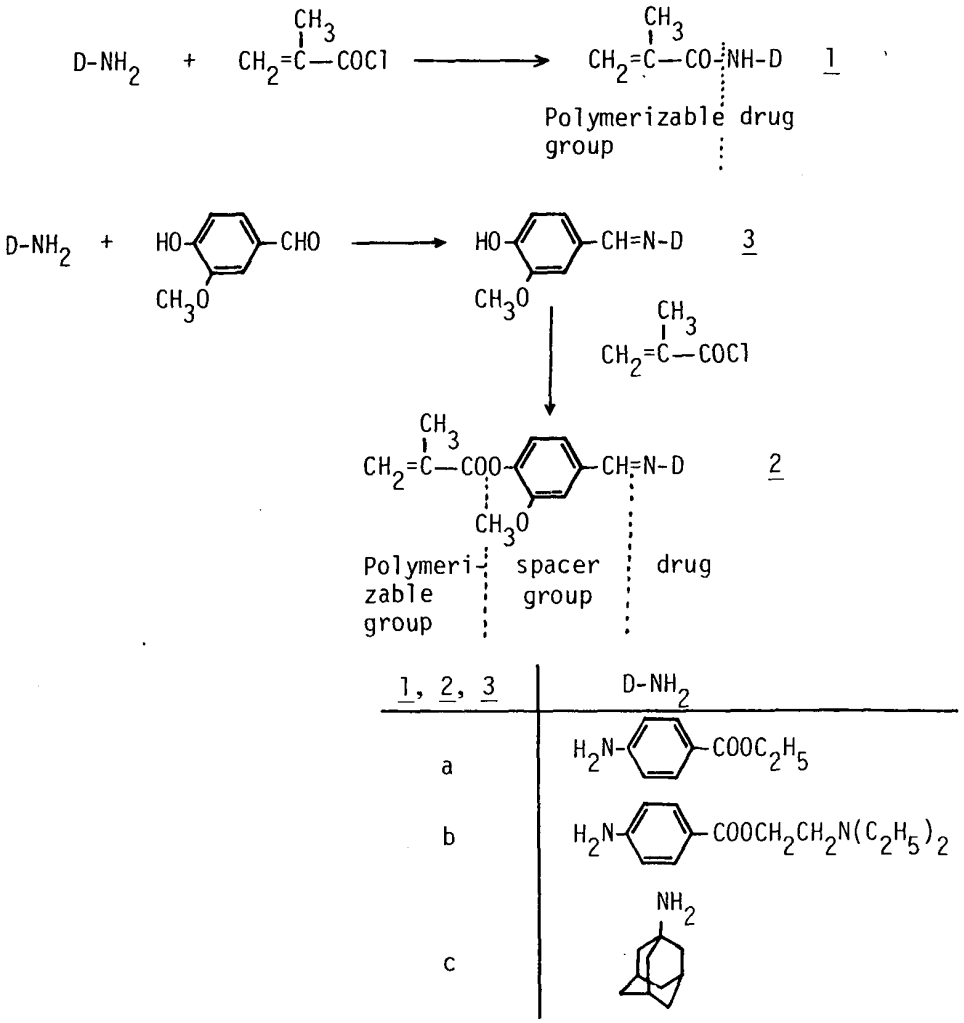

SCHEME 1.

out heterogeneously in the pH range 1-7.5 at 37°C. These compounds are expected to be the active ingredient releasing the drug and, therefore, solutions of pH 1 and about 7 were employed to simulate the pH of gastric juice and saliva, respectively. The hydrolysis of polymerizable anesthetic monomers was first carried out at 37°C, varying the pH. Both derivatives with spacer groups (2a and 2b) hydrolyzed to give the anesthetic in large yield at pH 1, as can be seen in Figs. 1 and 2. On the other hand, the rate of hydrolysis of the directly fixed drugs (1a and 1b) was low and hardly affected by the pH of the reaction media. Accordingly, these monomeric drugs with spacer groups will be appreciably hydrolyzed in gastric juice, but will not be hydrolyzed by saliva. The rate of drug release from each monomer and reaction time are shown in Fig. 3. The rate of hydrolysis of monomeric derivatives with spacer groups 2 was found to be very fast, while that of hydrolysis of derivatives without spacer group 1 was found to be slow. Consequently, the susceptibility of polymerizable derivatives to hydrolysis is greater when spacer groups are present. The rate of drug release of 1 is too slow for practical purposes.

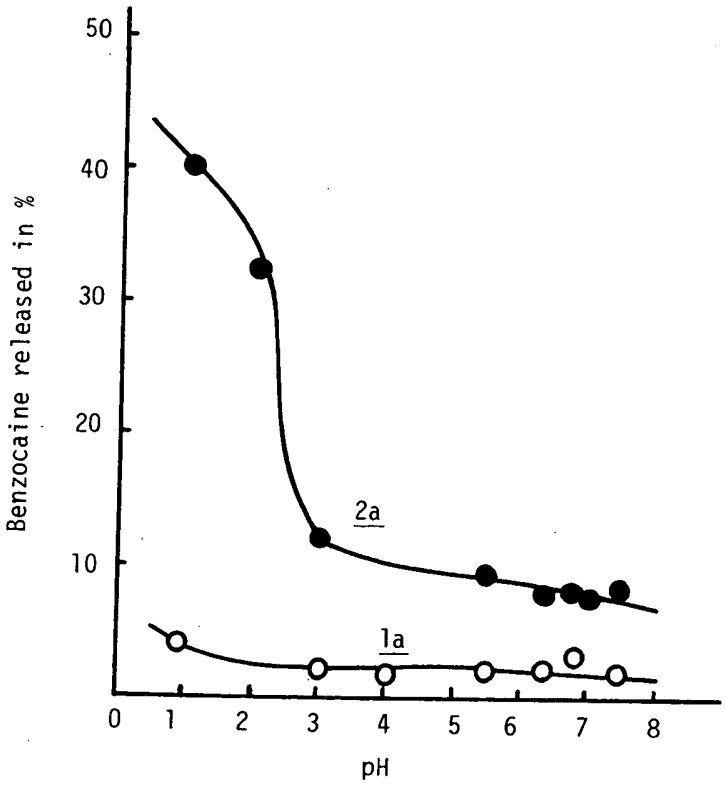

FIG. 1. Effect of pH on the hydrolysis of monomeric benzocaine derivatives without spacer 1a (○) and with spacer 2a ( ) at 37°C for 6 h. Sample: 50 mg.

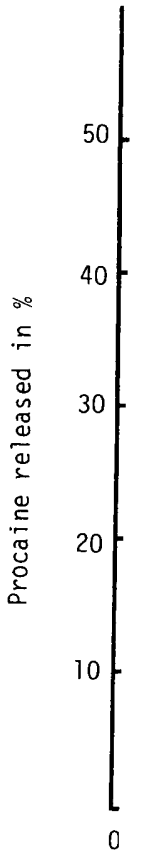

FIG. 2. Effect
derivatives witho
for 6 h. Sample:

Preparation a Derivatives

The monomeri
styrene (ST) and
drugs. All of the
aprotic solvents,
hexamethylphosph
ethyl ether. Char

The polymeric
at 37°C for 24 an
macromolecular
ingredients (Tabl

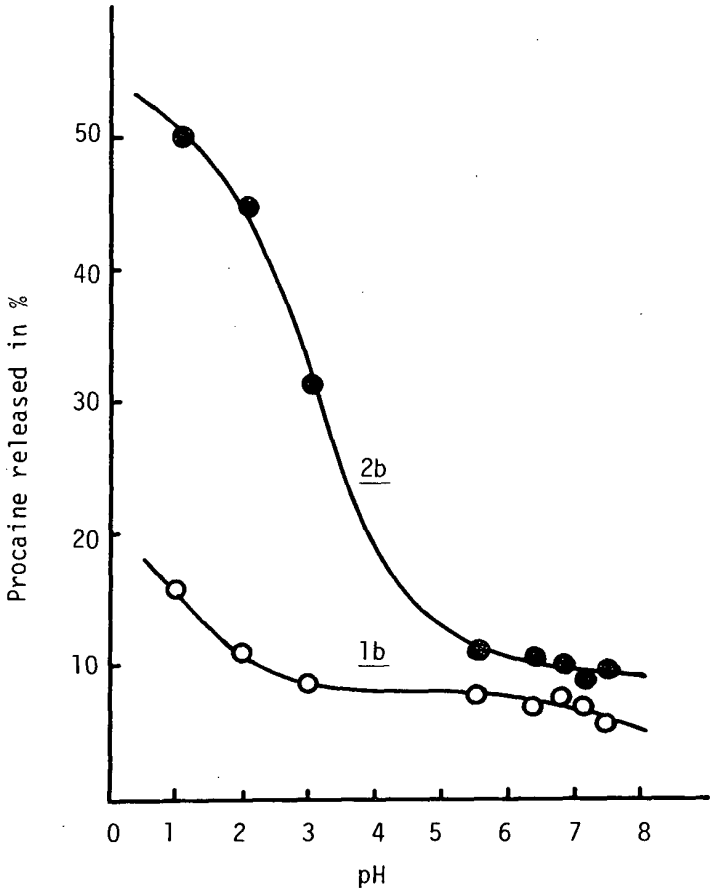

FIG. 2. Effect of pH on the hydrolysis of monomeric procaine derivatives without spacer 1b (○) and with spacer 2b (●) at 37°C for 6 h. Sample: 50 mg.

Preparation and Hydrolysis of Polymeric Derivatives

The monomeric derivatives were free-radical copolymerized with styrene (ST) and methyl methacrylate (MMA) to obtain the polymeric drugs. All of these macromolecular prodrugs were soluble in polar aprotic solvents, such as dimethylformamide, dimethylsulfoxide, and hexamethylphosphoramide, but insoluble in benzene, ethanol, and diethyl ether. Characterization data are shown in Table 1.

The polymeric derivatives were also hydrolyzed heterogeneously at 37°C for 24 and 48 h in order to study their potential use as the macromolecular prodrugs for the controlled slow release of active ingredients (Table 1). It was found that the copolymers with MMA

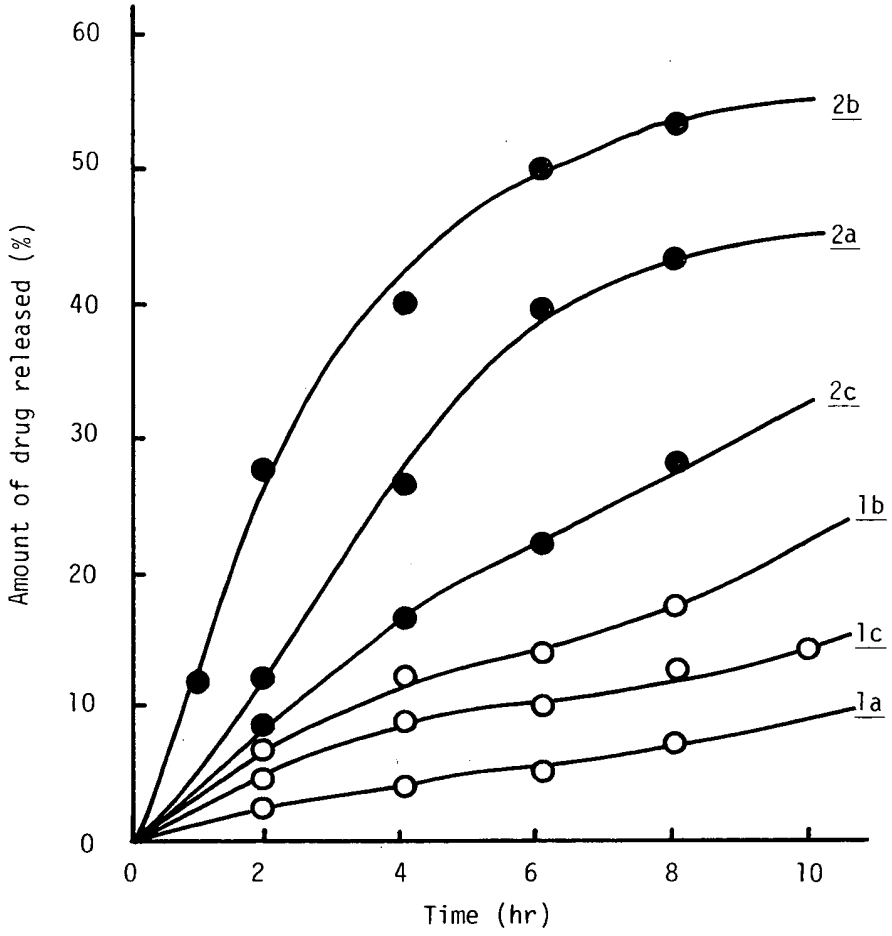

FIG. 3. Hydrolysis of monomeric drug derivatives without spacer 1 (○) and with spacer 2 (●) at 37°C, pH 1. Sample: 50 mg.

tend to be hydrolyzed more easily than those with ST. This might be because poly(methyl methacrylate) is more permeable to water than is poly(styrene) [21]. It was also found that the hydrolysis of copolymer with 2 occurred more easily than that of copolymer with 1. As for the monomers, the spacer group works effectively in all of the copolymers. These macromolecular prodrugs are then hydrolyzed acid-catalytically by gastric juice to remove local anesthetic or amantadine, nontoxic vanillin, and polymeric carrier residue.

The conclusions to be drawn from results are as follows: 1) vanillin as a spacer group plays an important role in hydrolysis, 2) these prodrugs can be hydrolyzed by gastric juice to give the free drug, 3) they are expected to increase the duration of drug action by controlled slow release of drug even though the prodrugs were not examined in vivo.

TABLE 1. Results of the Copolymerization of Monomeric Derivatives with Comonomer and Hydrolysis of Polymeric Derivatives

Monomeric derivatives, mmol	Comonomer, mmol	Polymerization time, h	Yield, %	$[\eta]$, dL/g	N content of copolymer, %	Mole fraction of drug unit in copolymer	Drug released,[a] %	
							24 h	48 h

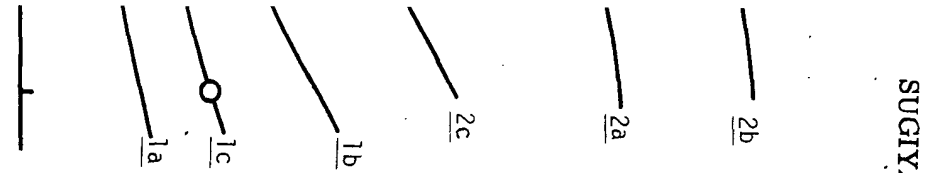

without spacer
0 mg.

This might be
to water than
lysis of copoly-
r with 1. As
in all of the co-
ydrolyzed acid-
c or amantadine,

lows: 1) vanil-
ysis, 2) these
free drug, 3)
n by controlled
t examined in

TABLE 1. Results of the Copolymerization of Monomeric Derivatives with Comonomer and Hydrolysis of Polymeric Derivatives

Monomeric derivatives, mmol	Comonomer, mmol	Polymerization time, h	Yield, %	$[\eta]$, dL/g	N content of copolymer, %	Mole fraction of drug unit in copolymer	Drug released,[a] %	
							24 h	48 h
1a 4.29	MMA 28.2	3.5	19.2	0.39	1.79	0.15	3.20	3.30
1a 4.29	ST 26.0	5.0	8.8	0.20	1.64	0.14	2.23	5.00
1b 3.29	MMA 28.2	3.5	14.5	0.13	2.56	0.11	12.7	16.0
1b 3.29	ST 26.0	6.0	27.8	0.15	2.23	0.10	11.9	15.2
1c 4.56	MMA 28.2	6.0	32.1	0.61	1.82	0.15	13.0	-
1c 4.56	ST 26.0	6.0	28.2	0.24	1.81	0.16	6.4	-
2a 2.72	MMA 28.2	3.5	19.1	0.27	1.79	0.19	16.8	24.3
2a 2.72	ST 26.0	5.0	16.4	0.33	1.72	0.19	14.4	22.1
2b 2.28	MMA 28.2	3.5	23.0	0.23	2.11	0.10	31.6	49.7
2b 2.28	ST 26.0	6.0	11.0	0.30	2.37	0.12	11.9	15.2
2c 2.83	MMA 28.2	6.0	33.2	0.55	1.90	0.08	27.7	-
2c 2.83	ST 26.0	6.0	15.3	0.13	2.90	0.15	18.3	-

[a]Hydrolysis of copolymers was carried out in aqueous solution of pH 1 at 37°C. Sample sizes: 500 mg.

REFERENCES

[1] L. G. Donaruma and O. Vogl, Polymeric Drugs, Academic, New York, 1978.
[2] H. Ringsdorf, J. Polym. Sci., Polym. Symp. Ed., 51, 135 (1975).
[3] J. A. Campbell, J. Pharm. Sci., 52, 76 (1963).
[4] B. Z. Weiner, M. Tahan, and A. Zilkha, J. Med. Chem., 15, 410 (1972).
[5] F. Lapicque and E. Dellacheaie, Makromol. Chem., 184, 277 (1983).
[6] A. A. Harris, A. K. Redersen, P. Stenberg, U. Ulmusten, and L. Wingerup, J. Pharm. Sci., 69, 1271 (1980).
[7] M. Asano, M. Yoshida, and I. Kaetsu, Kobunshi Ronbunshu, 39, 327 (1982).
[8] M. Asano, M. Yoshida, I. Kaetsu, K. Nakai, H. Yamanaka, H. Yuasa, and K. Shida, Ibid., 40, 525 (1983).
[9] J. Bartulin, M. Przybylsky, H. Ringsdorf, and H. Ritter, Makromol. Chem., 175, 1007 (1974).
[10] H. Ritter, Makromol. Chem., Rapid Commun., 3, 431 (1982).
[11] H. Ringsdorf, H. Ritter, and H. Rolly, Makromol. Chem., 177, 741 (1976).
[12] K. Kondo, A. Takimoto, and K. Takemoto, Makromol. Chem., Rapid Commun., 4, 341 (1983).
[13] V. Hoffmann, H. Ringsdorf, A. Seganova, and W.-H. Wagner, Makromol. Chem., 180, 837 (1979).
[14] A. Lääne, M. Haga, and A. Aaviksaar, Ibid., 184, 1339 (1983).
[15] J.-C. Soutif, F. M.-Moussounda, and J.-C. Brosse, Makromol. Chem., Rapid Commun., 4, 61 (1983).
[16] M. D. Purgett, W. Deits, and O. Vogl, J. Polym. Sci., Polym. Chem. Ed., 20, 2477 (1982).
[17] L. G. Donaruma and J. Razzano, J. Polym. Sci., 14, 244 (1971).
[18] B.-Z. Weiner and A. Zilka, J. Med. Chem., 16, 573 (1973).
[19] H. R. Allcock, P. E. Austin, and T. X. Neeman, Macromolecules, 15, 689 (1982).
[20] G. H. Stempel Jr., R. P. Cross, and R. P. Mariella, J. Am. Chem. Soc., 72, 2299 (1950).
[21] D. W. Morgan, Ind. Eng. Chem., 45, 2296 (1953).

Received July 23, 1985

Vinyl Polymeri
Compounds o
Selective Graft

N. MOSZNER, M.

Department of Ch
Friedrich Schille
6900 Jena, Germa

Grafting of me
sulfoxide-co-t
num(III) chlor
tained graft co
chromium(II)
amide. By thi
polymers can

In previous pa
transition metals
vanadium(III) chl
graft copolymeri
meric sulfoxides.
generated by the
and a polymer ba

$$P\text{–}X + Me^{Z+} -$$

STIC-ILL

From: Schnizer, Richard
Sent: Wednesday, March 26, 2003 3:18 PM
To: STIC-ILL
Subject: 09/627,787

Please send me a copy of:

Sugiyama, Kazuo, J. Macromol. Sci. Chem. (1986), A23(10): 1155-64
102 for broad claims

Lu et al, Bioconjugate Chem. (2000) 11(1): 3-7
Poss interveneing reference

Liso et al J. Controlled Release (1995) 33(3): 429-436)
102 for broad claims?

Rihoiva et al, J. Controlled Release (1985) 2:289-310

Not sure what this is

Omelyanko et al Controlled Release (1998) 53(1-3): 25-37)
Could have fluorescine attached to HPMA

Richard Schnizer, Ph.D.
Patent Examiner
Art Unit 1635
CM1 12E17
703-306-5441
Mail Box CM1 11E12

COMMUNICATIONS

Synthesis of Bioadhesive Lectin-HPMA Copolymer–Cyclosporin Conjugates

Zheng-Rong Lu,[†] Song-Qi Gao,[†] Pavla Kopečková,[†,‡] and Jindřich Kopeček*[,†,‡]

Departments of Pharmaceutics and Pharmaceutical Chemistry/CCCD, and Bioengineering, University of Utah, Salt Lake City, Utah 84112. Received July 26, 1999

An amino group containing cyclosporin A (CsA) derivative has been synthesized and conjugated to *N*-(2-hydroxypropyl)methacrylamide (HPMA) copolymer via an aromatic azo bond, which can be specifically cleaved by azoreductase activity in colon to release the drug for the treatment of colon diseases. Lectins, peanut (*Arachis hypogea*) agglutinin (PNA) and wheat germ agglutinin (WGA), have been conjugated to HPMA copolymer–CsA derivative conjugates (PCsA), respectively, to give bioadhesive conjugates. The PNA and WGA are the targeting proteins that can bind to diseased colon tissue and healthy tissue, respectively. There were on average four P(CsA) copolymer chains attached on one WGA molecule with a drug content of 16.0 wt % and five P(CsA) copolymer chains attached on one PNA molecule with a drug content of 11.5 wt %. The incubation of a P(CsA) copolymer with the rat cecal contents resulted in the cleavage of the azo bond and release of the cyclosporin derivative. The biological evaluation of the conjugates is under way.

Cyclosporin A (CsA)[1] is a lipophilic cyclic undecapeptide with unique immunosuppressive properties. It is widely used in organ transplantation and was also found to be effective in the treatment of inflammatory bowel diseases (IBD) (ulcerative colitis, Crohn's disease) (*1–3*). The oral administration of the drug has shown some success in the treatment of the IBD. However, it has been found that CsA was predominantly absorbed in the small intestine after oral administration (*4*), and significant nephrotoxicity and other toxic side effects were associated with the administration of high doses of CsA (*5*). A placebo-controlled trial showed that CsA enemas for ulcerative colitis were not efficacious because of its poor aqueous solubility and its low absorption via colon (*6*). Therefore, alternative ways are required to increase the aqueous solubility of CsA to deliver it specifically to the disease sites in the colon and enhance its efficacy with concomitant reduction of side effects.

The colon-specific bioadhesive, water-soluble polymeric delivery system may be one of the options to specifically deliver CsA to the colon (*7*). The CsA solubility can be dramatically increased by attachment to water-soluble polymers. The site-specific colon delivery can be achieved by the conjugation of the drug via an aromatic azo linkage and the introduction of biorecognizable moieties such as lectins. The specific azoreductase activities in the colon of many species (*8*) can cleave the azo linkage to release the drug (*7*). Lectins are proteins or glycoproteins of nonimmunological origin, capable of recognizing and binding to the antigens (carbohydrates) expressed in the tissue or on cell surface and have potential in oral colon-specific drug delivery (*9*). The differences in the structure of the carbohydrates result in the selective bioadhesion of lectins. For example, peanut (*Arachis hypogea*) agglutinin (PNA) binds to the Thomson–Friedenreich (TF) antigen, which has an increased expression in the diseased colon tissue (e.g., in ulcerative colitis). The binding of PNA to the diseased tissue is proportional to the severity of ulcerative colitis (*10*), whereas wheat germ agglutinin (WGA) binds to brush border and goblet cell mucins in healthy colon tissue (*11*). Previously, we conjugated lectins, PNA and WGA, to *N*-(2-hydroxypropyl)methacrylamide (HPMA) copolymer, a water-soluble drug carrier, and found that the polymeric conjugates showed different binding patterns in the healthy rat intestinal tissue (*12*). HPMA copolymer–WGA conjugate bound strongly to the intestinal tissue, and the HPMA copolymer–PNA conjugate bound minimally, but specifically. The results suggested that the lectin–HPMA

* To whom correspondence should be addressed. Phone: (+801) 581 4532. Fax: (+801) 581 3674. E-mail: Jindrich.Kopecek@m.cc.utah.edu.

[†] Department of Pharmaceutics and Pharmaceutical Chemistry/CCCD.

[‡] Department of Bioengineering.

[1] Abbreviations: AIBN, 2,2′-azobisisobutyronitrile; CsA, cyclosporin A; DCC, dicyclohexyl carbodiimide; DCU, dicyclohexyl urea; DMSO, dimethyl sulfoxide; HPMA, *N*-(2-hydroxypropyl)-methacrylamide; IBD, inflammatory bowel disease; MA, methacryloyl; MeBmt, 2-*N*-methyl-(*R*)-((*E*)-2-butenyl)-4-methyl-L-threonine; M_n, number average molecular mass; M_w, weight average molecular mass; ONp, *p*-nitrophenoxy; P(CsA), HPMA copolymer-CsA derivative conjugate; PBS, phosphate-buffered saline; PNA, peanut (*Arachis hypogea*) agglutinin; PNA-PCsA, peanut (*Arachis hypogea*) agglutinin-HPMA copolymer-CsA derivative conjugate; SEC, size-exclusion chromatography; THF, tetrahydrofurn; WGA, wheat germ agglutinin; WGA-PCsA, wheat germ agglutinin-HPMA copolymer-CsA derivative conjugate; wt %, weight percentage.

10.1021/bc990098a CCC: $19.00
Published on Web 12/10/1999

Scheme 1. Synthesis of Amino Group Containing CsA Derivative 3[a]

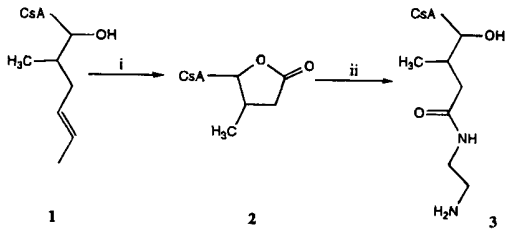

[a] (i) $NaIO_4$, $KMnO_4$, K_2CO_3, H_2O, t-BuOH, 14 h, 92%; (ii) $NH_2CH_2CH_2NH_2$, THF, reflux, 24 h, 60%.

Scheme 2. Synthesis of Monomer 9[a]

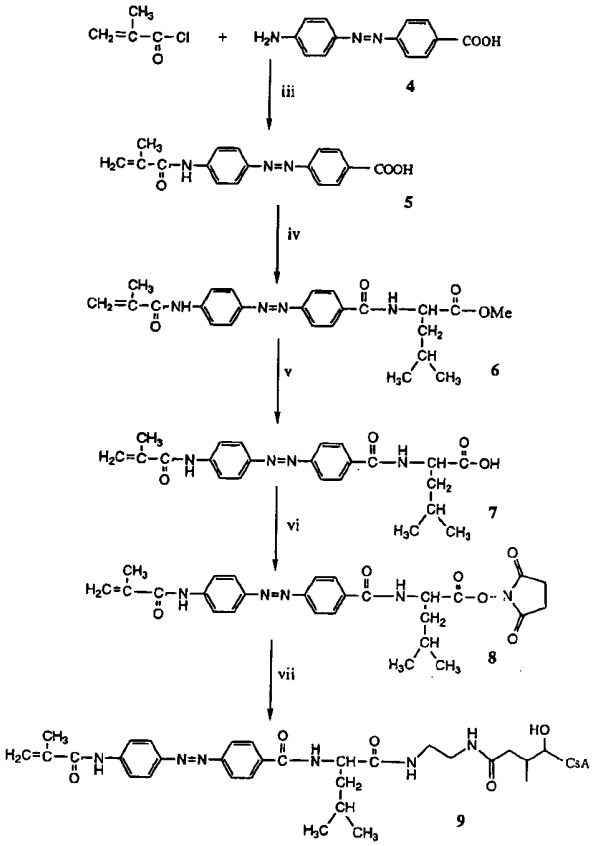

[a] (iii) Diisopropylethylamine, CH_2Cl_2, rt, overnight, 52%; (iv) L-leucine methyl ester hydrochloride, diisopropylethylamine, DCC, CH_2Cl_2, 4 °C, overnight, 57%; (v) NaOH, rt, 6 h, HCl, 81%; (vi) *N*-hydroxysuccinimide, DCC, THF/CH_2Cl_2 (1:1), 4 °C, overnight, 49%; (vii) 3, THF, rt, 24 h, 68%.

copolymer conjugates could be suitable carriers for colon site-specific delivery of CsA.

We report on the synthesis of lectin (PNA or WGA)–HPMA copolymer–CsA derivative conjugates for site-specific colon delivery. An HPMA copolymer precursor containing a CsA derivative and a reactive ester group was first synthesized by free-radical copolymerization of HPMA with a CsA-containing monomer **9** and MA-Gly-Gly-ONp in the presence of AIBN. The lectins (PNA and WGA) were conjugated to the copolymer precursor by reacting their amino groups with the active ester groups in the copolymer, respectively.

The CsA derivative-containing monomer **9** was designed and synthesized according to the procedure described in Schemes 1 and 2. An aromatic azo compound, 4-(4-aminophenylazo)benzoic acid (*13*), and L-leucine were employed as a biodegradable spacer between the polymerizable double bond and the CsA derivative. The aromatic azo bond can be cleaved to release the drug specifically by the azoreductase activity produced by microorganisms commonly present in the colon. The conjugation of CsA via aromatic azo bond might avoid the major side effect—fast absorption in small intestine and subsequent nephrotoxicity. The aromatic azo spacer has been successfully used in colon-specific delivery of 5-aminosalicylic acid, a potent drug for the treatment of ulcerative colitis (*8*, *14*). The L-leucine was introduced between the drug and the aromatic residue in order to free the CsA derivative completely by peptidase and/or aminopeptidase (*15*, *16*) after initial cleavage of the aromatic azo bond by the azoreductase activities.

CsA has a cyclic undecapeptide structure (structure 1)

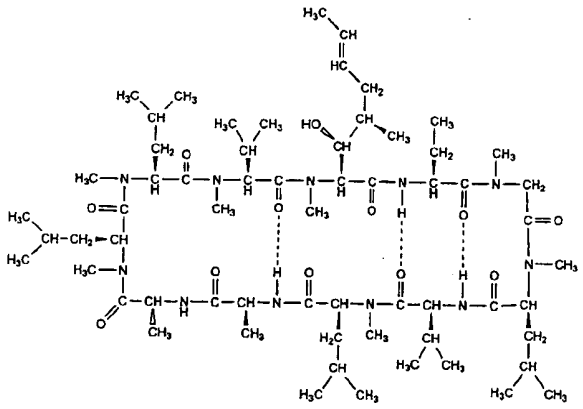

and has one functional group, the hydroxyl group on the 2-*N*-methyl-(*R*)-((*E*)-2-butenyl)-4-methyl-L-threonine (MeBmt) residue, which could be used as an attaching point in monomer synthesis. The attachment of CsA via the hydroxyl group to a polymerizable group would result in a monomer where the intact structure of CsA is maintained. However, the attempt to conjugate CsA to a monomer via the hydroxyl group was not successful because the hydroxyl group shows very low reactivity due to the steric hindrance. A reactive functional group, e.g., amino group, had to be introduced to CsA for the conjugation. The double bond on the MeBmt residue can be chemically modified to introduce an amino group, and it has been reported that the modified CsA maintained its pharmacological effectiveness (*17*–*19*). The conjugation of CsA derivative to HPMA copolymers may decrease the side effects associated with administration of CsA (*20*). Due to the combination of local and systemic actions of CsA releases in the colon (*21*), lower CsA plasma levels should be therapeutically effective when compared to intravenous administration.

A reactive amino group was introduced to MeBmt residue of CsA by the reaction of 1,2-ethylenediamine with a CsA lactone (**2**), Scheme 1. The CsA lactone was prepared by the oxidative cleavage of the double bond of the CsA using $NaIO_4$ and $KMnO_4$ (*22*). The lactone was refluxed with excess 1,2-ethylenediamine for 24 h in methanol. The solvent was removed, and solid residue was dissolved in CH_2Cl_2 and washed with water. The amino-functionalized CsA derivative (**3**) was obtained from the organic phase and was purified by silica gel chromatography. The compound **3** was characterized by proton NMR and electrospray mass spectrometry (m/z = 1248.38 (M^+ + 1), and the calculated molecular weight is 1247.73).

Scheme 3. Copolymerization of Monomer 9[a]

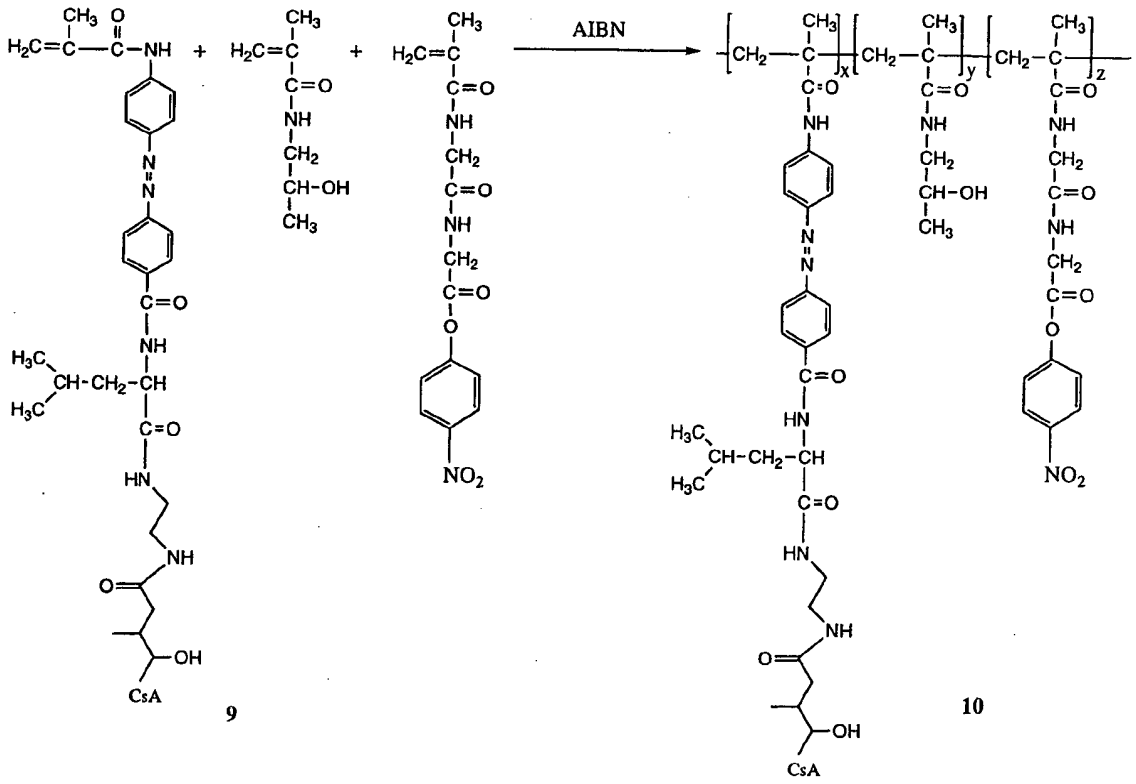

[a] HPMA and MA-Gly-Gly-ONp. AIBN, Acetone, 50 °C, 48 h, 76%.

The synthesis of the monomer **9** is shown in Scheme 2. 4-(4-Aminophenylazo)benzoic acid (**4**) was employed as a degradable spacer (*14*). The polymerizable residue, methacryloyl group, was introduced by reacting methacryloyl chloride with **4** in the presence of diisopropylethylamine to give compound **5**. L-Leucine methyl ester was coupled to compound **5** in the presence of DCC to form compound **7** after the hydrolysis of the ester group with dilute NaOH in methanol. The active ester **8** was synthesized by reacting compound **7** with *N*-hydroxysuccinimide in the presence of DCC. The CsA derivative containing monomer **9** was synthesized by the coupling reaction of compound **8** with **3**. The orange monomer **9** was isolated using silica gel chromatography. The intermediate reaction products and the monomer **9** were characterized by proton NMR and electrospray mass spectrometry. The *m/z* ($M^+ + 1$) of the monomer **9** was 1652.75 (calculated 1652.19).

The monomer **9** (90 mg), HPMA (210 mg), and MA-Gly-Gly-ONp (28 mg) were copolymerized in the presence of AIBN at 50 °C in acetone (Scheme 3).

Copolymer **10** was obtained with a yield of 76%. The number and weight average molecular masses of the copolymer were 17 500 and 25 900 Da, respectively, as determined by size-exclusion chromatography (SEC) using polyHPMA calibration, eluted with 30% acetonitrile containing PBS buffer. The content of the CsA derivative **3** in the copolymer was 0.20 mmol/g as determined spectrophotometrically at 360 nm based on the absorbance of the aromatic azo residue ($\epsilon = 2.5 \times 10^4\ M^{-1}\ cm^{-1}$, methanol). The content of the ONp active ester was 0.2 mmol/g (of copolymer) as determined spectrophotometrically at 400 nm based on the released *p*-nitrophenolate ($\epsilon = 1.8 \times 10^4\ M^{-1}\ cm^{-1}$, water) after hydrolysis of the copolymer in basic condition and separation using a Sephadex G-25 column. Because of the hydrophobicity of CsA derivative, the copolymer aggregated partially in PBS solution as shown by the SEC profile of the copolymer. The hydrophobic aggregation completely disappeared in the 30% (volume) acetonitrile containing PBS solution.

The lectins, WGA (molecular mass = 43 kDa) and PNA (molecular mass = 110 kDa), were bound to the HPMA copolymer–CsA derivative conjugate [P(CsA)] **10**, respectively, by reacting their amino groups with the *p*-nitrophenol ester of the copolymer. A high concentration of lectin or copolymer precursor should be avoided in the conjugation reaction because precipitation occurred due to lectin (especially the PNA) aggregation or cross-linking. However, a too low concentration of reactants might result in low yield of conjugate due to large amount of unreacted protein. The concentrations of lectin and polymer solutions were optimized to give higher yields. A 4 wt % concentration of copolymer solution and 1.7 wt % of WGA (1.5 wt % of PNA) were used in the conjugation. The lectin solution was added dropwise to the copolymer solution. The conjugation reaction was carried out at neutral pH (7.3) for 2 h at room temperature and left at 4 °C overnight after the pH was gradually raised to 8.0 with diluted NaOH. The unreacted *p*-nitrophenol ester was destroyed by raising the pH to 9.0 for a short period. The lectin–copolymer conjugates were separated from unconjugated copolymer and lectins by SEC. The isolated lectin–copolymer conjugates were dialyzed against deionized water, and lyophilized. The weight average molecular masses of the conjugates were determined by using SEC with a laser light scattering detector (Mini-Dawn, Wyatt). The molecular masses of the conjugates were 150 kDa for WGA–P(CsA) conjugate and 250 kDa for PNA–P(CsA) conjugate, respectively. The lectin contents were 36.5 wt % in the WGA–P(CsA) conjugate and 54.5 wt % in the PNA–P(CsA) conjugate, respec-

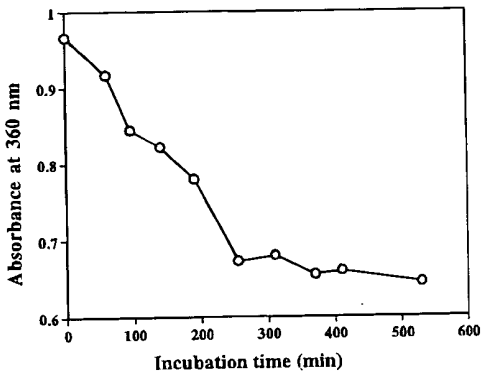

Figure 1. The time-dependent degradation of P(CsA) with rat cecal contents. The P(CsA) was incubated with preincubated cecum contents in N_2 atmosphere at 37 °C. The absorbance of aromatic azo bond at 360 nm was recorded at different time intervals.

tively, as determined by Lowry assay. The CsA derivative content was determined spectrophotometrically at 360 nm based on the aromatic azo residues. The contents of CsA derivative were 16.0 wt % in the WGA–P(CsA) conjugate and 11.5 wt % in the PNA–P(CsA) conjugate, respectively. There were on average four P(CsA) chains attached to one WGA molecule and five P(CsA) chains attached to one PNA molecule.

The lectins, especially PNA, have a tendency to aggregate and precipitate in aqueous solution. However, when the lectins were conjugated to the copolymer, the stability of the lectins was significantly increased. No precipitation was observed in the lectin–copolymer conjugate solution, pH 7.3 (1 wt %), during 1 month storage at 4 °C.

To verify the stability of the amide bond originating in the leucine residue in the GI tract, we incubated the P(CsA) with rat small intestine contents (10 wt %) at 37 °C. No significant release of the CsA derivative was detected after 5 h of incubation. The HPLC analysis of the methylene dichloride extract of the P(CsA) incubation mixture indicated that less than 1% of total CsA derivative was released. However, an 1 h incubation of Z-Ala-Ala-Leu-Nap (1 mM), used as a control, resulted in 50% of *p*-nitroaniline release. This indicates that the amide bond originating in the leucine residue in the P(CsA) side chains is considerably stable in conditions mimicking the small intestine.

The cleavage of the aromatic azo bond and the release of the CsA derivative were investigated by incubation of P(CsA) with rat cecal contents at 37 °C. The degradation of the aromatic azo bond was monitored by UV spectrophotometry at 360 nm, and the degradation kinetics is shown in Figure 1. The absorbance of the azo spacer at 360 nm decreased with increasing the incubation time and appeared to reach a plateau after 6 h. The incubation mixture was extracted with methylene chloride and the extract was analyzed by MALDI-TOF mass spectrometry. The *p*-amino-benzoyl-Leu-ED-CsA residue (m/z = 1519, + K^+) expected after the cleavage of the azo bond and free CsA derivative (m/z = 1248, **3** + H^+; 1287, **3** + K^+) were identified in MALDI-TOF mass spectra. Both compounds were present in a significant amount in the organic extract as determined by HPLC. As demonstrated above that the P(CsA) was stable in the small intestinal contents, however, in cecal contents the free CsA derivative was released in addition to the fragment resulting from the cleavage of the azo bond. This indicates that the CsA containing side chain in P(CsA) was resistant to endopeptidase activities. The ultimate cleavage of the amide bond originating in the leucine residue in the cecal contents suggests that the azo bond was cleaved first, followed by the cleavage of the amide bond by aminopeptidases. The results seem to validate the design of the conjugates and the importance of the colon-specific cleavage of the azo bond. The azoreductase activity of the colonic bacteria is suitable for site-specific delivery of drugs to the large intestine. This is based on the facts that the proteolytic activity in the colon is less than that of the small intestine and that the concentration of microbial flora present in the colon is orders of magnitude higher than in both the stomach and the small intestine (*7*).

In summary, the above results indicated that the HPMA copolymer–CsA derivative conjugate will be stable during the transport via GI tract but will specifically release the drug in the colon after cleavage of the azo bond by the azoreductase activities. The lectins, WGA and PNA, were conjugated to the P(CsA), respectively, to enhance the bioadhesion of the conjugate to the colon tissue (*23*). Further biological evaluation of the nontargeted and the lectin-targeted HPMA copolymer–CsA conjugates is ongoing.

ACKNOWLEDGMENT

The research project was supported in part by NIH Grant DK39544.

Supporting Information Available: Further experimental procedures. This material is available free of charge via the Internet at http://pubs.acs.org.

LITERATURE CITED

(1) Brynskov, J. (1993) Cyclosporin for inflammatory bowel disease: mechanisms and possible actions. *Scand. J. Gastroenterol. 28*, 849–857.

(2) Aiko, S., Conner, E. M., Fuseler, J. A., and Grisham, M. B. (1997) Effects of cyclosporine or FK506 in chronic colitis. *J. Pharmcol. Exp. Ther. 280*, 1075–1084.

(3) Wenzl, H. H., Petritsch, W., Aichbichler, B. W., Hinterleitner, T. A., Fleischmann, G., and Krejs, G. J. (1998) Short-term efficacy and long-term outcome of cyclosporine treatment in patients with severe ulcerative colitis. *Z. Gastroenterol. 36*, 287–293.

(4) Drewe, J., Beglinger, C., and Kissel, T. (1992) The absorption site of cyclosporin in the human gastrointertinal tract. *Br. J. Clin. Pharmacol. 33*, 39–43.

(5) Faulds, D., Goa, K. L., and Benfield, P. (1993) Cyclosporin: a review of its pharmacodynamic and pharmacokinetic properties, and therapeutic use in immunoregulatory disorders. *Drugs 45*, 953–1040.

(6) Sandborn, W. J., Tremaine, W. J., Schroeder, K. W., Batts, K. P., Lawson, G. M., Steiner, B. L., Harrison, J. M., and Zinsmeister, A. R. (1994) A placebo-controlled trial of cyclosporine enemas for mildly to moderately active left-sided ulcerative colitis. *Gastroenterology 106*, 1429–1435.

(7) Kopeček, J., and Kopečková, P. (1992) N-(2-Hydroxypropyl)-methacrylamide copolymers for colon-specific drug delivery. In *Oral Colon-Specific Drug Delivery* (D. R. Friend, Ed.) pp 189–211, CRC Press, Boca Raton, FL.

(8) Kopečková, P., Rathi, R. C., Takada, S., Říhová, B., Berenson M. M., and Kopeček, J. (1994) Bioadhesive N-(2-hydroxypropyl)methacrylamide copolymers for colon-specific drug delivery. *J. Controlled Release 28*, 211–222.

(9) Lehr, C.-M. (1999) Lectin-mediated drug delivery - the second generation of bioadhesives. *Abstracts Ninth Int. Symp. Recent Adv. Drug Delivery Syst.*, p 12, Salt Lake City, UT, February 22, 1999.

(10) Cooper, H. S., Farano, P., and Coapman, R. A. (1987) Peanut lectin binding sites in colon of patients with ulcerative colitis. *Arch. Pathol. Lab. Med. 111*, 270–275.

(11) Philips, T. E., and Frisch, E. B. (1990) Secretory glycoconjugates of a mucin-synthesizing human colonic adenocarcinoma cell line. Analysis using double labeling with lectins. *Histochemistry 93*, 311−317.

(12) Wróblewski, S., Kopečková, P., Říhová, B., and Kopeček, J. (1998) Lectin-HPMA copolymer conjugates: potential oral drug carriers for targeting diseased tissues. *Macromol. Chem. Phys. 199*, 2601−2608.

(13) Jaffe, C. L., Lis, H., and Sharon, N. (1980) New cleavable photoreactive heterobifunctional cross-linking reagents for studying membrane organization. *Biochemistry 19*, 4423−4429.

(14) Grim, Y., and Kopeček, J. (1991) Bioadhesive water-soluble polymeric drug carriers for site-specific oral drug delivery. Synthesis, characterization, and release of 5-aminosalicylic acid by *Streptococcus faecium in vitro*. *New Polym. Mater. 3*, 49−59.

(15) Kopečková, P., Ikesue, K., and Kopeček, J. (1992) Cleavage of oliogopeptide *p*-nitroanilides attached to N-(2-hydroxypropyl)methacrylamide copolymers by guinea pig intestinal enzymes. *Makromol. Chem. 193*, 2605−2619.

(16) Ikesue, K., Kopečková, P., and Kopeček, J. (1993) Degradation of proteins by guinea pig intestinal enzymes. *Intl. J. Pharm. 95*, 171−179.

(17) Říhová, B., Jegorov, A., Strohalm, J., Matha, V., Rossmann, P., Fornùsek, L., and Ulbrich, K. (1992) Antibody-targeted cyclosporin A. *J. Controlled Release 19*, 25−40.

(18) Říhová, B., Strohalm, J., Plocová, D., Šubr, V., Šrogl, J., Jelínková, M., Šírová, M., and Ulbrich, K. (1996) Cytotoxic and cytostatic effects of anti-Thy 1.2 targeted doxorubicin and cyclosporin A. *J. Controlled Release 40*, 303−319.

(19) Šťastný, M., Ulbrich, K., Strohalm, J., Rossmann, P., and Říhová, B. (1997) Abnormal differentiation of thymocytes induced by free cyclosporine is avoided when cyclosporine bound to N-(2-hydroxypropyl)methacrylamide copolymer carrier is used. *Transplantation 63*, 1818−1827.

(20) Von Graffenried B., and Krupp, P. (1986) Side effects of cyclosporin in renal transplant recipients and in patients with autoimmune disease. *Transplant. Proc. 18*, 876−883.

(21) Sandborn, W. J. (1995) A critical review of cyclosporine therapy in inflammatory bowel disease. *Inflam. Bowel Dis. 1*, 48−63.

(22) Paprica, P. A., Margaritis, A., and Petersen, N. O. (1992) Preparation of novel Cyclosporin A derivatives. *Bioconjugate Chem. 3*, 32−36.

(23) Wróblewski, S., Berenson, M., Kopečková, P., and Kopeček, J. (1999) Biorecognition of HPMA copolymer - lectin conjugates as an indicator of differentiation of cell-surface glycoproteins in development, maturation and diseases of human and rodent tissues. *J. Biomed. Mater. Res.* (in preparation).

BC990098A